ABSTRACT

Title: IDENTIFYING AND UNDERSTANDING NORTH AMERICAN CARBON CYCLE PERTURBATIONS FROM NATURAL AND ANTHROPOGENIC DISTURBANCES

Christopher S.R. Neigh, Doctor of Philosophy, 2008

Directed By: Professor and Chair John R.G. Townshend
Department of Geography

Carbon dioxide accumulating in our atmosphere is one of the most important environmental threats of our time. Humans and changing climate, separately or in concert, have affected global vegetation, biogeochemical cycles, biophysical processes, and primary production. Recent studies have found temporary carbon stores in North American vegetation due to land-cover land-use change, but have yet to characterize regional mechanisms across the continent. This research implemented multi-resolution remote sensing data, coupled with ecosystem simulations, to determine the importance of fine-scale disturbance in our understanding of dynamics that drove and/or perturbed carbon sequestration in North America from 1982 through 2005.

The research involved three components: 1) identified large regions with natural and anthropogenic vegetation disturbances; 2) determined causes of disturbances with high-spatial resolution data and mapped associative fine-scale

land cover dynamics; and 3) used prior empirical observations in simulations to quantify mechanisms that altered carbon pathways.

Investigation of normalized difference vegetation index data from the NOAA series of Advanced Very High Resolution Radiometers found regions in North America that experienced marked increases in photosynthetic capacity at various times from 1982 to 2005. Inspection of anomalies with multi-resolution data from Landsat, IKONOS, aerial photography, and ancillary data revealed a wide range of causes: climatic influences; severe drought and subsequent recovery; irrigated agriculture expansion; insect outbreaks followed by logging and subsequent regeneration; and forest fires with subsequent regeneration.

Fine-scale land cover change dynamics were included in Carnegie-Ames-Stanford approach simulations to enhance replication of carbon cycle processes found in empirical observations. Integration of multi-resolution remote sensing data, with carbon ecosystem process modeling, improved regional understanding and accounting of dynamic fine-scale spatial-temporal North American ecosystem carbon balance by a total of ~10 – 250 teragrams of carbon. Coarse resolution simulations could fail to identify important local scale drivers which impact regional carbon balance.

IDENTIFYING AND UNDERSTANDING NORTH AMERICAN CARBON CYCLE PERTURBATIONS FROM NATURAL AND ANTHROPOGENIC DISTURBANCES

by

Christopher S.R. Neigh

Dissertation submitted to the Faculty of the Graduate School of the
University of Maryland, College Park, in partial fulfillment
of the requirements for the degree of
Doctor of Philosophy
2008

Advisory Committee:

Professor John R.G. Townshend, Chair
Adjunct Professor Compton J. Tucker
Professor Ruth DeFries
Professor Samuel Goward
Associate Professor Irwin Forseth

To my Wife,

Gina…

For love & support during my Graduate Studies

&

My Mother…

For love & raising me to achieve my dreams

Foreword

Portions of my Dissertation have been previously published in the peer reviewed literature with my advisors Professor John R.G. Townshend and Adjunct Professor Compton J. Tucker as co-authors. These publications and associative research were conducted under grants from the National Aeronautical and Space Administration. Dr. Compton J. Tucker was the Principal Investigator with the majority of tasks being carried out by myself in an effort to successfully complete my PhD studies. The following two publications have appeared in the literature:

Neigh, C.S.R., Tucker, C.J., & Townshend, J.R.G. (2007). Synchronous NDVI and surface temperature trends in Newfoundland: 1982-2003. *International Journal of Remote Sensing, 28*, 2581-2598

Neigh, C.S.R., Tucker, C.J., & Townshend, J.R.G. (2008). North American Vegetation Dynamics observed with multi-resolution satellite data. *Remote Sensing of Environment, 112*, 1749-1772

Acknowledgements

I would like to thank Dr. Dan Slayback for processing AVHRR images and discussion of NDVI trend significance, Dr. Jorge Pinzon for producing the GIMMS 'g' dataset and discussion of evaluation of climate influences to NDVI, and Dr. Molly Brown for discussion of NDVI processing artifacts and implications of scale in coarse resolution data. I am grateful to Nuno Carvalhais for collaboration and implementation of land-cover land-use change in carbon simulations in CASA and development of disturbance modules. I would also like to thank Dr. G. Jim Collatz, for collaboration and discussion of modeling ecosystem dynamics with land-cover land-use change. I also thank the members of my committee, Professor Ruth DeFries, Professor Samuel Goward, and Associate Professor Irwin Forseth for their guidance.

I am particularly grateful to my co-advisors, Professor John Townshend and Adjunct Professor Compton Tucker, for their mentorship and guidance during the course of my PhD studies. The combination of their insight and wealth of knowledge produced a learning experience that fostered my academic growth.

Table of Contents

List of Tables

List of Figures

List of Acronyms

AVHRR	Advanced Very High Resolution Radiometer
BOREAS	Boreal Ecosystem-Atmosphere Study
CASA	Carnegie-Ames-Stanford Approach
CCSP	Climate Change Science Program
CFS	Canadian Forest Service
CVA	Change Vector Analysis
ETM+	Enhanced Thematic Mapper plus
FAO	Food and Agriculture Organization
FPAR	Fraction of absorbed Photosynthetically Active Radiation
GIMMS	Global Inventory Modeling and Mapping Studies
GISS	Goddard Institute for Space Studies
GLCF	Global Land Cover Facility
GPCP	Global Precipitation Climatology Project
GPP	Gross Primary Production
GPS	Global Positioning System
IGBP	International Geosphere Biosphere Program
ISCCP	International Satellite Cloud Climatology Project
LAI	Leaf Area Index
LCLUC	Land-Cover Land-Use Change
MODIS	Moderate Resolution Imaging Spectroradiometer
MSC	Meteorological Service of Canada

MSS	Multispectral Scanner
NASA	National Aeronautical and Space Administration
NASS	National Agriculture Statistics Service
NBP	Net Biome Production
NEP	Net Ecosystem Production
NECB	Net Ecosystem Carbon Balance
NOAA	National Oceanic Atmospheric Administration
NPP	Net Primary Production
PAR	Photosynthetically Active Radiation
PCA	Principal Component Analysis
ppm	parts per million
R_h	Heterotrophic Respiration
UNESCO	United Nations Educational Scientific and Cultural Organization
USDA	United States Department of Agriculture
SR	Simple Ratio
TC	Tasseled Cap
TM	Thematic Mapper

Chapter 1. Introduction

1.1 The Global Carbon Cycle

Carbon is a fundamental element for life on Earth that cycles among reservoirs of organic material in the biosphere, as a gas in the atmosphere, dissolved in the hydrosphere and locked in sediments in the lithosphere (Schlesinger 1997). The cycle is highly variable and difficult to measure producing accounting uncertainties due to complex biological, chemical, and physical processes (Houghton 2003; Sabine et al. 2004; Schaefer et al. 2002). Currently, a global imbalance exists with carbon dioxide (CO_2) accumulating in the atmosphere from human use of Earth resources (CCSP 2007; IPCC 2007). These activities are known to have large impacts on the carbon cycle and it is critical to understand the dynamics of the controlling processes if informed policy decisions are to be made regarding the future sustainability of climate (Houghton 2007; IPCC 2007). Crucial quantitative information about the locations of the uptake and release of carbon is provided by satellite remote sensing. Although, few studies have quantified fine-scale human induced land-cover land-use change impacts to carbon derived from multi-resolution satellite data.

CO_2 is a trace greenhouse gas in our atmosphere transparent to sun light while absorbing surface radiant heat. Change in the atmospheric concentration of CO_2 has forced detrimental climate change (IPCC 2007), alone it is accountable for +55% of the change in the Earth's radiation balance (IPCC 2001). Due to increasing levels of CO_2 substantial global climate changes are

projected to occur through spatial-temporal patterns of biosphere-atmosphere interactions of fluxes of carbon, water and energy (CCSP 2007; IPCC 2007).

Over the past 11,000 years until the 18th century, atmospheric CO_2 varied less than 25 parts per million (ppm) or ~9% (Joos and Prentice 2004). Since the Industrial Revolution, a steady accumulation of CO_2 occurred as humans burned fossil fuels which took millennia to store in the lithosphere (Figure 1.1 A). As a consequence, CO_2 increased ~100 ppm, from preindustrial concentrations of ~280 ppm (IPCC 2001), to 380 ppm in 2005 (Keeling and Whorf 2005), a 35% increase over a brief ~150 years.

The biosphere has been a repository of atmospheric carbon through photosynthesis absorbing CO_2 in plant biomass (IPCC 2007). Over the past two centuries it has sequestered ~300 Gt ± 50% reducing emissions so that only ~40% remains (Sabine et al. 2004) (Figure 1.1 B, difference between red and blue curves). Climate change could reduce and/or remove natural repositories of carbon, accelerating accumulation of CO_2 in the atmosphere which could result in detrimental feedbacks to climate (Fung et al. 2005). Observed from ice-cores, concentrations of CO_2 are greater than any period from the past 420,000 years due to the inability of ecosystems to capture increasing emissions (CCSP 2007; IPCC 2007). A warming trend has begun and will continue for future centuries due to thermal inertia of oceans and other climate change factors (Hansen et al. 2005; Hansen 2007). Understanding and accounting for carbon is critical

considering an altered carbon cycle can change global climate (Foley and Ramankutty 2004; Houghton 2007).

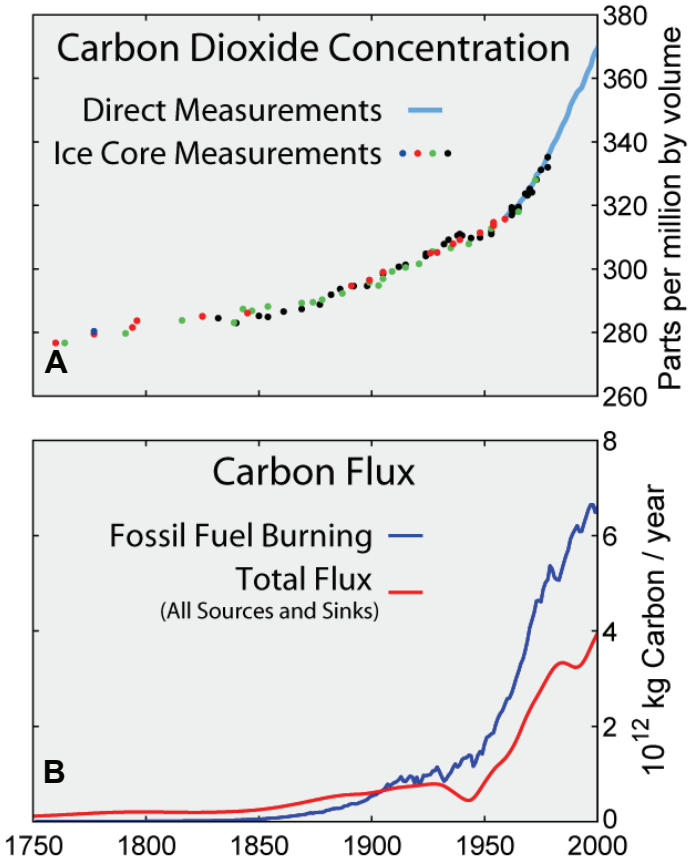

Figure 1.1 A) Atmospheric CO_2 concentration and B) carbon emissions and total flux of carbon that remains in the atmosphere. Difference is due to the biosphere sink. (http://www.globalwarmingart.com/wiki/Image:Carbon_History_and_Flux_Rev_png)

Components of the cycle critical to understand the biosphere sink have been defined in a number of terms. Gross primary production (GPP) is CO_2 assimilated through photosynthesis or the process by which plants draw carbon from the atmosphere. Net primary production (NPP), is a measure of GPP minus plant respiration, while net ecosystem production (NEP) is a measure of NPP minus soil respiration (Randerson et al. 2002). None of these measurements explicitly account for disturbance possibly driven by humans (e.g. harvest,

logging, and fire) which motivated the development of net biome productivity (NBP) introduced by Schulze and Heimann (1998), that includes carbon losses off site (Figure 1.2). NBP is representative of the total carbon balance with inclusion of episodic disturbance events and is the quantity sought after in this investigation.

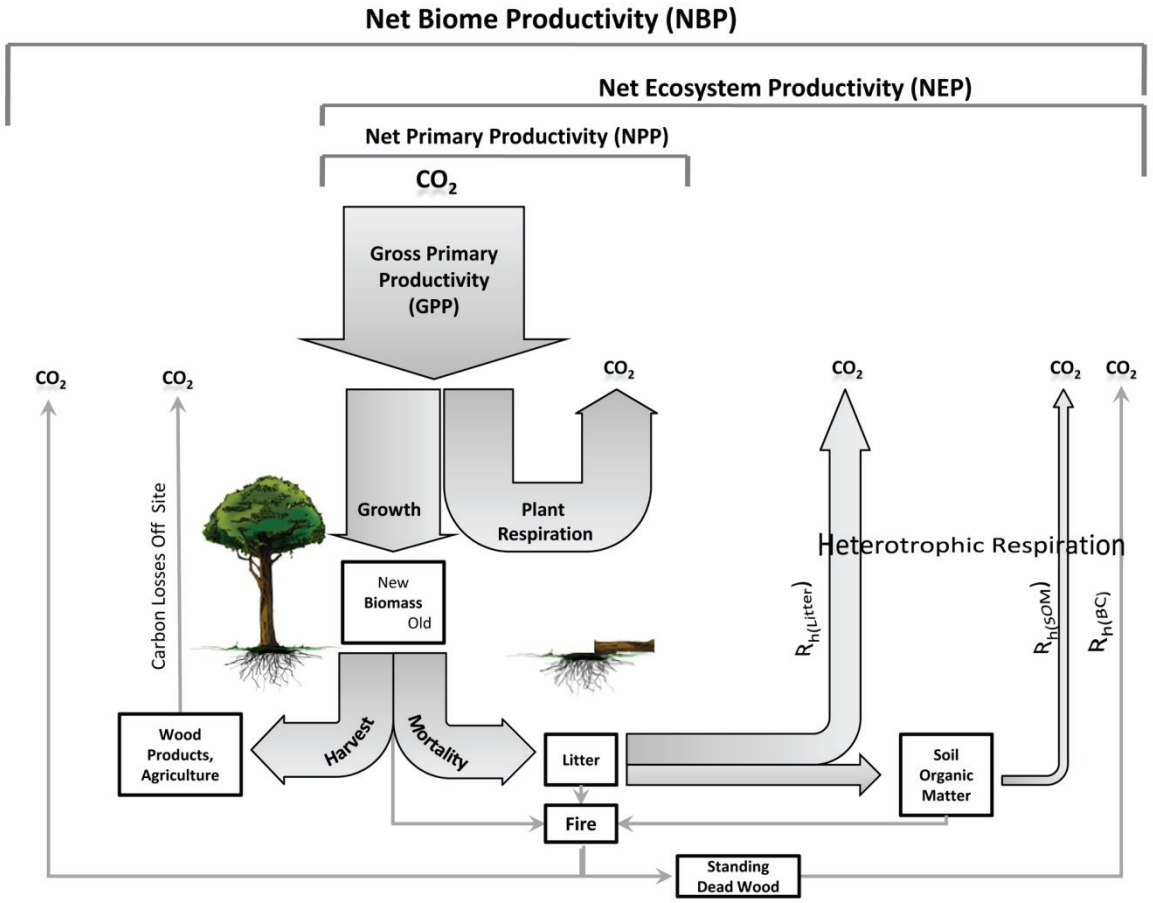

Figure 1.2 A conceptual scheme of the carbon cycle through ecosystems with input through photosynthesis and balance between autotrophic (plant respiration) and heterotrophic (soil) respiration. Disturbance to the carbon cycle is captured in harvest and mortality through fire, logging, and agriculture harvesting. Inclusion of these disturbance processes that impact the carbon cycle in ecosystems is referred to as net biome productivity (NBP), adapted from (Schulze et al. 2000).

1.2 The North American Carbon Cycle

North America alone has been predicted to account for 50% of the terrestrial carbon sink and more than 25% of the variability in the global carbon cycle (CCSP 2007; Goodale et al. 2002; Gurney et al. 2002; Pacala et al. 2001). However, the future of the sink is highly uncertain due to climate feedbacks to vegetation productivity and large errors exist when calculating inter-annual fluxes (i.e. the missing carbon sink) (Angert et al. 2005; Breshears et al. 2005; Chen et al. 2006; Friedlingstein et al. 2006; Nowak et al. 2004). Loss of the North American sink could alter the global carbon balance which has regional to global climate change consequences (Canadell et al. 2007; Hansen et al. 2005). Projected changes include: increased heat index (IPCC 2007), intensified precipitation events, increased risk of drought (Breshears et al. 2005), changes in North Atlantic Ocean circulation (Nazarenko et al. 2007), and rising sea level 0.2 – 0.6 m (IPCC 2007), and perhaps more (Rahmstorf 2007) by 2100. Models have suggested a continental warming of 1° - 3° C over the next century to a maximum of 3.5° - 7.5° C in northern North America (IPCC 2007). These phenomena could result in detrimental impacts inhibiting species from carrying out life sustaining activities.

1.3 Multi-Resolution Satellite Observations Integrated in Carbon Modeling

Satellite remote sensing of disturbance and vegetation state, linked to process models, provide the most promising approach for studying carbon fluxes at regional scales. Disruption of vegetation growth contributes to the rise in CO_2

providing ‘pulses’ of emission from lack of gross primary production. Knowing the time, location and magnitude of vegetation disturbance is currently a major uncertainty in global carbon cycle studies (Candell et al. 2000; CCSP 2007; Houghton 2007; Wofsy and Harris 2002). A coupled approach can investigate disturbance and reduce errors associated to the missing sink.

Work initiated herein seeks to identify and characterize carbon sinks in North America observed as increasing anomalous trends within the National Oceanic and Atmospheric Administration (NOAA) series of polar orbiting advanced very high resolution radiometers (AVHRRs) normalized difference vegetation index (NDVI) data. AVHRR anomaly images were generated by year as the average May to September growing season value per pixel relative to1982 to 2005 mean NDVI. Areas will be selected for further study if they met two criteria: 1) a contiguous region greater than 2,000 km^2 with a trend greater than 0.1 NDVI at a 98% confidence interval; and 2) high resolution remote sensing data and corresponding validation were also available for analysis for the 1982 to 2005 time period. Modeling the carbon cycle with remote sensing data as a primary driver of ecosystem dynamics in isolated regions where vegetation productivity is increasing (i.e. anomaly locations) will establish a refined spatial-temporal focus to identify and understand North American carbon sinks. This investigation will combine positive qualities of Landsat (30 m x 30 m resolution) and AVHRR (bimonthly observations) data to deduce regional scale carbon cycle disturbances. Merged analysis of both satellite-derived measurements into a

radiation use efficiency model driven by NDVI and altered for different carbon cycle processes will produce quantitative estimates of regional carbon processes. An improved understanding of regional human and climate induced impacts to net biome productivity (NBP) will allow better management to take place to optimize sequestration of CO_2 (Caldeira et al. 2004; Dixon et al. 1994).

1.4 Research Objectives

The goal of this research is to develop an improved assessment and understanding of ecosystem disturbances that alter the terrestrial carbon balance of North America. The hypothesis is that increases in vegetation production shown by remote sensing data represent sinks of atmospheric carbon sequestered in biomass. This will be examined through empirical studies of remote sensing data and through application and refinement of carbon simulation modeling.

To achieve this goal the following activities were carried out:

1. Analyze NDVI anomalies on decadal periods to identify significantly large variation in vegetation productivity over the period of 1982 to 2005, 1982 to 1991, 1992 to 1999, and 1992 to 2005 (Chapter 3);
2. Quantify human induced land-cover land-use change(s) within regions of increased NDVI (Chapter 3);

3. Characterize disturbance to vegetation productivity, whether driven by climate or land-cover land-use change in regions of increased NDVI (Chapter 3 and Chapter 4);
4. Simulate net biome productivity (NBP) of ecosystems with disturbance in North America to improve understanding of carbon cycle dynamics (Chapter 4);
5. Compare net ecosystem production (NEP) to net biome production (NBP) to derive importance of fine scale data in simulations that account for disturbance (Chapter 4).

1.5 Outline of Dissertation

This dissertation consists of five chapters with two primary goals. Chapter 1 introduces the carbon cycle and motivates the investigation performed herein. Chapter 2 reviews literature relevant to the terrestrial carbon cycle and our current knowledge. In Chapter 3, land-cover land-use change and climate dynamics are investigated in regions of North America that experienced marked increases in NDVI. Chapter 4 integrates fine-scale knowledge gained from detailed investigations of vegetation dynamics into simulations that were developed to replicate carbon cycle ecosystem disturbance dynamics to calculate net biome productivity. Finally, Chapter 5 summarizes results and explores potential impacts to our understanding of North American net biome productivity.

Chapter 2. Literature Review

2.1 Previous North American Carbon Cycle Studies

Uncertainties of future climate change have not improved appreciably over the past 30 years due to lack of understanding of individual physical processes, complex interactions among processes, and the chaotic nature of the climate system (Roe and Baker 2007). Accounting for gigatonnes (10^9, billion metric tonnes) of carbon per year (Gt C yr^{-1}) in terrestrial sinks of carbon with atmospheric inversions studies (studies that subtract known emissions from atmospheric measurements) still have high values of model error due to a limited number of flux towers and complexity of atmospheric transport models (models that simulate atmospheric circulation relative to tower locations) (Baker et al. 2006; Pacala et al. 2001). Error associated to model estimates is referred to as the "missing" carbon sink. Refining estimates with more advanced accounting measures or models, including fine-scale regional estimates of non-respiratory carbon losses, will improve our understanding of complex processes in the carbon cycle in an effort to constrain important North American missing sinks.

2.2 Previous Methods Used to Understand the Carbon Cycle

A number of previous works identified carbon sinks produced with ecosystem dynamics through forest statistics (Caspersen et al. 2000; Dong et al. 2003), crop statistics (Hicke et al. 2004; Lobell et al. 2002), coarse resolution satellite data (Dong et al. 2003; Myneni et al. 1997; Nemani et al. 2003; Potter et al. 2003a; Potter 1999), and atmospheric inversion modeling (Baker et al. 2006;

Deng et al. 2007; Gurney et al. 2004; Patra et al. 2005). Book keeping and inversion studies have found a terrestrial sink of carbon in the North American continent that has offset emissions. Older investigations found the sink accounted for 0.5 ± 0.6 Gt C yr^{-1} (Bousquet et al. 1999; Fung et al. 1997; Hicke et al. 2002; Houghton et al. 1999; Potter et al. 2003b) to more recent studies that have found 1.3 ± 0.4 Gt C in 2003 (Deng et al. 2007); which accounts for nearly half of North American annual CO_2 emissions and nearly half of the global annual carbon sink (CCSP 2007). Deficiencies in both accounting methods exist because sink size varies through time due to climate impacts to plant absorption rates of CO_2. Current land-based studies include only a portion of atmosphere-to-ground processes, while atmospheric inversion studies include all the processes of terrestrial stores of carbon in wood product reservoirs, and exported products from agriculture and logging but they are not able to define the fine-scale region or processes of sequestration (Baker et al. 2006; Deng et al. 2007; Pacala et al. 2001).

2.3 Coarse Satellite Observations of Vegetation Productivity

Coarse resolution satellite estimates from the National Oceanic and Atmospheric Administration (NOAA) series of polar orbiting Advanced Very High Resolution Radiometers (AVHRRs) have been used in an attempt to find missing sinks at global and continental scales but they are limited in their ability to monitor human scale influences (e.g. logging and agriculture practices) to land use that may significantly impact carbon sequestration (Neigh et al. 2008). At

this coarse scale, regional human induced land cover change impacts to terrestrial vegetation productivity processes are not explicitly known due to large mixed pixels. To identify where and when a disturbance has occurred at continental or global scales requires multi-spatial-temporal remote sensing data.

Red and near-infrared remote sensing data have proven useful to calculate vegetation indices over a wide variety of regions and across the globe (Hicke et al. 2003; Hicke et al. 2002; Lotsch et al. 2003; Lucht et al. 2002; Nemani et al. 2003). Changes in normalized difference vegetation index (NDVI) across North America are thus important because they represent variability in vegetation photosynthetic capacity and carbon sequestration. NDVI (Tucker 1979) is calculated from channel 1 (0.58-0.68 μm) and channel 2 (0.72-1.10 μm) from the NOAA AVHRR series of polar orbiting satellites as:

$$NDVI = (Channel\ 2 - Channel\ 1)/(Channel\ 2 + Channel\ 1) \quad (2.1)$$

NDVI variations have been previously reported over the 1982 to 1991 period by Myneni et al. (1997) through1982 to 1999 period by Tucker *et al.* (2001), Slayback et al. (2003) and Zhou et al. (2001) and through 2003 by Bunn et al. (2006), and Goetz et al. (2006). NDVI is often used as a surrogate for primary production, because it exhibits a near linear relationship with the fraction of absorbed photosynthetically active radiation by the vegetation canopy and net primary productivity (Myneni et al. 1995; Sellers 1985; Sellers 1987).

Utilizing the same AVHRR NDVI data in carbon simulation modeling, recent studies have calculated net primary production (NPP) for North America (Hicke et al. 2002; Potter et al. 2007a; Potter et al. 2003b). Potter et al. (1999) estimated from 1990-1995 the United States had a 0.3% annual increase in forest extent contributing to a 0.1 Gt C yr^{-1} to more recently 0.3 Gt C yr^{-1} NPP sink (Potter et al. 2007a). Potter et al. (2007b) also recently integrated fine-scale climate and MODIS data to investigate NEP from 2000 – 2004. However, all of these studies did not calculate total carbon balance including altered carbon pathways as net biome productivity (NBP). Further research is needed to refine estimates of North American sink status, to identify fine-scale mechanisms that perturb carbon sequestration while understanding sensitivity of carbon pools to climate and anthropogenic land-cover change.

2.4 Disturbance Impacts to Carbon Cycling

Disturbance is defined within landscape ecology as any relatively discrete event in time that disrupts population, community, or ecosystem structure and changes resources, substrate availability, or the physical environment (Pickett and White 1985). Disturbance has been defined thoroughly in ecology, but the definition is not sufficient for the regional and continental context using satellite remote sensing. The definition of disturbance is relative to the spatial and temporal dimensions of the system investigated and must be explicitly derived from relevant community dimensions (Allen and Starr 1982). This investigation will explore relatively short-term disturbances within the ecological context of 1–

24 years over community, ecoregion, and continental scales of 10^2 to 10^6 m^2 using satellite data, and ancillary datasets. Disturbance on a regional scale alters biophysical process which in turn changes biogeochemical cycling (Figure 2.1).

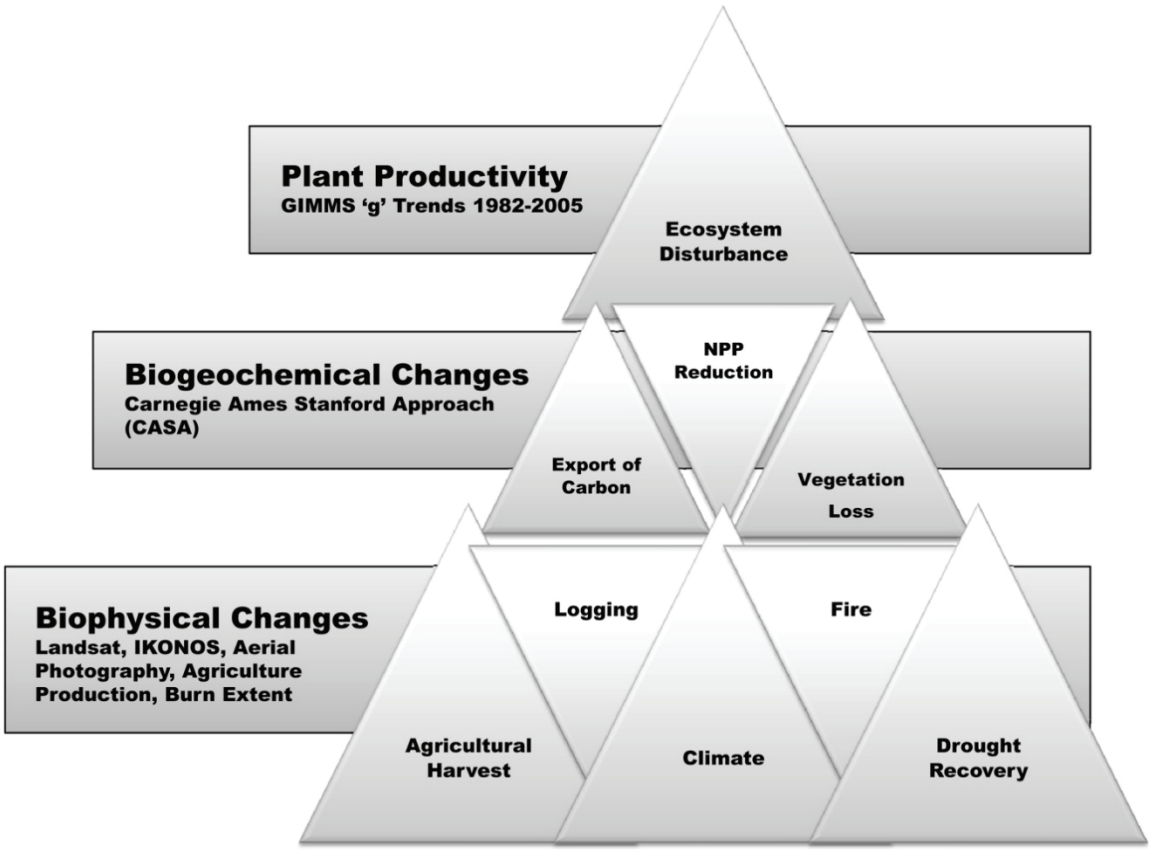

Figure 2.1 Carbon-related ecosystem disturbance classification adapted in this analysis. Biophysical changes to vegetation were captured with remote sensing data, and biogeochemical changes were analyzed with the Carnegie-Ames-Stanford Approach (CASA), to understand carbon cycle dynamics associated to terrestrial biophysical changes in North America. The triangle with subset interlaced triangles symbolizes interacting components of ecosystem (dynamics) in relation to objectives of this research.

Understanding vegetation productivity and state of disturbance regimes in select North American ecosystems from multi-resolution satellite data will provide information of carbon storage in the biosphere due to intense disturbances. A

foremost descriptor of disturbance within the human and natural division is that both must be discrete in time, in contrast to chronic stress or background variability; and both must cause a notable change in the state or functioning of the system. Human disturbances primarily occur as land use conversion of natural lands to agriculture and urban development. This investigation will incorporate multi-resolution multi-temporal datasets to capture and understand processes reported in the literature such as changes in agriculture practices, logging, insect outbreaks, drought, fire and climate influences to terrestrial vegetation productivity and the carbon cycle.

2.5 Land-Cover Land-Use Change Impacts to the Carbon Cycle

Nearly half of the carbon sink in North America is believed to occur as a result of land-cover land-use change from forest regrowth from agriculture abandonment (CCSP 2007). Other processes of accumulation are estimated to result from land-use change including management practices such as: fire suppression (Dixon et al. 1994; Houghton 1999, 2003), agroforestry (Ciais et al. 1995; Dixon et al. 1994; Houghton 2003), woody encroachment (Pacala et al. 2001); reduced tillage of agricultural lands (Ogle et al. 2003; Pacala et al. 2001; Paustian et al. 2000; Randerson et al. 1997; Six et al. 2004), more effective fertilization and pest management (Ciais et al. 1995; Ogle et al. 2003), higher yielding cultivars and shifts to more productive crop types (e.g., wheat to corn) (Hicke et al. 2002; Hicke et al. 2004; Lobell et al. 2002).

Mechanisms of carbon storage not related to land-use change include: nitrogen deposition (Ciais 1995; Friedlingstein et al. 1995; Houghton et al. 1998); changes in growing season duration (e.g., warming in the High Latitudes and more favorable climate for growth) (Hicke et al. 2002; Houghton et al. 1998); CO_2 fertilization (Ciais 1995; Friedlingstein et al. 1995); and changes in regional rainfall patterns (Ciais et al. 2005; Hicke et al. 2002). Other recent investigations have found change in vegetation productivity in the higher northern latitudes related to climate but have lacked detailed assessment of local scale variability that may be due to physical changes in vegetation structure or composition (Clein et al. 2000; McGuire et al. 2000; Nemani et al. 2003; Sitch et al. 2007; Sitch et al. 2003; Soja et al. 2007).

Known studies have yet to characterize disturbance to carbon storage at a fine-scale with remote sensing data and modeling across North America to understand land-cover land-use change coupled with climate ecosystem dynamics. Forest accounting studies do not include climatic influences to vegetation productivity or rates of soil respiration (Houghton et al. 1999; Schimel et al. 2001); and inversion methods do not reveal the exact location of change. However, the approach of coupling fine-scale remote sensing data and simulation modeling negates deficiencies with other methods. While Masek and Collatz (2006) integrated forest statistics, remote sensing, and biogeochemical modeling to evaluate carbon cycle implications, this was only applied in forested regions of the United States where detailed forest inventory data existed.

Research performed in this investigation recognized a lack of land-cover change information derived from fine-scale satellite data as input for ecosystem carbon simulations in prior investigations (Hicke et al. 2002; Potter et al. 2007a; Potter et al. 2003c), and contributed information to improve our knowledge of transient pools of carbon. This investigation intended to produce an assessment of natural and anthropogenic LCLUC "disturbances" in primary production (hereafter referred to as "Disturbance") in North America from 1982 to 2005, identify where and when a disturbance has occurred, determine vegetation land cover characteristics of the disturbed region, and simulate the carbon cycle dynamics to develop an enhanced mechanistic understanding of the temporal-spatial scale sensitivity of the North American carbon balance in regions of increased primary production.

Chapter 3. North American Vegetation Dynamics Observed with Multi-Resolution Satellite Data.

3.1 Introduction

Land cover and land use change strongly influence terrestrial biogeophysical and biogeochemical process (Brovokin et al. 2004; DeFries et al. 1999; Houghton 1999). Humans and changing climate, separately or in concert, have affected global vegetation, biogeochemical cycles, biophysical processes, and primary production. To infer North America vegetation changes, a 1982 to 2005 record of normalized difference vegetation index (NDVI) data was used. This approach, using 8-km NDVI data from the (NOAA) National Oceanic and Atmospheric Administration Advanced Very High Resolution Radiometer (AVHRR) instruments, has previously identified large-scale spatial and temporal patterns of vegetation response to climate (Lotsch et al. 2005; Myneni et al. 1997; Nemani et al. 2003; Zhou 2003). Previous work by others, (Goetz et al. 2005; Gong and Shi 2003; Ichii et al. 2002; Myneni et al. 1997; Nemani et al. 2003; Slayback et al. 2003; Tucker et al. 2001; Zhou et al. 2001), has addressed continental scale phenomena of changes in photosynthetic capacity since 1981-1982 from NDVI data. Investigations with coarse resolution data are limited in the ability to identify specific regional or local land use and land cover change mechanisms that could be responsible for NDVI anomalies.

A number of natural factors influence North American vegetation and primary production, and hence the NDVI: warming and possible reduced Arctic snow cover (Chapin et al. 2000; Dye and Tucker 2003); altered plant community

structure (Epstein et al. 2004; Sturm et al. 2005; Sturm et al. 2001; Tape et al. 2006); reduced permafrost extent and effects upon vegetative growth (Hobbie et al. 2002; Stokstad 2004); insect and pathogen outbreaks (Ayres and Lombardero 2000); severe drought (Angert et al. 2005; Barber et al. 2000; Ciais et al. 2005; Dai et al. 2004; Lotsch et al. 2005); and forest fire regimes (Flannigan et al. 2000). Anthropogenic influences on vegetation productivity include: more intensive agriculture practices (Malhi et al. 2001; Sainju et al. 2002); expansion of irrigated agriculture (Lemly et al. 2000; Tilman 1999); decreasing productivity by removing biomass through urban expansion (Imhoff et al. 2000; Masek et al. 2000); and logging and subsequent regeneration (Howard et al. 2004). This analysis was undertaken to understand vegetation dynamics at a regional scale in North America, to explore possible mechanisms that can affect continental-scale primary production. Interest was focused on investigating NDVI anomalies and determining what caused them, through the combined use of AVHRR NDVI, Landsat, IKONOS, aerial photography, and ancillary data.

NDVI data from the NOAA series of AVHRR instruments over the past 24 years have shown variations in photosynthetic capacity across large areas of North America (Slayback et al. 2003). These observed NDVI trends have occurred in a variety of regions, implying possibly a variety of cause(s) (Goetz et al. 2005; Pickett and White 1985; Tucker et al. 2001). Although a number of recent studies have found marked variations in NDVI throughout the Northern Hemisphere, they have not attributed these changes to regional factors that may

include natural disturbances and/or human alterations to ecosystem functioning (Gong and Shi 2003; Lotsch et al. 2005; Lucht et al. 2002; Myneni et al. 2001; Myneni et al. 1997; Nemani et al. 2003; Slayback et al. 2003; Tucker et al.; Zhou et al. 2001). It is important to identify and quantify land cover type, because changes in land cover can alter ecosystem functioning and carbon storage (Baldocchi and Amthor 2001; Olson 1975).

NDVI (Tucker 1979) is calculated from channel 1 (0.58-0.68 μm) and channel 2 (0.72-1.10 μm) from the NOAA AVHRR series of polar orbiting satellites as:

$$NDVI = \frac{(Channel\ 2 - Channel\ 1)}{(Channel\ 2 + Channel\ 1)} \quad (3.1)$$

NDVI has been found to have a strong linear relationship to the fraction of absorbed photosynthetically active radiation (FPAR), the radiation that drives photosynthesis (0.4 -0.7μm) (Myneni et al. 1995; Sellers 1985). FPAR is the main determinant of net primary productivity (NPP) of the ecosystem (Monteith 1981). NDVI changes across North America are thus important because they represent variability in vegetation photosynthetic capacity. Few investigations have explored regional vegetation changes in North America responsible for the observed increases in Northern Hemisphere NDVI (Jia et al. 2003; Stow et al. 2003; Walker et al. 2003); this investigation seeks to understand regional vegetation dynamics across the North American Continent observed by increases in the AVHRRs' NDVI.

3.2 Methods and Data

3.2.1 AVHRR NDVI

The Global Inventory Modeling and Mapping Studies (GIMMS) version "g", 1982 to 2005 bimonthly AVHRR NDVI record (Tucker et al. 2005) was used because a consistent inter-calibrated data set is critical for long-term vegetation studies. These data, at 8-km (64 km^2) resolution and bimonthly intervals, have been processed to account for orbital drift, minimize cloud cover, compensate for sensor degradation, and effects of stratospheric volcanic aerosols (Brown et al. 2004; Tucker et al. 2005). The GIMMS NDVI data records are accessible from the University of Maryland's Global Land Cover Facility (www.landcover.org).

The first step of analysis was to identify regions using AVHRR NDVI anomalies for further investigation. Next, Landsat data were used to understand AVHRR NDVI anomalies in terms of land cover at the 30 m scale. AVHRR anomaly images were generated by year as the average May to September growing season value with a least squares linear fit applied per pixel relative to four distinct time periods between1982 to 2005 with values excluded from analysis that do not meet the 98% confidence interval fit. Areas were selected for further study if they met two criteria: 1) a contiguous region was greater than 2,000 km^2 with a trend greater than 0.1 NDVI anomaly at a 98% confidence interval; and 2) high resolution remote sensing data and corresponding validation were also available for analysis for the 1982 to 2005 time period.

A lengthening of the growing season may increase plant growth, increase biomass formation, and increase carbon sequestration (Menzel and Fabian 1999). Nemani, et al. (2003), suggested multiple mechanisms affecting net primary productivity (NPP): nitrogen deposition, CO_2 fertilization, forest regrowth, temperature, precipitation and solar radiation. Recovery from disturbance in forest ecosystems has been noted to produce a net terrestrial carbon sink by which NPP exceeds heterotrophic respiration (R_h) due to enhanced resource availability, and reduced detritus input into the soil (Odum 1969). Regions with increasing NDVI were selected to explore possible changes in ecosystem functioning due to conversion and/or recovery of vegetation. It was acknowledged that some local changes may not result in a trend at the AVHRR pixel scale, for example sub-pixel changes could lead to increases and decreases which resolve to null at 8 km pixel scale.

3.2.2 Landsat

Landsat data were acquired for the same areas that had greater than 0.1 NDVI anomaly values. First data from NASA's orthorectified global Landsat data set (also called the "GeoCover" data set) were used because these data have less than a 50 m root mean square location error among the 1970s, 1990, and 2000 data layers (Tucker et al. 2004) and are available free of charge from the Global Land Cover Facility at the University of Maryland. Additional Landsat data were acquired for other time periods as needed and coregistered these data to the corresponding GeoCover data. When possible, data selection focused on

similar dates during peak growing season months with least amount of cloud cover available to reduce phonological errors introduced to classification of 1975, 1990, and 2000 epoch data layers. From an independent dataset used for accuracy assessment, it was found variation between dates within data layers did not have a significant impact on land cover classification or change detection.

A methodology was developed to determine land cover for three time periods (> 150 scenes), to quantify land cover changes that could be responsible for trends in NDVI (Table 3.1). The International Geosphere Biosphere (IGBP) classification was used because of its simplicity in defining North American vegetation types. These vegetation types include: evergreen needleleaf forest; mixed evergreen needleleaf and broadleaf deciduous forest; broadleaf deciduous forest; dwarf trees and shrubs; short vegetation C4 grasslands; agriculture C3 grasslands; water; barren lands; clouds and snow and ice (Table 3.2).

Table 3.1 Landsat scenes used in investigation, bold indicates duplicates for overlap.

	WRS1	MSS	WRS2	TM	ETM	MSS-2	TM-2	ETM-2
Yukon	64011	7/13/76	61011	6/30/88	9/2/00			
	67011	**7/6/78**	**61011**	**6/30/88**	**9/2/00**			
	64012	9/4/78	61012	7/18/92	7/19/00			
	67012	**7/6/78**	**61012**	**7/18/92**	**7/19/00**			
	67011	7/6778	63011	6/28/91	9/19/01			
	67012	**7/6/78**	**63012**	**6/30/92**	**8/31/00**			
	71012	7/20/76	63012	6/30/92	8/31/00			
Northern	39019	9/16/76	37019	8/30/87	9/29/01			
Saskatchewan	40020	9/6/73	37020	8/30/87	9/29/01			
	41019	9/21/79	39019	9/2/89	6/10/02			
	41019	**9/21/79**	**37019**	**8/30/87**	**9/29/01**			
	41020	**8/4/76**	**38020**	**6/2/93**	**9/4/01**			
	42020	**9/21/74**	**39020**	**6/6/92**	**6/10/02**			
	42020	9/21/74	38020	6/2/93	9/4/01			
	43019	8/5/78	41019	8/5/91	6/5/01			

Table 3.1 (*continued*) Landsat scenes used in investigation, bold indicates duplicates for overlap.

	WRS1	MSS	WRS2	TM	ETM	MSS-2	TM-2	ETM-2
	43019	**8/5/78**	**39019**	**9/2/89**	**6/10/02**			
	44020	5/25/73	41020	9/11/87	6/2/00			
	44020	**5/25/73**	**39020**	**6/6/92**	**6/10/02**			
Southern	38025	7/23/76	35025	7/1/88	7/26/00	9/18/79	9/3/88	4/21/00
Saskatchewan	38026	7/13/78	35026	8/11/91	7/8/99	5/15/79	9/28/91	4/21/00
& North Dakota	39025	7/18/79	36025	8/25/88	8/5/88	9/19/79	10/12/88	5/20/02
	39026	7/18/79	36026	9/3/91	8/5/01	9/19/79	7/17/91	10/8/01
Oklahoma	32034	6/14/79	30034	7/25/92	7/5/99	9/30/79	4/4/92	11/26/99
Panhandle	32035	6/14/79	30035	9/27/92	7/5/99	9/30/79	4/4/92	11/26/99
	33034	7/13/77	31034	7/8/89	7/14/00	5/15/78	10/28/89	5/11/00
	33035	7/13/77	31035	7/8/89	8/13/99	4/18/78	10/28/89	5/11/00
Quebec	14026	8/12/78	13026	8/27/89	7/19/01			
	14026	**8/12/78**	**15026**	**5/18/88**	**8/21/02**			
	14027	8/1/75	13027	8/27/89	8/23/02			
	16026	9/23/72	14026	8/26/86	6/5/00			
	15027	10/31/75	14027	6/10/87	5/20/00			
	16026	**9/23/72**	**15026**	**5/18/88**	**8/21/02**			
	16027	6/10/75	15027	5/13/86	6/15/01			
	17026	4/30/76	16026	8/3/90	8/25/01			
	17027	6/2/75	16027	8/3/90	8/25/01			
Newfoundland	03026	8/8/75	03026	7/31/87	10/1/01			
& Labrador	03027	5/15/74	03027	9/9/90	10/1/01			
	04025	7/14/73	04025	8/25/88	10/11/02			
	04026	7/14/73	04026	8/31/90	8/5/01			
	04027	9/24/73	04027	8/31/90	9/1/01			
	05023	8/22/76	05023	9/20/89	9/16/02			
	05024	9/02/74	05024	8/6/90	9/16/02			
	06025	9/13/72	05025	8/6/90	8/12/01			
	05026	8/22/76	05026	8/9/91	6/6/01			
	06026	**9/26/73**	**05026**	**8/9/91**	**6/6/00**			
	05027	6/4/74	05027	8/9/91	6/6/00			
	06023	6/30/76	06023	8/18/92	9/20/01			
	08023	**10/3/72**	**06023**	**8/18/92**	**9/20/01**			
	08022	**7/8/75**	**06023**	**8/18/92**	**9/20/01**			
	06024	10/19/72	06024	6/15/92	9/20/01			
	07024	**7/19/73**	**06024**	**6/15/92**	**9/20/01**			

Table 3.2 Class Definitions for evaluation protocol

Class	Criteria
(NE) Needleleaf Evergreen Forests	Needleleaf Evergreen Trees > 3 m in height, Continuous Canopy > 30%
	(MXF) Mixed Forests Mixed Needleleaf Evergreen and Deciduous Trees > 3 m in height, Continuous Canopy > 30%
(BD) Broadleaf Deciduous Forests	Broadleaf Deciduous Trees > 3 m in height, Continuous Canopy > 30%
(DTS) Dwarf Trees/Scrublands	Trees and Shrubs >1 and < 3 m in height, Continuous Canopy > 30%
(SVEG) Short Vegetation C3 Grasslands	Herbaceous Vegetation < 1 m in height, Sparse Canopy Density < 50%
(AG) Agriculture C4 Grasslands	Annual Crops, Sparse Canopy Density < 50%
(W) Water	Open Water Surfaces > 20%
(B) Barren/Bare Soil/Urban	Human Built Structures, Roads, Bare Soil > 20%
(C) Clouds/Snow	Clouds, Cloud Shadow, and Snow Cover > 20%

Coregistration between additional images in agriculture regions was carried out to avoid misregistration errors that could be confused with land cover change (Townshend et al. 1992). A minimum of 25 ground control points distributed over the image were selected between the orthorectified base image and the added image. A root mean square error of less than 0.25 pixels was used as the maximum threshold for error before the image was used in analysis. All Landsat images were processed in a similar manner with the same accuracy.

When using multispectral data, changes in surface reflectance have been associated with changes in vegetation cover and extent. Generally, a higher reflectance is associated with sparse vegetation cover, and a lower reflectance is associated with dense vegetation or water in visible wavelengths. When investigating pixel response to changes in land cover, deforestation will typically increase pixel brightness (darker vegetation to lighter soil) whereas afforestation

and succession would decrease pixel brightness (bare soil to vegetation) (Jensen 2006). This simple observation was used to quantify variance in land cover. Radiance values are used in my analysis because the selected study sites have marked changes in land surface red and near infrared spectral reflectance observed by coarse resolution 8 km AVHRR. The spectral changes observed between vegetated and non-vegetated pixels at Landsat 30 m resolution visible with 8 km AVHRR far outweigh the influences of sun angle, variability in atmospheric attenuation, and sensor degradation.

3.2.2.1 Classification

A number of change detection transforms have been applied to Landsat data: Principal Component Anaylsis (PCA), tassel cap (TC), and change vector analysis (CVA) (Crist and Cicone 1984; Kauth et al. 1979; Richards 1984). These methods all identify change in multi-temporal data and have been enhanced with hybrid methods (Guild et al. 2004; Jin and Sader 2005; Lanjeri et al. 2004; Lunetta et al. 2002; Nackerts et al. 2005; Rigina 2003; Warner 2005). To adequately account for temporal changes in vegetation cover, my analysis developed two methods to stratify multispectral observations into thematic maps of land cover and land cover change. The first method was developed for the boreal zone where variance in red and near-infrared spectral reflectance is observed from forest to non-forest changes. Method two required adaptation to identify interannual land-cover land-use changes that may be difficult to distinguish in regions of intense agriculture. Deriving an assessment of annual

active productivity within a region of crops that are rotated seasonally required an approach to capture all of the active croplands from native short and tall grass prairies. Both methods are based on change detection algorithms currently in use (Guild et al. 2004; Lanjeri et al. 2004).

A base map was first generated from the 2000 image from the red (Channel 3), near infrared (Channel 4), and mid infrared (Channel 5) from the Landsat Enhanced Thematic Mapper plus (ETM+). An unsupervised ISODATA classification was performed on these channels due to their ability to discriminate vegetation density and type while exhibiting reduced atmospheric contamination that commonly affects the blue and green visible wavelengths. ISODATA is a standard clustering algorithm available in most image processing software packages and is based on procedures in which cluster centers are iteratively determined sampled means (Tou and Gonzales 1974). If a scene contains atmospheric constituents, multiple iterations of the classification were performed to mask and eliminate cloud, cloud shadow, and haze cover. This was necessary to minimize atmospheric contamination that alters the class distribution structure. That was the basis for selecting and distinguishing the classification cover types.

Once a base map of recent land cover was derived, the classification process reverted in time to define locations of change in land cover and mask the current thematic map for prior land cover types (Figure 3.1). A similar method

has been performed by Lanjeri et al. (2004). This method was applied to reduce misclassifications between dates with no land cover changes.

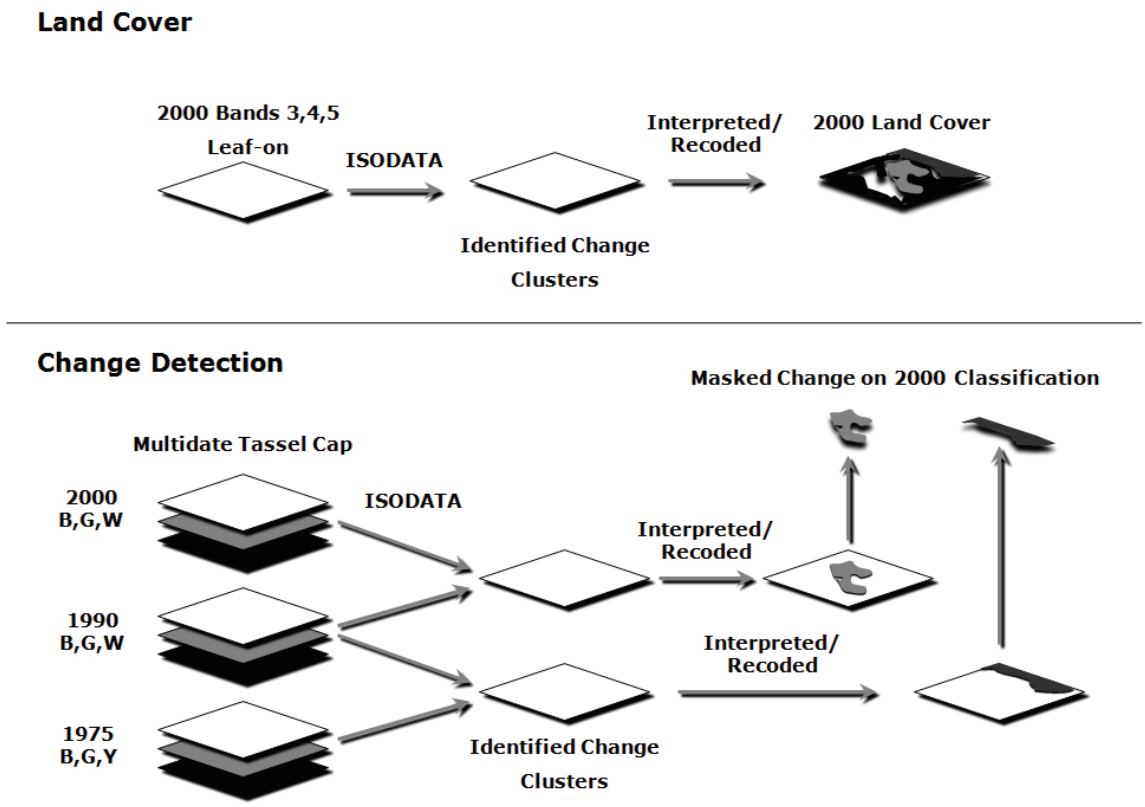

Figure 3.1 Diagrammatic representation of the land cover classification method developed to extract thematic information from multi-temporal Landsat data. Channels 3, 4 and 5 from Landsat-7 were first processed in an unsupervised method into ~50 classes that were aggregated into the 9 International Geosphere Biosphere Program land cover types. Subsequently, all reflective channels were used to produce a multi-date "tassel cap" transformation of brightness, greenness and wetness (B,G,W; Y, yellowness for Multispectral Scanner data) for each time period and then subjected to an unsupervised aggregation to produce areas of change for each of the three time periods. The three time periods were then compared to identify changes from 2000 to 1990 and 1990 to 1970s, respectively. This approach was used in the Mackenzie River Delta, Northern Saskatchewan, Southern Quebec, and Newfoundland study areas.

Change detection was subsequently performed once a base thematic map had been developed for each anomaly area. A linear tassel cap transformation was first applied to the multi-date images reducing multispectral redundancy to

indices of brightness, greenness, and wetness (Crist and Cicone 1984; Huang et al. 2002). The linear tassel cap also enhanced differences in brightness, greenness, and wetness that may occur between multi-date images. The weights of the linear tassel cap transformation were fixed, were sensor specific, and were not scene dependent (Guild et al. 2004). The sensor specific weights of the linear tassel cap transformation aid in normalizing between sensors for change detection analysis. Finally, an unsupervised ISODATA clustering algorithm was performed to all transformed images to group similar spectral vectors into 'change' and 'no change' clusters from the bi-temporal images (Richards 1993).

The same procedure was also performed in agriculture regions with the modification of adding an additional pair of images from the same year as the base period of investigation (Figure 3.2). This was done to capture crop rotation during a growing season while distinguishing irrigated agriculture from fallow croplands and natural grasslands. Irrigated agriculture generally had an enhanced signature of wetness and greenness compared to non-irrigated vegetation in the semi-arid high plains environment.

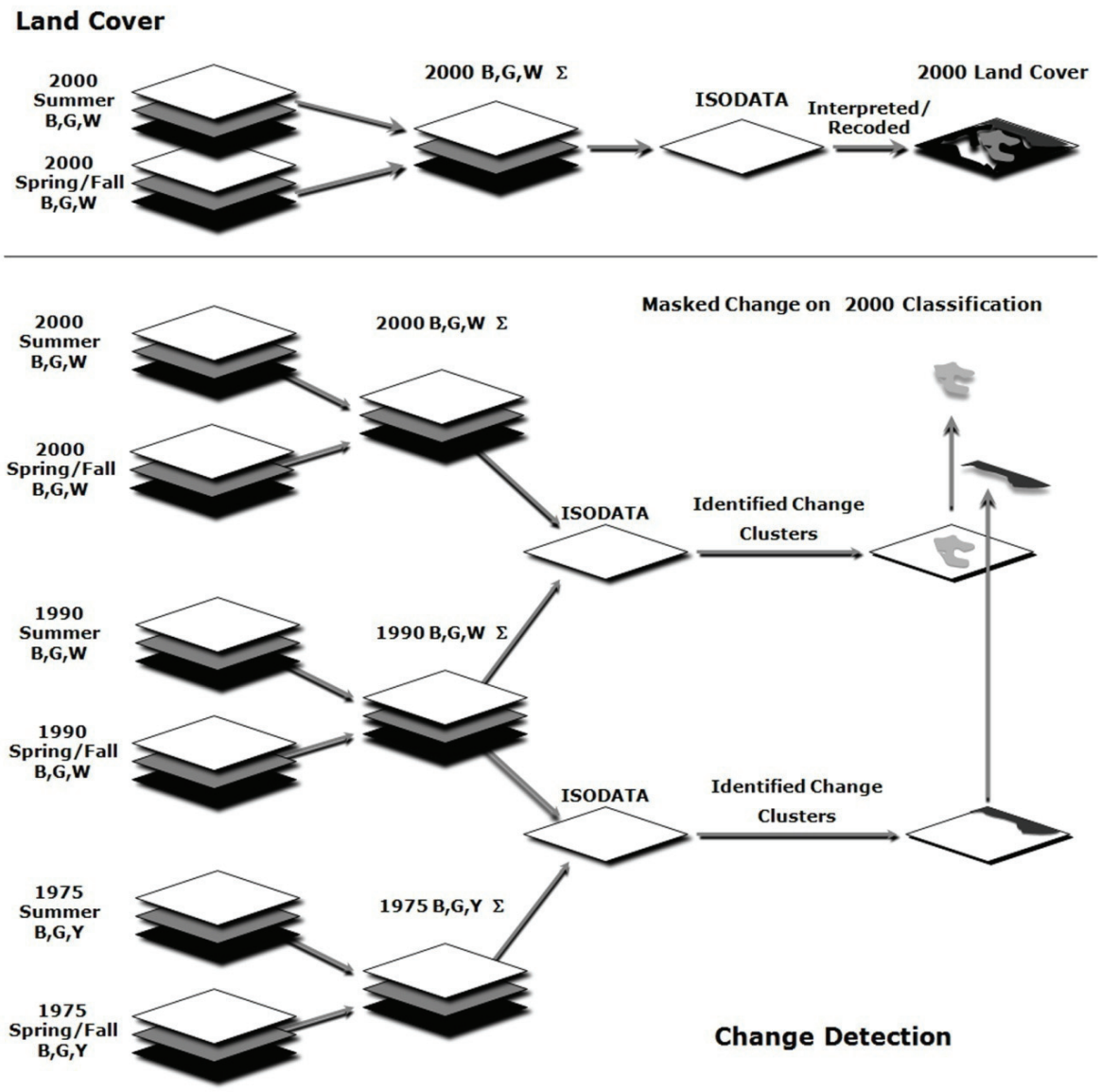

Figure 3.2 Land cover change classification algorithm diagramming steps to extract thematic data from Landsat data for the Southern Saskatchewan and Oklahoma "Panhandle" agricultural study areas. Method two was adapted for regions with irrigated agriculture to capture inter annual variability in crop productivity. Performing a transformation on multi-date tassel cap images of brightness, greenness, and wetness (B,G,W; Y, yellowness for Multispectral Scanner data), then calculating the sum (Σ) captured active irrigated agriculture while distinguishing between fallow agriculture and native grasslands.

3.2.2.2 Validation of Land Cover Maps

Accuracy assessment of land cover maps incorporated two levels of stratification. This was performed to capture two separate indicators of accuracy: map accuracy and an assessment of change. The sample design contains three components similar to Stehman & Wickham, (2006), that were used for the National Land Cover Assessment: (1) the sample design, that determines the spatial locations at which the reference data were obtained; (2) the response design, that details how the reference data were obtained; and (3) the analysis plan for producing the accuracy assessments. Error matrices were then created between the thematic map and reference data. Matrices were constructed with the rows representing the map land cover and columns representing the reference land cover.

The sample design employed nested hierarchical partitions to stratify the sampling distribution. Each study region was subdivided into two by two degree cells. The spatial extent of the maps developed for analysis in this investigation were large with study areas ranging from ~8 to ~18 million hectares. Multiplied times six study regions, and three temporal periods map production contained ~324 million hectares. An adequate sampling of validation data from in situ field surveys was impractical and cost prohibitive due to the spatial extent of the maps. A cost effective large sampling method was employed to develop an adequate validation reference dataset for cross comparison.

3.2.2.2.1 IKONOS & Aerial Photography

The validation dataset was derived from very high-resolution (~0.5 – 2 m) archived digital aerial photography from the United States Geological Survey (http://earthexplorer.usgs.gov) and National Air Photo Library Natural Resources Canada (http://airphotos.NRCan.gc.ca), IKONOS high resolution remote sensing imagery (1 – 4 m), and in situ field plot surveys with aerial over flights of Global Position System (GPS) referenced photography (Table 3.3 and 3.4). The 2000 Landsat analyses were validated the most, because they were the most current satellite information (Figure 3.3). The 1990 and 1975 Landsat data was investigated with digital aerial photography from a similar time period to verify observed changes in cover types. Unfortunately a very limited amount of high-resolution aerial photography data existed for the selected study regions in 1975. This limitation was reported in accuracy assessments as the number of samples used in the confusion matrix as comparisons of dates between air photos and Landsat scenes. Accuracy assessment of historical maps is vital due to the implications of land-cover land-use change within disturbance-modified ecosystems. Biogeochemical-modeled results rely on remote sensing input datasets to derive quantitative estimates of carbon (Potter et al. 1993; Powell et al. 2004).

Table 3.3 Archived aerial photography used in validation of land cover maps, derived from United States Geological Survey National Aerial Photography (http://earthexplorer.usgs.gov), and National Air Photo Library Natural Resources Canada (http://airphotos.NRCan.gc.ca).

Yukon & Northwest Territories

Landsat	Date	Air photo ID	Date	Air photo ID	Date
060011	06/30/88	A26750_152	08/03/85		
061011	07/18/92	A26748_19	08/03/85		
064012	09/04/78	A26724_55	07/10/85		
061012	07/16/00	A31865_112	08/06/04		
067011	07/06/78	A24953_32	07/09/78		
063011	09/19/01	A31863_41	04/08/05	A31872_25	08/17/04
067012	07/06/78	A25776_142	06/25/81		
063012	06/30/92	A27122_151	07/10/87		
063012	08/31/00	A31873_054	08/22/04		

Northern Saskatchewan

Landsat	Date	Air photo ID	Date	Air photo ID	Date
037019	08/30/87	A27626_31	07/12/90		
037019	08/30/87	A27626_22	07/12/90		
042020	09/21/74	A22486_58	08/06/71		
043019	08/05/78	A22508_52	07/06/71	A22510_81	07/19/71
041020	09/11/87	A25930_59	11/08/81		

Southern Saskatchewan & Dakotas

Landsat	Date	Air photo ID	Date	Air photo ID	Date
035025	07/01/88	A27300_021	07/11/88		
038025	07/23/76	A24379_216	05/15/76		
035026	08/11/91	W03711027	08/18/92	W03671148	07/13/91
038026	07/13/78	P800201079	08/24/80	P800205171	08/27/80
038026	07/13/78	P800143093	07/31/80		
039026	09/19/79	P800205072	08/27/80		

Texas Oklahoma Panhandle

Landsat	Date	Air photo ID	Date	Air photo ID	Date
031035	07/08/89	P003462041	04/14/91		
033034	07/13/77	DSD013002	06/24/75	DSD042047	06/13/76
033034	07/13/77	DSD000903	06/20/75		
033035	07/13/77	DSD006070	07/01/75		

Quebec

Landsat	Date	Air photo ID	Date	Air photo ID	Date
013026	08/27/89	A27304_14	06/27/88		
014026	08/12/78	A24060_181	07/29/75		
013027	08/27/89	A27010_104	08/23/86	A26900_152	05/13/86
015027	10/31/75	A24061_99	07/29/75		
015026	05/18/88	A27531_144	07/21/89		
015026	08/21/02	1614248	06/06/03		
017027	06/02/75	A24042_260	07/27/75		

Table 3.3 (continued)

Labrador & Newfoundland

Landsat	Date	Air photo ID	Date	Air photo ID	Date
002026	05/27/75	A24979_12	07/28/78		
003026	07/31/87	A26783_194	08/02/85		
004026	7/14/73	A25876_5	09/05/81		
004026	08/31/90	A26704_42	06/25/85	A26784_21	08/03/85
004027	08/31/90	A26706_137	06/25/85		
005024	08/06/90	A31461_11	06/28/85		
005026	08/09/91	A26704_136	06/24/85	A26782_72	8/04/85
005026	08/09/91	A26704_205	06/24/85		
005027	06/04/74	A25808_73	07/17/81	A26340_71	08/01/83

Table 3.4 IKONOS imagery used in validation of land cover maps.

Northern Saskatchewan

Landsat	Date	IKONOS ID	Date	IKONOS ID	Date
037019	09/29/01	po_203787	07/04/01		

Southern Saskatchewan

Landsat	Date	IKONOS ID	Date	IKONOS ID	Date
035026	07/08/99	po_92042	05/02/02	po_92469	05/2/02

Texas Oklahoma Panhandle

Landsat	Date	IKONOS ID	Date	IKONOS ID	Date
030035	07/05/99	po_91921	05/06/02		
031035	05/11/00	po_38124	05/23/00	po_47261	08/27/00

Quebec

Landsat	Date	IKONOS ID	Date	IKONOS ID	Date
015026	08/21/02	po_20381	06/06/03		

Labrador & Newfoundland

Landsat	Date	IKONOS ID	Date	IKONOS ID	Date
003026	10/01/01	po_20535	09/16/03		

Figure 3.3 Example of validation efforts from Newfoundland. (A) A black and white geo-referenced digital air photo was obtained from the Canadian Government (id A26784_21, 8/03/1985). (B) A low altitude oblique aerial photograph that I took with the GPS coordinates of the location of the camera. (C) A Landsat multi-spectral image using bands 4, 5, and 3 to represent red, green, and blue colors, respectively (path 4 row 26, 8/05/2001).

3.2.3 Ancillary Data

Once the primary cause of land cover change was identified with Landsat regional analysis, ancilary fire, logging, agriculture production, temperature, and precipitation data were used to investigate these factors as possibly contributing to NDVI trends within the areas studied. Fire and logging extent datasets were derived from the Canadian forest service (NRC 2007) and were reported annually by province in hectares. A fire database from the boreal ecosystem-atmosphere study (BOREAS) that spans from 1945 to 1996 was also used (Sellers et al. 1997). Agriculture production data were derived from the United States Department of Agriculture (USDA) National Agriculture Statistics Service (NASS) (USDA 2007) for areas selected for study in the U.S. Data were reported by county, crop type, and production method.

Influences of temperature and precipitation were investigated with daily meteorological station data (where available) from the Meteorological Service of

Canada (MSC) in regions with NDVI trends with no land cover change (MSC 2007). Analyses were performed to investigate whether drought, or a change in growing season length had occurred. The beginning of the growing season was calculated as the first appearance of five consecutive days with the daily average surface temperature, $T = (T_{max} + T_{min}) / 2$, above 5° C and the end of the growing season as the last occurrence of five consecutive days of temperature with $T >$ 5° C (Feng and Hu 2004; Frich et al. 2002).

3.3 Results

NDVI anomalies in the AVHRR data revealed six areas for investigation with high-resolution data to evaluate land-cover land-use change. Six contiguous regions based on two assumptions: (I) A contiguous region greater than 2,000 km^2 has an NDVI trend greater than 0.1 from selected observational periods and; (II) High resolution remote sensing data and corresponding validation data were available for intensive analysis for the entire AVHRR record. Six regions were selected that met these criteria: (1) the Mackenzie River Delta; (2) Northern Saskatchewan; (3) Southern Saskatchewan; (4) Oklahoma Panhandle; (5) Southern Quebec; and (6) Newfoundland (Figure 3.4). Four areas that experienced large-scale NDVI trends were not investigated due to a lack of high-resolution remotely sensed data (Northern Quebec, Labrador, South Eastern Nunavut, and Northern Manitoba).

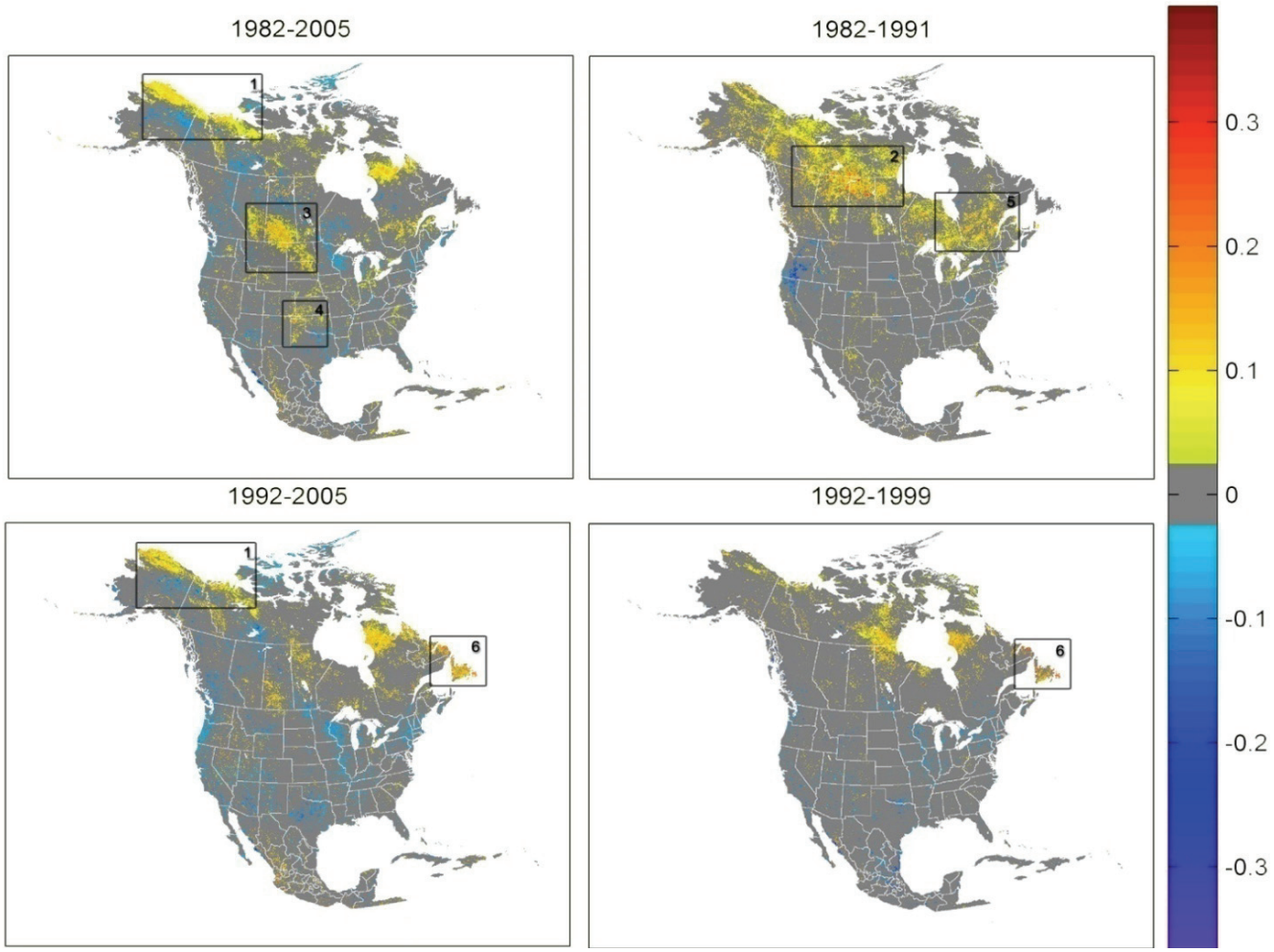

Figure 3.4 May to September annual AVHRR NDVI trends for selected periods between 1982 and 2005. Areas were selected for more detailed study where NDVI increases were greater than 0.1 NDVI units for the various time periods for regions > 2,000 km^2 and high resolution remote sensing and ground data were available. Six regions met these criteria among 4 different time periods: (1) The Mackenzie River Delta area; (2) Northern Saskatchewan; (3) Southern Saskatchewan; (4) the Oklahoma Panhandle and adjacent areas; (5) Southern Quebec; and (6) Newfoundland.

3.3.1 The Arctic Slope of Alaska, Yukon, and Northwest Territory

A large area of North America bordering the Arctic Ocean in Alaska and Canada, roughly from 60° to 70° N exhibited a zone of NDVI increases from 1982 to 2005. The Mackenzie River Delta area of Canada was selected for investigation, because numerous high-resolution aerial photographs are available for the entire AVHRR record.

The Mackenzie River Delta study region is located in the Arctic Circle where extreme variations in solar insulation and temperature are the norm. Winter extends nine months in this region, and the surrounding landscape is underlain with continuous permafrost while the land cover consists primarily of alpine tundra to open lichen woodland (Archibold 1995). The river delta has a unique ecosystem to neighboring lands due to the northward flow of warm waters to the Arctic Circle. The depth of the permafrost controls nutrient availability and vegetative cover while temperature exerts considerable control over permafrost depth and the active organic soil layer in surrounding ecosystems (Pavelsky and Smith 2004). Chen et al. (2003), noted a decline of 22% in the permafrost zone from 1940 to 1995 in northwestern Canada. Higher temperatures have increased the active soil layer depth and extent while extending growing season length.

This area is located just above the Northern limit of the North American boreal forest and has little anthropogenic disturbance. The largest concentration

of human settlement in the region is Inuvik (68°18'N, 133°30'W), which has 3,600 residents (Figure 3.5). The lack of human occupation implied the observed anomaly was not associated with human alterations of land cover but the change in vegetation was related to climate.

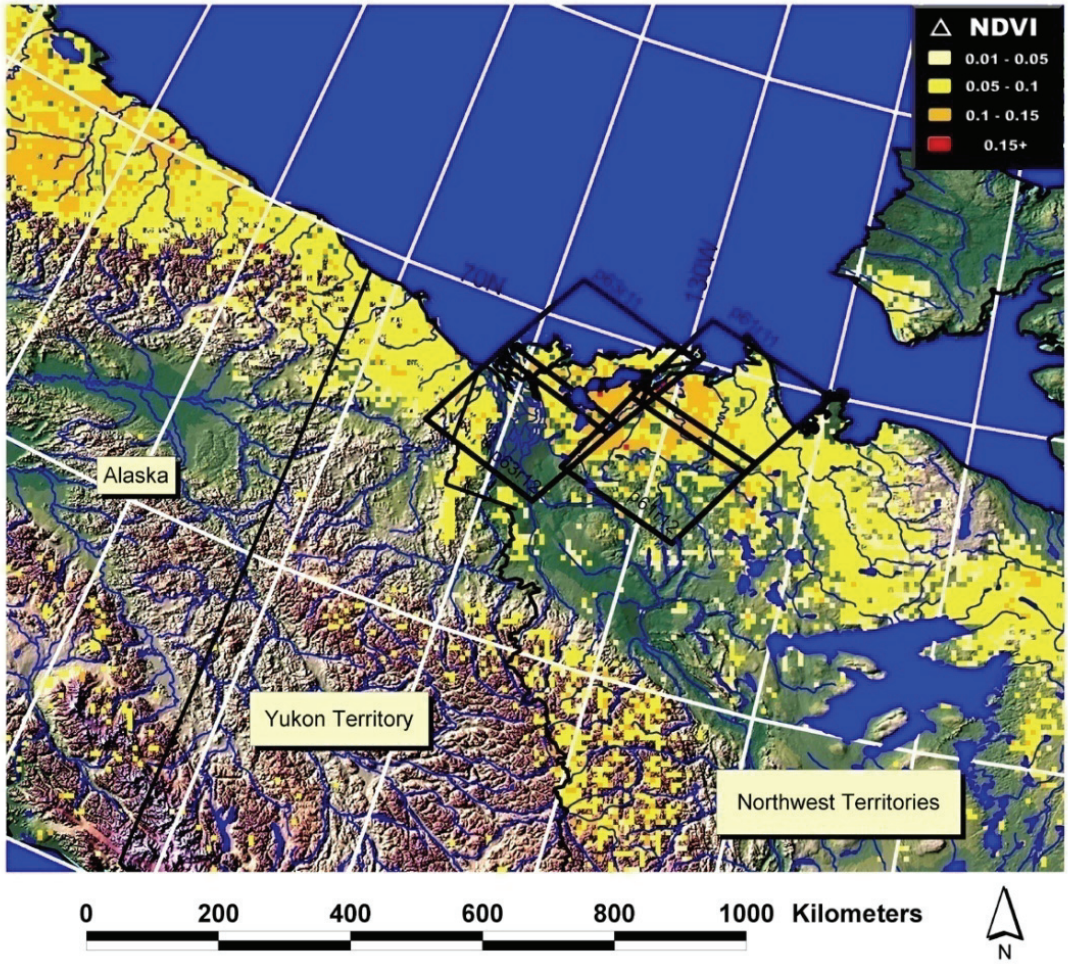

Figure 3.5 Yukon and Northwest Territories study region with Landsat scenes used in land cover investigation of the trend (Δ) in NDVI.

3.3.1.1 Land Cover

Land cover results for this region indicated minor changes in vegetation cover from 1976 to 2000. Maps contained ~80,000 km^2 and dwarf trees and

shrubs increased by ~720 km^2 (+ < 1% change in area), short vegetation grassland declined ~950 km^2 (-1% change in area), and water extent changed by ~400 km^2 (+ < 1% change in area) (Figure 3.6, A and B). The largest event was a fire that burned ~710 km^2, reducing vegetation to barren lands (+ < 1% in area). Map accuracy ranged from 92.8% to 94.5% (Table 3.5).

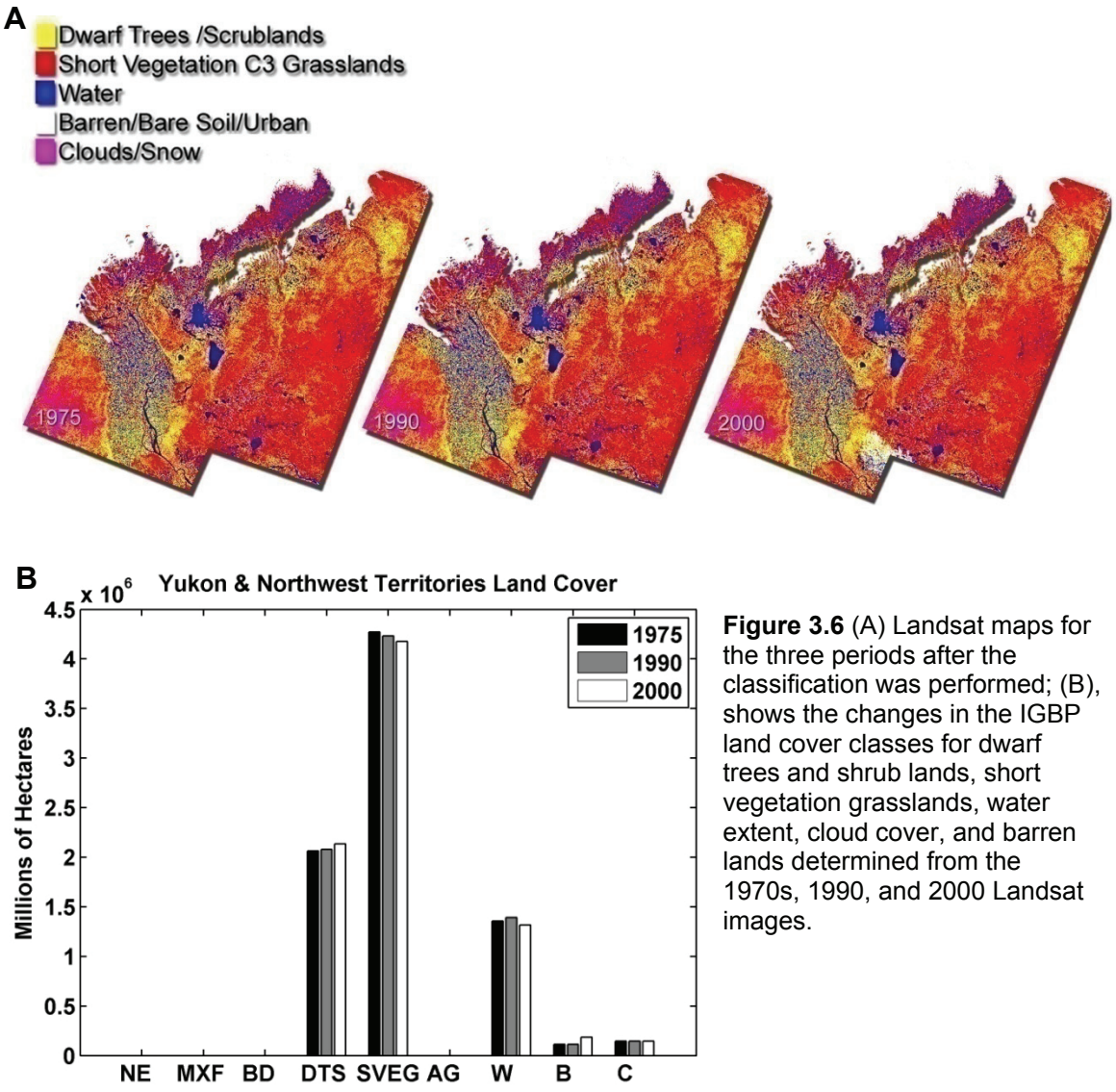

Figure 3.6 (A) Landsat maps for the three periods after the classification was performed; (B), shows the changes in the IGBP land cover classes for dwarf trees and shrub lands, short vegetation grasslands, water extent, cloud cover, and barren lands determined from the 1970s, 1990, and 2000 Landsat images.

Table 3.5 Error Matrices for Yukon.

Air Photo & IKONOS Reference Data		*Ne*	*Mbn*	*Bd*	*Dts*	*Sveg*	*Ag*	*W*	*B*	*C*	Map %
MSS	*Ne*	0	0	0	0	0	0	0	0	0	0.0
Mapped Data	*Mbn*	0	0	0	0	0	0	0	0	0	0.0
	Bd	0	0	0	0	0	0	0	0	0	0.0
	Dts	0	0	0	1494	161	0	33	0	0	26.0
	Sveg	0	0	0	118	1096	0	46	248	0	53.8
	Ag	0	0	0	0	0	0	0	0	0	0.0
	W	0	0	0	17	4	0	5281	0	0	17.1
	B	0	0	0	0	0	0	0	262	0	1.4
	C	0	0	0	0	0	0	0	0	0	1.8
Producer's Accuracy		-	-	-	91.7	86.9	-	98.5	51.4	0	-
User's Accuracy		-	-	-	88.5	72.7	-	99.6	100.0	-	-
Sample %		-	-	-	18.4	13.5	-	64.9	6.3	-	-
Overall Accuracy 92.8%											
Kappa Statistic 87.4%											
TM	*Ne*	0	0	0	0	0	0	0	0	0	0.0
Mapped Data	*Mbn*	0	0	0	0	0	0	0	0	0	0.0
	Bd	0	0	0	0	0	0	0	0	0	0.0
	Dts	0	0	0	376	620	0	9	0	0	26.1
	Sveg	0	0	0	194	9269	0	19	248	0	53.2
	Ag	0	0	0	0	0	0	0	0	0	0.0
	W	0	0	0	0	38	0	19967	0	0	17.5
	B	0	0	0	0	22	0	0	262	0	1.4
	C	0	0	0	0	0	0	0	0	0	1.8
Producer's Accuracy		-	-	-	66.0	93.2	-	99.8	51.4	-	-
User's Accuracy		-	-	-	37.4	95.3	-	99.8	92.3	-	-
Sample %		-	-	-	1.3	31.0	-	66.8	1.7	-	-
Overall Accuracy 96.3%											
Kappa Statistic 92.2%											
ETM	*Ne*	0	0	0	0	0	0	0	0	0	0.0
Mapped Data	*Mbn*	0	0	0	0	0	0	0	0	0	0.0
	Bd	0	0	0	0	0	0	0	0	0	0.0
	Dts	0	0	0	2648	145	0	0	0	0	26.8
	Sveg	0	0	0	233	2611	0	10	175	0	52.5
	Ag	0	0	0	0	0	0	0	0	0	0.0
	W	0	0	0	0	0	0	4454	0	0	16.6
	B	0	0	0	25	0	0	0	326	0	2.3
	C	0	0	0	0	0	0	0	0	0	1.8
Producer's Accuracy		-	-	-	91.1	94.7	-	99.8	65.1	-	-
User's Accuracy		-	-	-	94.8	86.2	-	100.0	92.9	-	-
Sample %					26.4	26.0	-	44.4	5.0	-	-
Overall Accuracy 94.5%											
Kappa Statistic 91.8%											

Landsat imagery was limited in applicability to define the spectral differences between short vegetation grasslands and dwarf trees and shrubs. This excluded the ability to define subtle vegetative growth on a decadal basis. Extensive multi-temporal high-resolution data are needed to evaluate if expansion of shrub lands has occurred. This remote area has incurred limited human disturbance implying that alterations to this ecosystem have been induced by abiotic factors. Plant growth increased as warmer temperatures extend the growing season length (Figure 3.7).

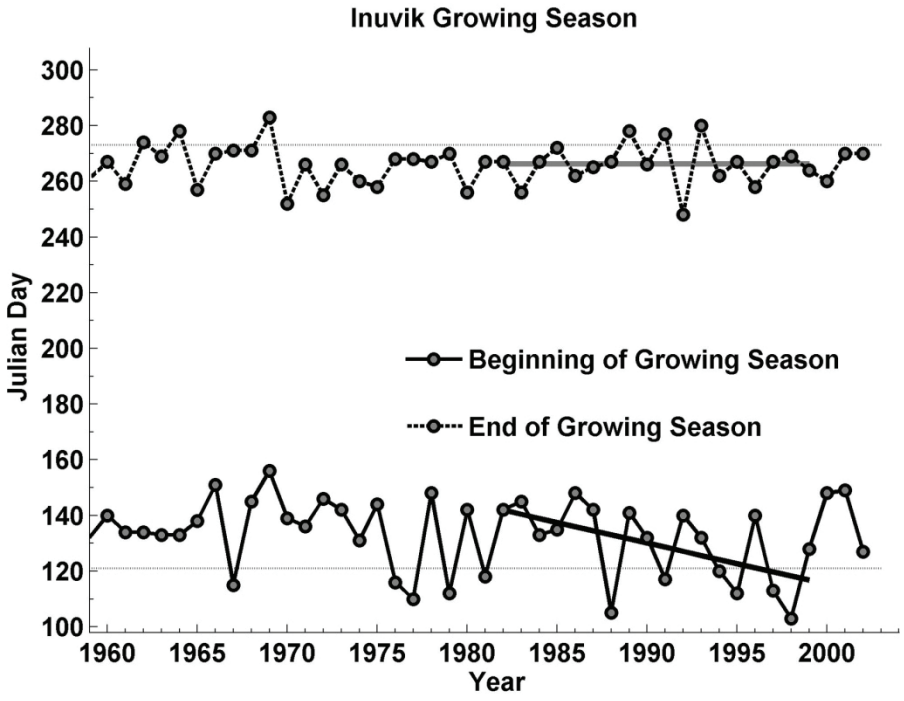

Figure 3.7 The growing season length calculated from 1960-2002 from meteorological station data located in Inuvik.

3.3.1.2 Climate

Higher surface temperatures during late winter and early spring have been reported in the high Arctic of North America (Hansen et al. 1999). I found an increase in warmer temperatures was associated with a corresponding increase

in NDVI in this region. Warming resulted in an earlier start of the growing season. Temperatures increased ~2º ± 1º from March to August while the beginning of growing season was ~15 days earlier (from mid May to early May) over the same 1982-1999 time period. Warming in this region enhanced May to August NDVI by permitting a longer growing season (Figure 3.8 and 3.9). Results captured an increase in photosynthetic capacity (duration and amplitude) of vegetation due to longer available periods of productive growth due to earlier onset of spring. An in depth quantitative analysis of climate influence to vegetation productivity is beyond the scope of this work; these phenomena will be investigated with simulation modeling in the future. As suggested by Sturm et al., (2005), abiotic and/or sun-target-sensor influences have altered vegetation dynamics in this region.

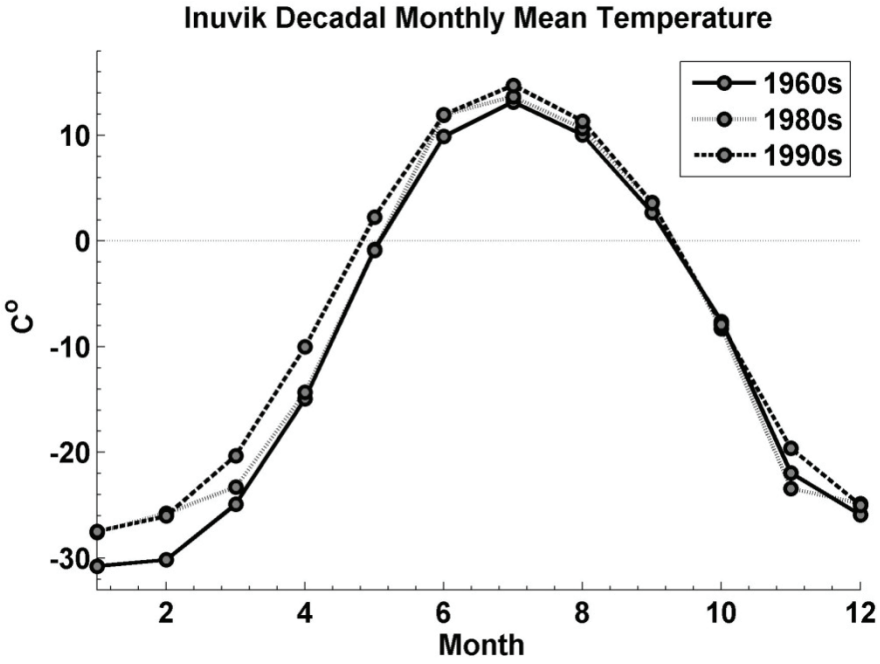

Figure 3.8 The mean monthly Inuvik decadal surface air temperature.

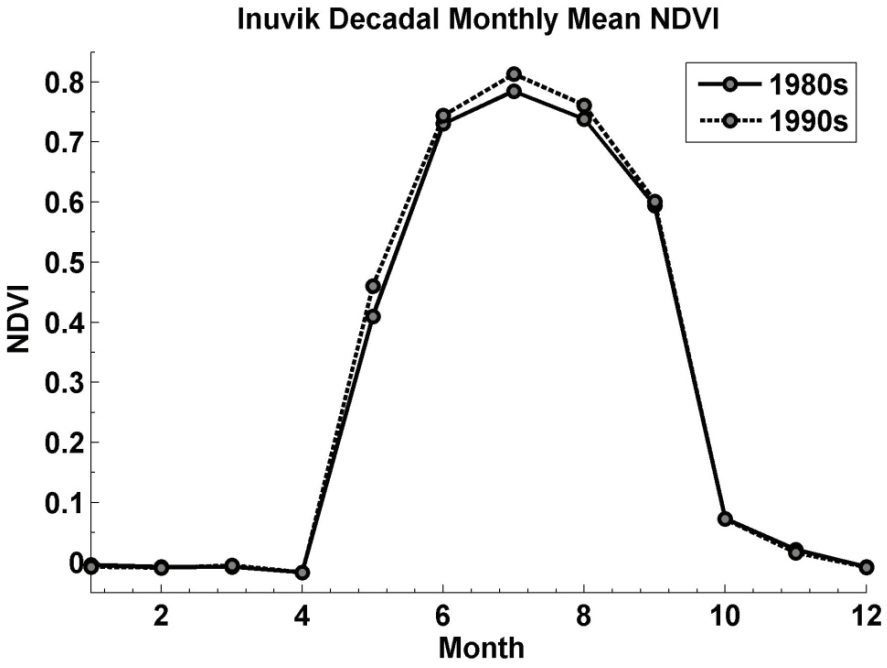

Figure 3.9 The resultant NDVI increases during the growing season.

3.3.2 Northern Saskatchewan

The Northern Saskatchewan study region lies on the boundaries of two ecoregions, the closed boreal forest and the open lichen woodland. The division between closed spruce-feather moss boreal forests and open lichen woodland is abrupt in the northern boundaries of the provinces of Manitoba and Saskatchewan. This boreal ecoregion is a small portion of the North American boreal forest that covers ~10° of latitude, but it is a floristically poor biome (Jarvis et al. 2001). Two species are nearly ubiquitous in this region, white spruce (*P. glauca*) and black spruce (*P. marinana*) with other species of larch or tamarack (*L. laricina*), balsam fir (*A. balsamea*), balsam poplar (*P. banksiana*), trembling aspen (*P. tremuloides*) and white or paper birch (*B. papyrifera*) are intermixed depending on the age of the current successional state. Extensive peat bogs

and muskegs sporadically dot the landscape among dense stands of conifers as remnants of glacial times of the past (Figure 3.10).

There is little human interference with the land cover in this region because access is limited. However, fire is one of the most important disturbances in this region (Wein and MacLean 1983; Wright and Heinselman 1973). Boreal forests are very productive following fire events. Amiro et al., (2000), found that aboveground NPP increased linearly for the first 15 years following forest fires in Canada and steady states of aboveground NPP were not present until 20+ years after fires. Carbon storage in this ecosystem is closely related to fire history, as fire is a major disturbance that alters community structure and vegetative productivity.

The average fire frequency is ~60 years depending on forest type in North American boreal forests (Archibold 1995). Fire frequency in the boreal zone has increased due to increased warming and associated drying over the past 20 years (Amiro et al. 2001). Typically 9,000-10,000 fires burn in coniferous forest across Canada, which annually consume more than 20,000 km^2 or 0.6% of the forested area (Higgins and Ramsey 1992). This variation in stand age with fire revisit times can be seen in conifer energetics, as peak photosynthesis has been observed in NDVI to vary throughout the life cycle of boreal stands (Kasischke 1997).

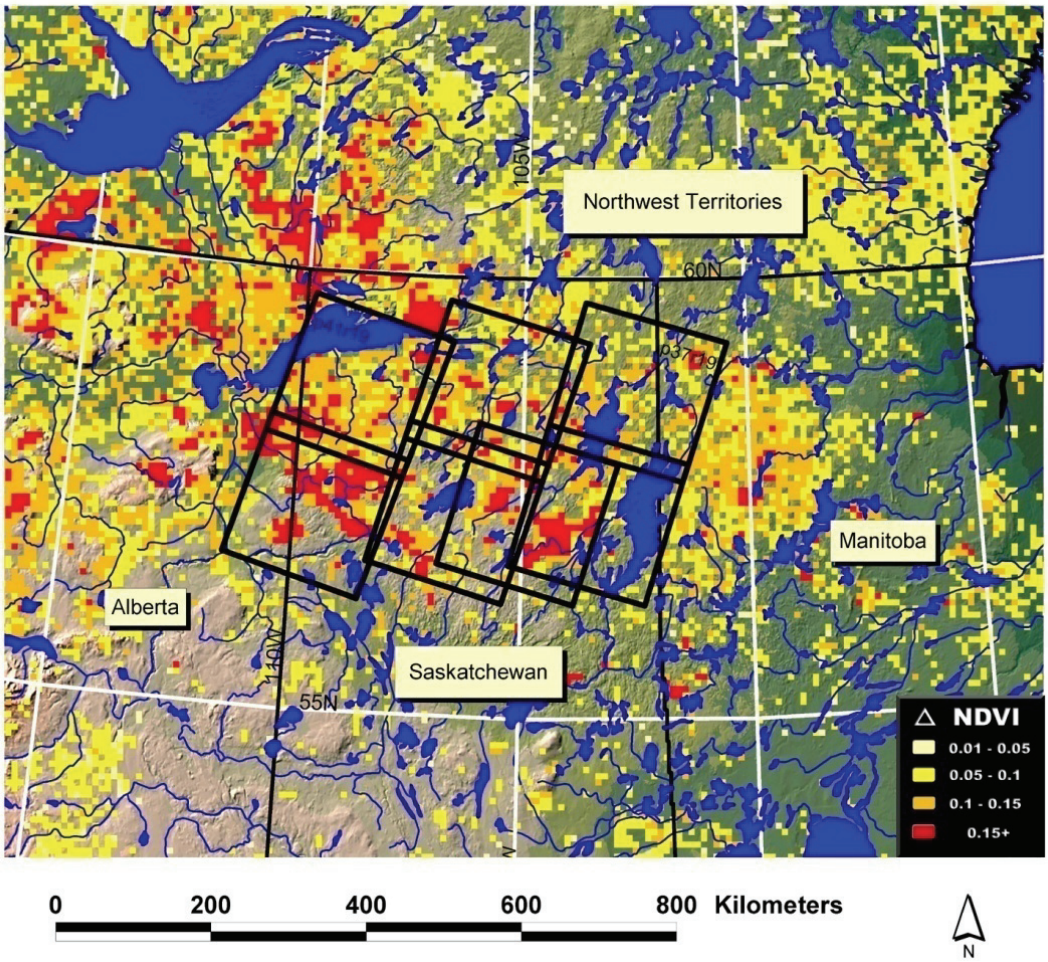

Figure 3.10 A diagrammatic representation of the Northern Saskatchewan study area with trend (Δ) in NDVI 1982-1991, and Landsat scene locations.

3.3.2.1 Land Cover

Land cover analyses for this region indicate marked changes in vegetation cover. Maps contained ~160,000 km^2 with the largest changes occurring between short vegetation grasslands and needle leaf evergreen forests. During the study, needleleaf evergreen forests declined by ~13,000 km^2 (-8% change in area), dwarf trees and shrubs declined by ~8,000 km^2 (-5% change in area), while short vegetation grasslands increased by ~2,000 km^2 (+13% change in

area) (Figure 3.11 A, B, C, and D). Map accuracy ranged from 89.9% to 97.6% (Table 3.6). Extensive wildfire burn scars were observed in Landsat TC data as decreases in brightness, greenness, and wetness. All anniversary scene pairs over the thirty-year period revealed extensive burn scars from boreal fires. No other apparent changes in land cover or land use were observed, as this region is located in a remote region outside the impact zone of anthropogenic land use change. Ancillary data from the Canadian Forest Service indicated extensive burn scars in this region. Recently burned forests were found with recovering young forest stands to be the cause for the observed NDVI anomaly.

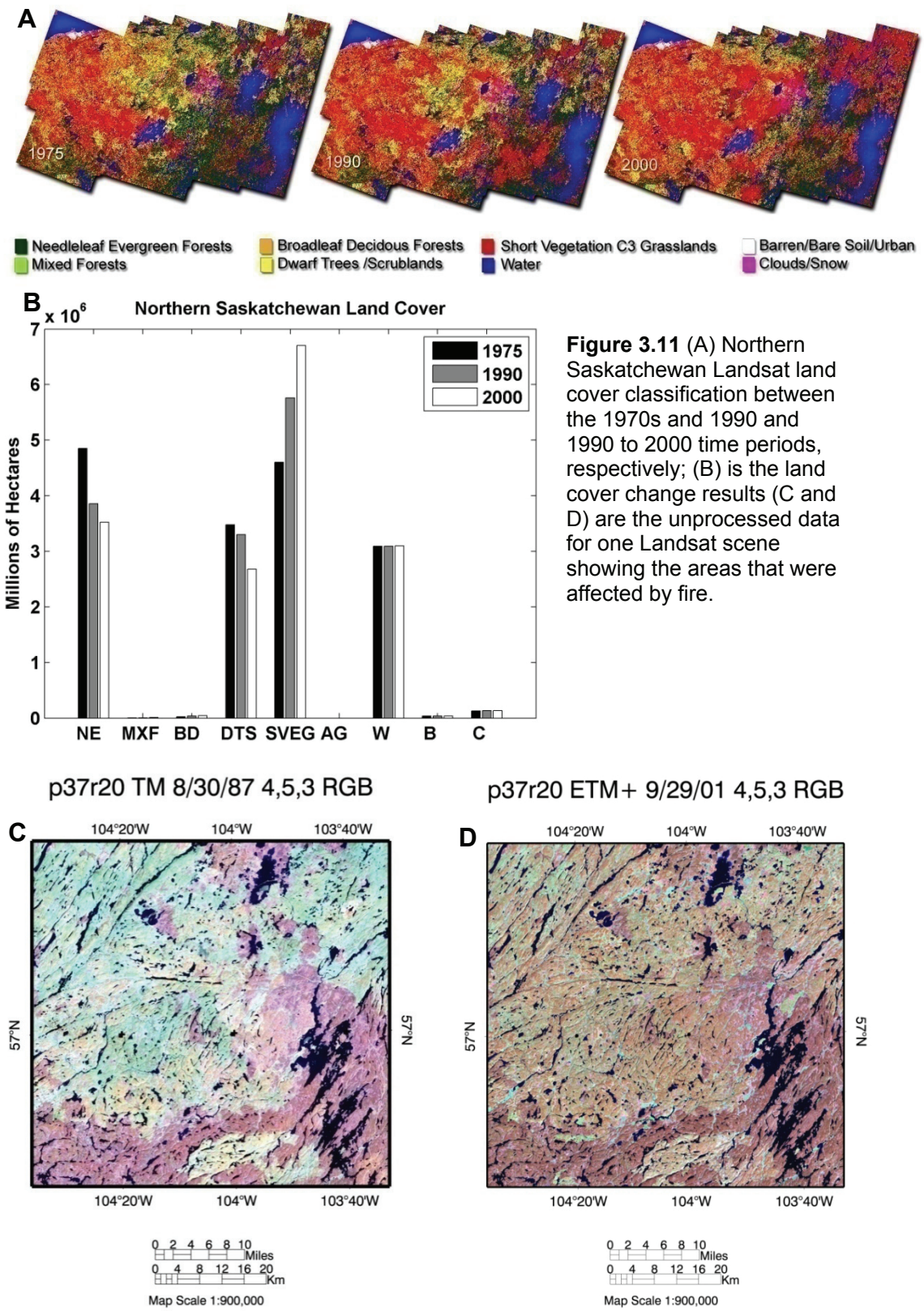

Figure 3.11 (A) Northern Saskatchewan Landsat land cover classification between the 1970s and 1990 and 1990 to 2000 time periods, respectively; (B) is the land cover change results (C and D) are the unprocessed data for one Landsat scene showing the areas that were affected by fire.

Table 3.6 Error Matrices for Northern Saskatchewan.

Air Photo & IKONOS Reference Data		*Ne*	*Mbn*	*Bd*	*Dts*	*Sveg*	*Ag*	*W*	*B*	*C*	Map %
MSS	*Ne*	399	0	0	125	5	0	0	0	0	29.9
Mapped Data	*Mbn*	0	0	0	0	0	0	0	0	0	0.0
	Bd	0	0	0	0	0	0	0	0	0	0.2
	Dts	13	0	0	426	28	0	0	0	0	21.4
	Sveg	5	0	0	26	149	0	0	0	0	28.4
	Ag	0	0	0	0	0	0	0	0	0	0.0
	W	2	0	0	0	0	0	836	0	0	19.1
	B	0	0	0	0	0	0	0	0	0	0.2
	C	0	0	0	0	0	0	0	0	0	0.8
Producer's Accuracy		95.2	-	-	73.8	81.9	-	100.0	-	-	-
User's Accuracy		75.4	-	-	91.2	82.8	-	99.8	-	-	-
Sample %		23.1	-	-	31.9	10.1	-	46.2	-	-	-
Overall Accuracy 89.9%											
Kappa Statistic 89.7%											
TM	*Ne*	3694	0	0	125	159	0	0	0	0	23.8
Mapped Data	*Mbn*	0	0	0	0	0	0	0	0	0	0.0
	Bd	0	0	0	0	0	0	0	0	0	0.2
	Dts	19	0	0	426	89	0	0	0	0	20.3
	Sveg	72	0	0	26	1315	0	0	0	0	35.5
	Ag	0	0	0	0	0	0	0	0	0	0.0
	W	1	0	0	0	38	0	2114	0	0	19.1
	B	0	0	0	0	22	0	0	0	0	0.2
	C	0	0	0	0	0	0	0	0	0	0.8
Producer's Accuracy		97.6	-	-	73.8	81.0	-	100.0	-	-	-
User's Accuracy		92.9	-	-	79.8	93.1	-	98.2	-	-	-
Sample %		50.2	-	-	7.6	21.5	-	28.0	-	-	-
Overall Accuracy 97.6%											
Kappa Statistic 89.7%											
ETM	*Ne*	3538	0	0	31	161	0	0	0	0	21.7
Mapped Data	*Mbn*	0	0	0	0	0	0	0	0	0	0.0
	Bd	0	0	0	0	0	0	0	0	0	0.1
	Dts	7	0	0	95	151	0	0	0	0	16.5
	Sveg	57	0	0	24	1993	0	0	0	0	41.3
	Ag	0	0	0	0	0	0	0	0	0	0.0
	W	0	0	0	0	0	0	2126	0	0	19.1
	B	0	0	0	0	0	0	0	0	0	0.2
	C	0	0	0	0	0	0	0	0	0	0.8
Producer's Accuracy		98.2	-	-	63.3	86.5	-	100.0	-	-	-
User's Accuracy		94.9	-	-	37.5	96.1	-	100.0	-	-	-
Sample %		46.5	-	-	1.9	29.7	-	27.4	-	-	-
Overall Accuracy 94.7%											
Kappa Statistic 92.0%											

3.3.2.2 Fire and Logging

Large fires (>200 hectares) were noted in 1980, 1981, 1993, 1994, and 1995 (Figure 3.12), while area logged for all of Saskatchewan has remained relatively stable, fluctuating between 160 km^2 and 250 km^2 per year throughout the province. The most extensive fire occurred in 1981, burning over 22,455 km^2 or over three hundred fifty, 8 km^2 AVHRR pixels across the entire province. The second most extensive fire event occurred in 1995 burning over 16,400 km^2.

A fire event spatial database from the BOREAS was used as a surrogate to the Landsat land cover evaluation (Sellers et al. 1997). A similar method to Domenikiotis et al., (2002) was used to verify the spatial extent of fire events. Similar results to the Landsat data in annual fire extent support that fire recovery is producing increases in NDVI. A majority of the large fire events occurred in Northern Saskatchewan. Large-scale wildfires are a natural part of this ecosystem reoccurring at intervals that are started from a number of different means and can be observed in NDVI data (Kasischke 1997). Fire recovery in this study region was the primary factor in the observed increases in NDVI. Higher near infrared reflectance values in Landsat data were observed for recovering vegetation in burned regions than for forests that were not burned.

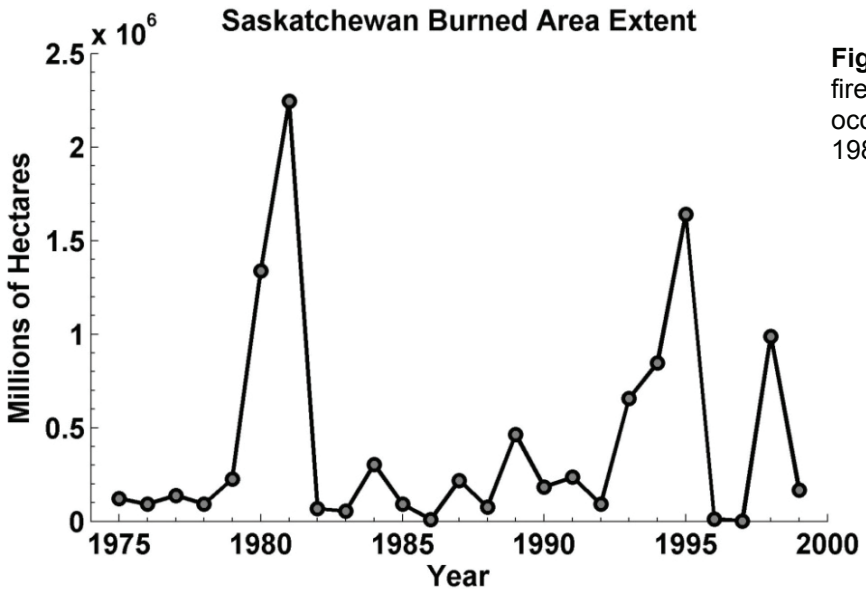

Figure 3.12 Extensive fires (> 1 million hectares) occurred in years 1980-1981 and 1995.

Growth is often limited in coniferous forest by mineral poor soils with productivity controlled by nutrient cycling (Cole and Rapp 1981). Deep beds of feather mosses of Schreber's feather moss (*P. schreberi*) and mountain fern moss (*H. splendens*) typically form the understory of forests within this study area. These mosses insulate the ground and reduce decomposition because of low soil temperatures. Fires release nutrients stored in mosses much faster than decomposition and therefore enhance growth at post fire sites (Auclair et al. 1976; vanCleve et al. 1983). Albedo declines in burn scar sites and this can increase the soil temperature by absorbing more solar radiation. AVHRR NDVI anomalies observed from 1982 through 1991 were from these ecosystems that were in recovery from the extensive fires that occurred in 1980 and 1981. The anomalies observed in this case were not due to direct abiotic influences on productivity; they are attributable to ecosystem recovery and nutrient enhancement from large-scale fire disturbance events.

3.3.3 Southern Saskatchewan & the Dakotas

The Southern Saskatchewan and Dakotas study region lies in the northern boundaries of the Great Plains. This area is commonly referred to as the 'Prairie Pothole' region because of ancient glacial depressions. Several hundred thousand small (< 100 ha), shallow (maximum depth < 5 m) pothole lakes lie in depressions that extend over 776,900 km^2 in the American Midwest and Western Canada (Covich et al. 1997). Stream drainage is primarily absent in this region, and numerous wetlands have formed between mounds of glacial till that dot the landscape. A diverse aquatic ecosystem exists here where playas, pothole lakes, ox-bow lakes, springs, groundwater aquifers, and intermittent and ephemeral streams are responsive to climatic fluctuations (Winter and Rosenberry 1998). Many of the wetlands are underlain by low-permeability glacial till making groundwater exchange slow. This forces these wetlands to be highly dependent upon precipitation for their water supply. Precipitation and evapotranspiration act as the largest forcing on the extent of surface water (Covich et al. 1997; Winter and Rosenberry 1998).

Most of the prairie that existed before human occupation has been replaced with agro ecosystems where vegetation productivity is controlled with fertilizers and irrigation (Goudrian et al. 2001). Agro ecosystems are managed and improved with new technology to produce crops nearer to their maximum physiological potential. Changes in land use in agro ecosystems to enhance productivity are achieved by: extensification (expanding the area of cultivated

land); and/or intensification (increasing the number of cropping cycles sown on a particular area of land or by increasing the yield per unit area), or both (Gregory et al. 1999).

This region is heavily modified by agriculture where upland areas produce primarily sorghum, corn and wheat. During the growing season, precipitation is a limiting factor to growth. Irrigation networks are not extensively developed as this region has enough rainfall to support most crops compared to the Southern High Plains. Droughts are common throughout the high plains. Trenberth et al., (1988), noted a drought in 1988 in the northern and eastern high plains; this was the only climatic event in the region concurrent with the AVHRR NDVI observations. This region is well populated around urban centers and agriculture is the primary land cover type. The NDVI anomaly followed the Missouri Coteau, a large topographic feature that was formed by glacial deposition. It separates two major biogeographic zones of the Great Plains and Central Lowlands (Figure 3.13).

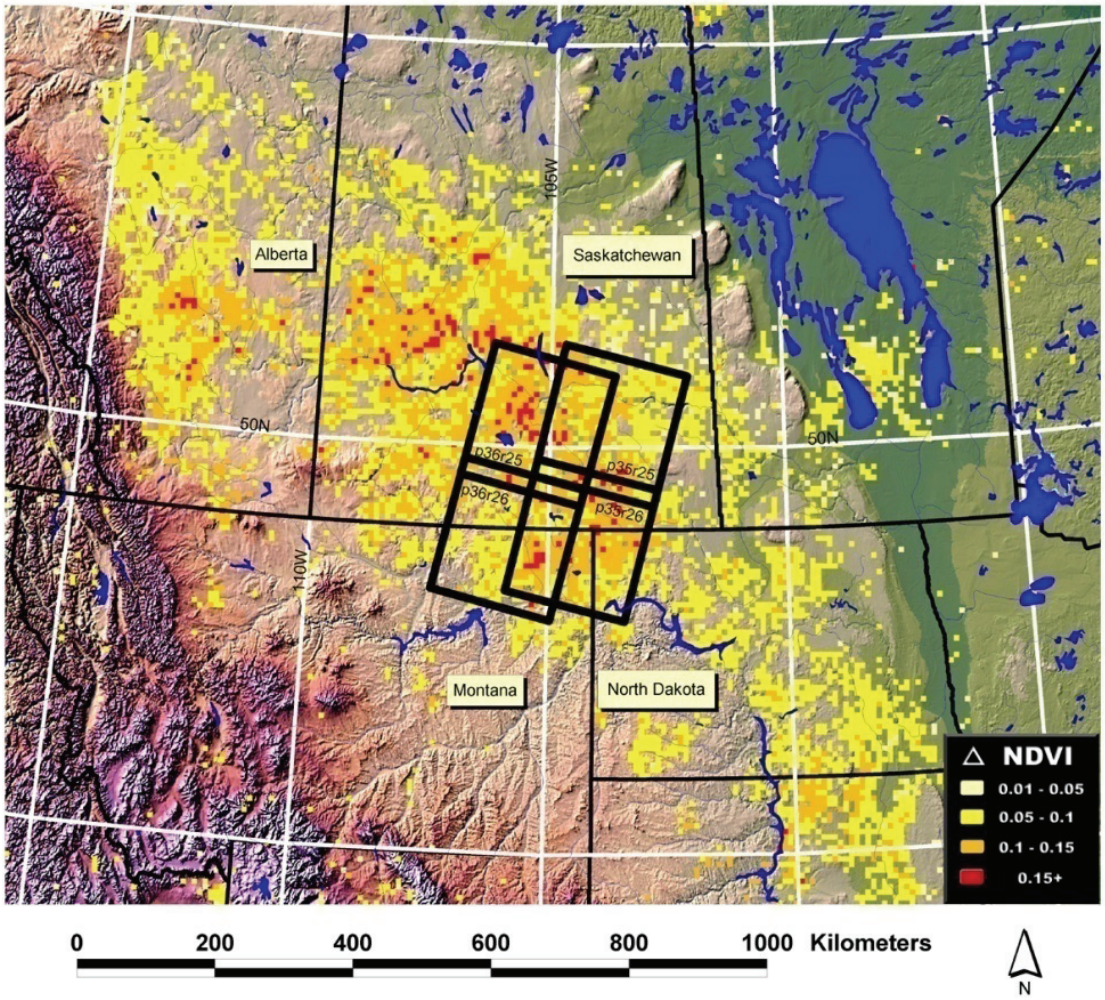

Figure 3.13 The Southern Saskatchewan study region experienced a marked NDVI increase from 1982 to 2005.

3.3.3.1 Land Cover

Land cover results for this region indicated marked changes in vegetation cover. Maps contained ~90,000 km^2, and during observations agriculture fluctuated by ~7,460 km^2 and stabilized near 1970s extent, short vegetation grassland declined ~5,930 km^2 (-11% change in cover type), barren lands increased by ~4,190 km^2 (+50% change in cover type), and water extent changed by ~860 km^2 (+46% change in cover type). Map accuracy ranged from

88.9% to 93.6% (Table 3.7). The drought in 1988 is apparent in the reduction of agriculture extent in the 1990 map and recovery in the 2000 map (Figure 3.14, A and B).

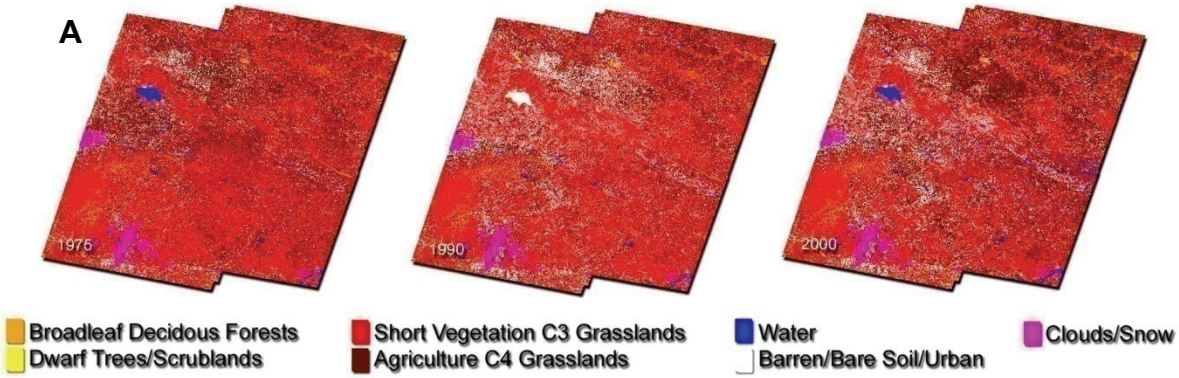

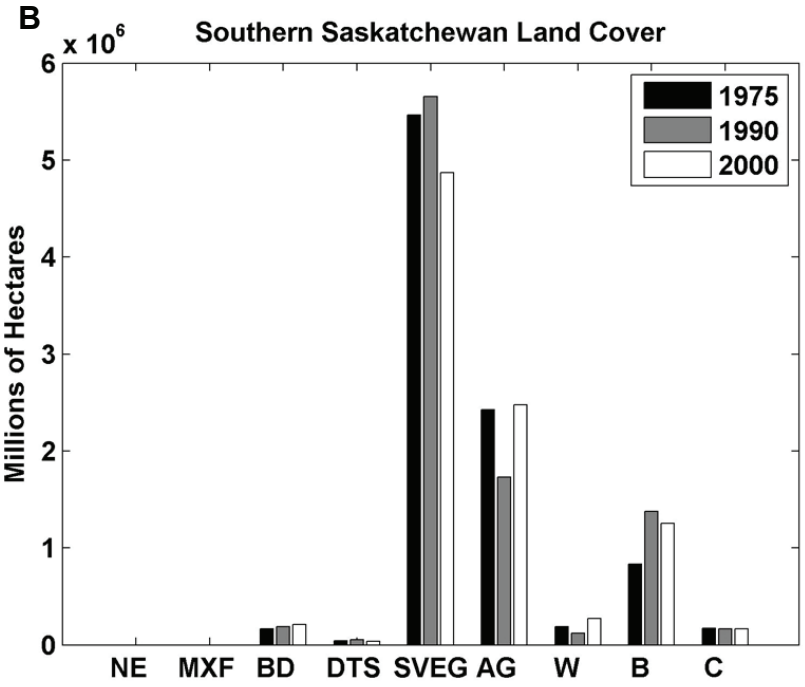

Figure 3.14 (A) The Southern Saskatchewan classified areas from the three GeoCover time periods, (B) shows the changes in land cover change for region.

Table 3.7 Error Matrices for Southern Saskatchewan & Dakotas.

Air Photo & IKONOS Reference Data		*Ne*	*Mbn*	*Bd*	*Dts*	*Sveg*	*Ag*	*W*	*B*	*C*	Map %
MSS	*Ne*	0	0	0	0	0	0	0	0	0	0
Mapped Data	*Mbn*	0	0	0	0	0	0	0	0	0	0
	Bd	0	0	230	65	52	80	0	0	0	1.8
	Dts	0	0	0	98	0	0	4	57	0	0.5
	Sveg	0	0	74	7	11631	952	13	63	0	58.8
	Ag	0	0	83	19	0	7634	1018	69	0	26.1
	W	0	0	0	45	0	0	2163	0	0	2
	B	0	0	4	0	60	133	67	1166	0	9
	C	0	0	0	0	0	0	0	0	0	0
Producer's Accuracy		-	-	58.8	41.9	99.0	86.8	66.2	86.1	-	-
User's Accuracy		-	-	53.9	61.6	91.3	86.5	98.0	81.5	-	-
Sample %		-	-	1.7	1.0	51.2	38.4	14.2	5.9	-	-
Overall Accuracy 88.9%											
Kappa Statistic 82.8%											
TM	*Ne*	0	0	0	0	0	0	0	0	0	0
Mapped Data	*Mbn*	0	0	0	0	0	0	0	0	0	0
	Bd	0	0	169	0	21	35	0	0	0	0.9
	Dts	0	0	0	0	0	0	0	0	0	1.9
	Sveg	0	0	15	0	10253	97	1	256	0	65.1
	Ag	0	0	61	21	364	1785	3	29	0	13.5
	W	0	0	0	0	39	0	10	0	0	0.3
	B	0	0	0	0	28	0	0	2019	0	18.1
	C	0	0	0	0	0	0	0	0	0	0.1
Producer's Accuracy		-	-	69.0	0.0	95.8	93.1	71.4	87.6	-	-
User's Accuracy		-	-	75.1	0.0	96.5	78.9	20.4	98.6	-	-
Sample %		-	-	1.6	0.1	70.4	12.6	0.1	15.2	-	-
Overall Accuracy 93.6%											
Kappa Statistic 86.4%											
ETM	*Ne*	0	0	0	0	0	0	0	0	0	0
Mapped Data	*Mbn*	0	0	0	0	0	0	0	0	0	0
	Bd	0	0	149	16	11	50	0	0	0	2.2
	Dts	0	0	0	0	0	0	0	0	0	0.4
	Sveg	0	0	31	14	3466	288	0	103	0	52.5
	Ag	0	0	25	0	86	2311	0	25	0	26.7
	W	0	0	0	0	0	0	651	0	0	2.9
	B	0	0	2	0	100	5	0	653	0	13.5
	C	0	0	0	0	0	0	0	0	0	1.8
Producer's Accuracy		-	-	72.0	0.0	94.6	89.1	100.0	83.6	-	-
User's Accuracy		-	-	65.9	0.0	90.2	94.4	100.0	85.9	-	-
Sample %		-	-	2.9	0.4	50.7	35.9	9.0	10.8	-	-
Overall Accuracy 91.2%											
Kappa Statistic 86.7%											

No extensive changes in land use were noted in this region and the land cover is primarily composed of agriculture (corn, wheat, sorghum) and rangeland for cattle grazing. Large increases in standing water (prairie potholes or sloughs) were observed in the Landsat record spanning from 1972-2000. Previous fall precipitation has been found to account for 63% to 65% of the variation in the number of wetland basins (Larson 1995). Apparent dramatic increases in wetland size have been recorded from increases in precipitation and may contribute to observed crop yield. Land cover change does not appear to be the motivator for the observed change in vegetation dynamics in this region. Climate impacting dry land agriculture produced the NDVI anomaly.

The drought ended in 1992 and the NDVI AVHRR anomaly appeared during the 1982-2000 period because of recovery (Trenberth et al. 1988; Winter and Rosenberry 1998). Increases in precipitation influenced dry-land crop production in this area by enhancing plant growth. Near infrared reflectance was observed to increase with crop production in Landsat (Figure 3.15, A and B). Corn production was noted to be highly variable and was limited by erratic precipitation patterns (USDA, 2006). Winter et al., (1998), noted conditions to be the wettest on record over the past 130 years, and potentially the past 500 years. The responses of wetlands and agricultural lands to increased precipitation was consistent with the observed NDVI anomalies.

3.3.3.2 Crop Data

To verify if abiotic changes were enhancing vegetation photosynthetic capacity, the National Agriculture Statistics Service (NASS) records were investigated (http://www.nass.usda.gov). Sequential seasonal vegetation indices profiles revealed crop canopy emergence, maturation, and senescence. These measurements have been related to crop condition and yield (Benedetti and Rossini 1993; Boissard et al. 1993; Doraiswamy and Cook 1995; Labus et al. 2002; Rasmussen 1992). Marked increases in wheat production have been noted, which impacted the NDVI.

Yields of wheat increased in three selected Northeastern Montana counties within the NDVI anomaly area. Acres of wheat production rose more than 40% (>400 km^2), and a marked increase was noted after the 1988 drought (Figure 3.15 C). Increases in yield were associated with the increased precipitation after the drought of 1988, returning crop production in this region to its normal state. Adjacent counties to the anomaly region were also investigated and they did not have a marked increase in production. The primary limiting factor to growth in this area was precipitation which increased substantially and caused the observed NDVI anomaly.

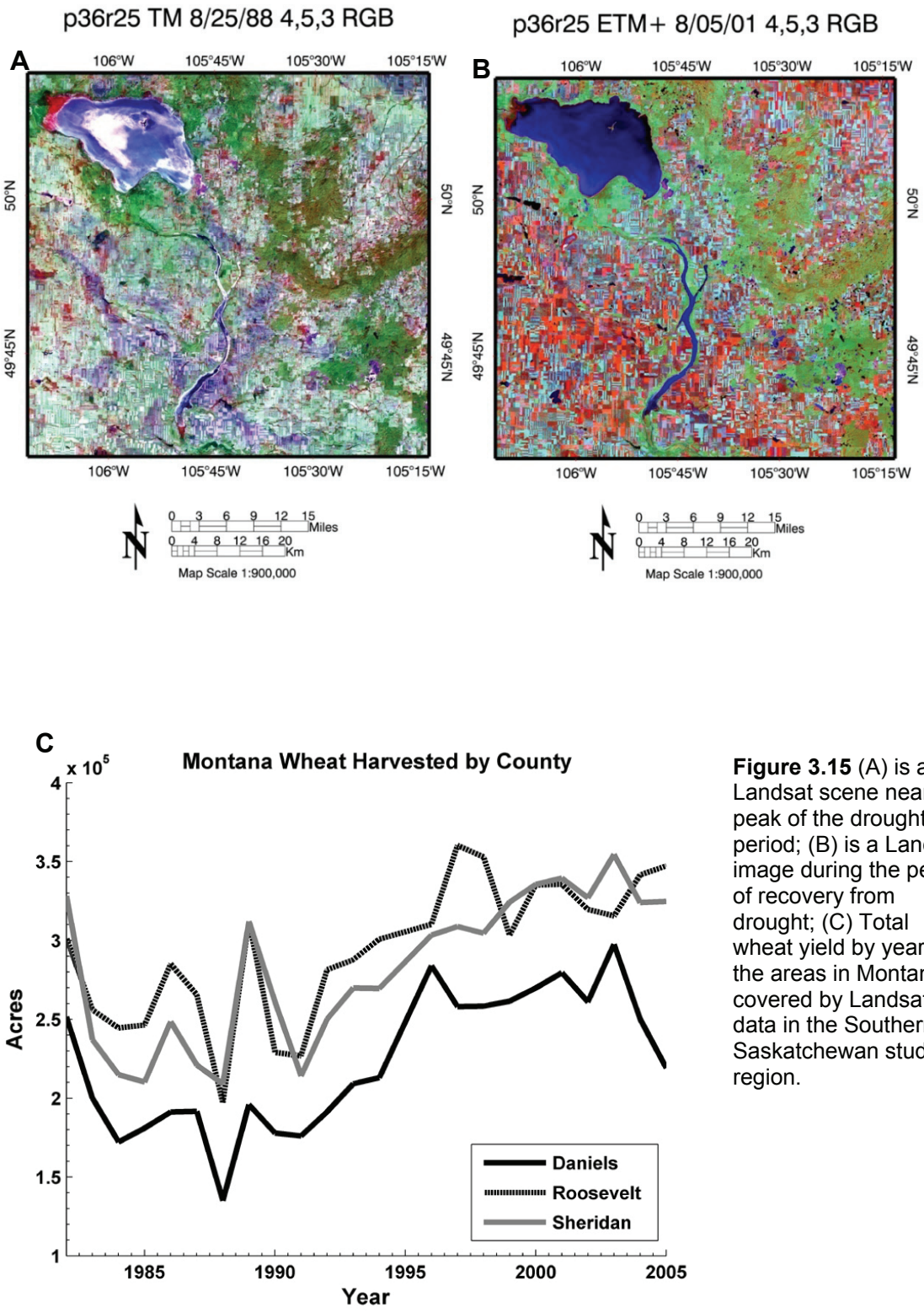

Figure 3.15 (A) is a Landsat scene near the peak of the drought period; (B) is a Landsat image during the period of recovery from drought; (C) Total wheat yield by year for the areas in Montana covered by Landsat data in the Southern Saskatchewan study region.

3.3.4 High Plains

The Oklahoma Panhandle study area is dominated by human land use of agriculture and pasture land. A similar agro ecosystem to the Southern Saskatchewan and Dakotas study region exists here. The landscape consists of flat to irregular plains where sedimentary bedrock is overlain by alluvial deposits. The High Plains have a semi-arid environment where precipitation is the limiting climatic variable to vegetation growth. Precipitation has been found to spatially and temporally modulate NDVI in Kansas (Wang et al. 2001). Over the past 20 years, variations in crop type and production have varied substantially. Although the spatial/temporal heterogeneity of crop type and production can possibly cause the observed change in AVHRR NDVI, this semi arid region is heavily reliant on irrigation to grow more productive crops. Irrigation practices and crop selection were found to explain the NDVI anomalies observed (Figure 3.16).

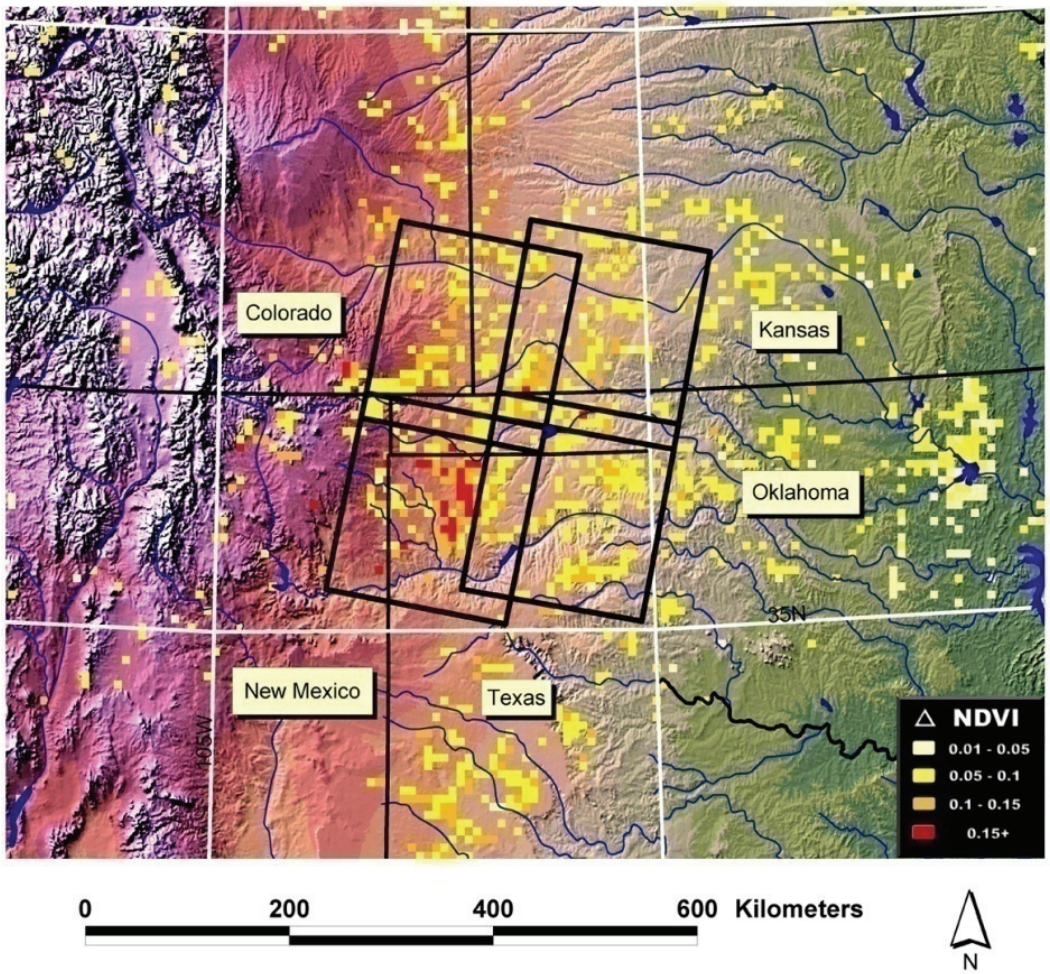

Figure 3.16 An area of expanded irrigated agriculture in the "Panhandle" area of Colorado, Kansas, New Mexico, Oklahoma, and Texas that was identified as having experienced a marked NDVI increase from 1982 to 2005.

3.3.4.1 Land Cover

Marked changes in land cover were found in Northern Texas, Oklahoma, and Kansas. Landsat analysis revealed changes in irrigation extent. ~100,000 km^2 was mapped and during observations agriculture increased by ~2,850 km^2, short vegetation grassland declined ~4,860 km^2, barren lands increased by ~1,650 km^2, and water extent changed by ~160 km^2. Map accuracy ranged from

87% to 91% (Table 3.8). Center pivot agriculture expansion was pervasive throughout this region (Figure 3.17, A and B).

Expansion of irrigated agriculture is largely constrained by access to the Ogallala aquifer. Water in this aquifer is considered a nonrenewable resource because it was formed from melt water from the Rocky Mountains during the Pliestocene era. The High Plains aquifer in this region has experienced a >30% decline in ground water over the past 40 years (Scanlon et al. 2005). Standard practices consist of dry land farming (completely reliant on rain) and furrow and dike irrigation (flooding fields). Using center pivot irrigation over previous irrigation practices has tripled production (biomass) and consumed less water (Opie 2000). Enhanced production was due to the center pivot's ability to more evenly and accurately irrigate fields. Expansion of center pivot irrigation in this region from 1972 – 2000 was marked and evident at the Landsat resolution (Figure 3.17, A and B, and Figure 3.18).

Abiotic variability did not impact vegetation in this region. Normal precipitation ranges 30 – 50 cm of rain a year, when a majority of the crops (corn, wheat and sorghum) require up to 76 – 101 cm (for corn) during the growing season. The deficit of precipitation relative to evaporation ranges from 20 – 160 cm (Covich et al. 1997). Droughts are common in this area and tend to occur every 20 years and can last between 5 – 10 years (Opie 2000). The most severe drought occurred in the 1930's (Great Dust bowl) and the second during the 1950's (Little Dust bowl). More recent droughts, although minor in comparison,

have occurred during the late 1970s, late 1980s and most recently in 1996 (Covich et al. 1997). The 1988 drought did not impact this region with the severity incurred in the north central United States and parts of the North East (Trenberth et al. 1988). Dry spells do not impact the farmers to the extent of previous years because of the development of the high plains aquifer irrigation networks, which now extend for more than 16,000 km^2 (www.hpwd.com). A heavy reliance on ground water has been developed to offset the irregular patterns of precipitation.

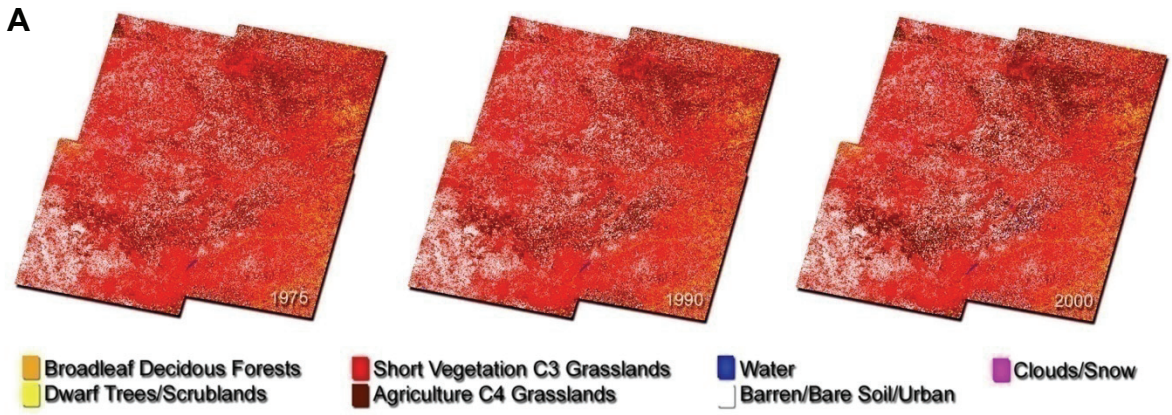

Figure 3.17 (A) The classified Landsat data for three GeoCover time periods, (B) shows the decrease in natural vegetation to irrigated agriculture over the 1970s to 2000 time period.

Table 3.8 Error Matrices for Oklahoma Panhandle.

Air Photo & IKONOS Reference Data		*Ne*	*Mbn*	*Bd*	*Dts*	*Sveg*	*Ag*	*W*	*B*	*C*	Map %
MSS	*Ne*	0	0	0	0	0	0	0	0	0	0
Mapped Data	*Mbn*	0	0	0	0	0	0	0	0	0	0
	Bd	0	0	131	0	0	0	0	0	0	0.9
	Dts	0	0	112	55	0	0	0	0	0	1.9
	Sveg	0	0	31	17	28109	400	0	1100	0	66.8
	Ag	0	0	0	7	119	2434	0	52	0	12.4
	W	0	0	0	0	0	0	16	57	0	0.3
	B	0	0	2	0	1843	57	5	6926	0	17.6
	C	0	0	0	0	0	0	0	0	0	0.1
Producer's Accuracy		-	-	47.5	69.6	93.5	84.2	76.2	85.1	-	-
User's Accuracy		-	-	100.0	39.2	94.8	93.2	21.9	78.4	-	-
Sample %		-	-	0.7	0.2	79.8	7.7	0.1	21.6	-	-
Overall Accuracy 90.8%											
Kappa Statistic 78.9%											
TM	*Ne*	0	0	0	0	0	0	0	0	0	0.0
Mapped Data	*Mbn*	0	0	0	0	0	0	0	0	0	0.0
	Bd	0	0	164	0	1	0	0	0	0	0.9
	Dts	0	0	0	0	0	0	0	0	0	1.9
	Sveg	0	0	24	0	8720	45	0	122	0	65.1
	Ag	0	0	22	0	417	773	0	49	0	13.5
	W	0	0	6	0	0	0	99	0	0	0.3
	B	0	0	0	0	447	1	0	2849	0	18.1
	C	0	0	0	0	0	0	0	0	0	0.1
Producer's Accuracy		-	-	75.9	-	91.0	94.4	100.0	94.3	0	-
User's Accuracy		-	-	99.4	-	97.9	61.3	94.3	86.4	0	-
Sample %		-	-	1.7	-	76.0	6.5	0.8	24.0	0	-
Overall Accuracy 91.7%											
Kappa Statistic 83.1%											
ETM	*Ne*	0	0	0	0	0	0	0	0	0	0
Mapped Data	*Mbn*	0	0	0	0	0	0	0	0	0	0
	Bd	0	0	55	0	0	0	0	0	0	1.0
	Dts	0	0	0	0	0	0	0	0	0	2.0
	Sveg	0	0	47	0	2340	12	0	2110	0	62.0
	Ag	0	0	0	0	0	3255	0	10	0	15.2
	W	0	0	0	0	0	0	22	0	0	0.4
	B	0	0	0	0	50	37	0	10351	0	19.2
	C	0	0	0	0	0	0	0	0	0	0.1
Producer's Accuracy		-	-	53.9	-	97.7	98.5	100.0	83.0	-	-
User's Accuracy		-	-	100.0	-	51.9	99.7	100.0	99.2	-	-
Sample %		-	-	0.6	-	14.9	20.6	0.1	77.8	-	-
Overall Accuracy 87.6%											
Kappa Statistic 77.3%											

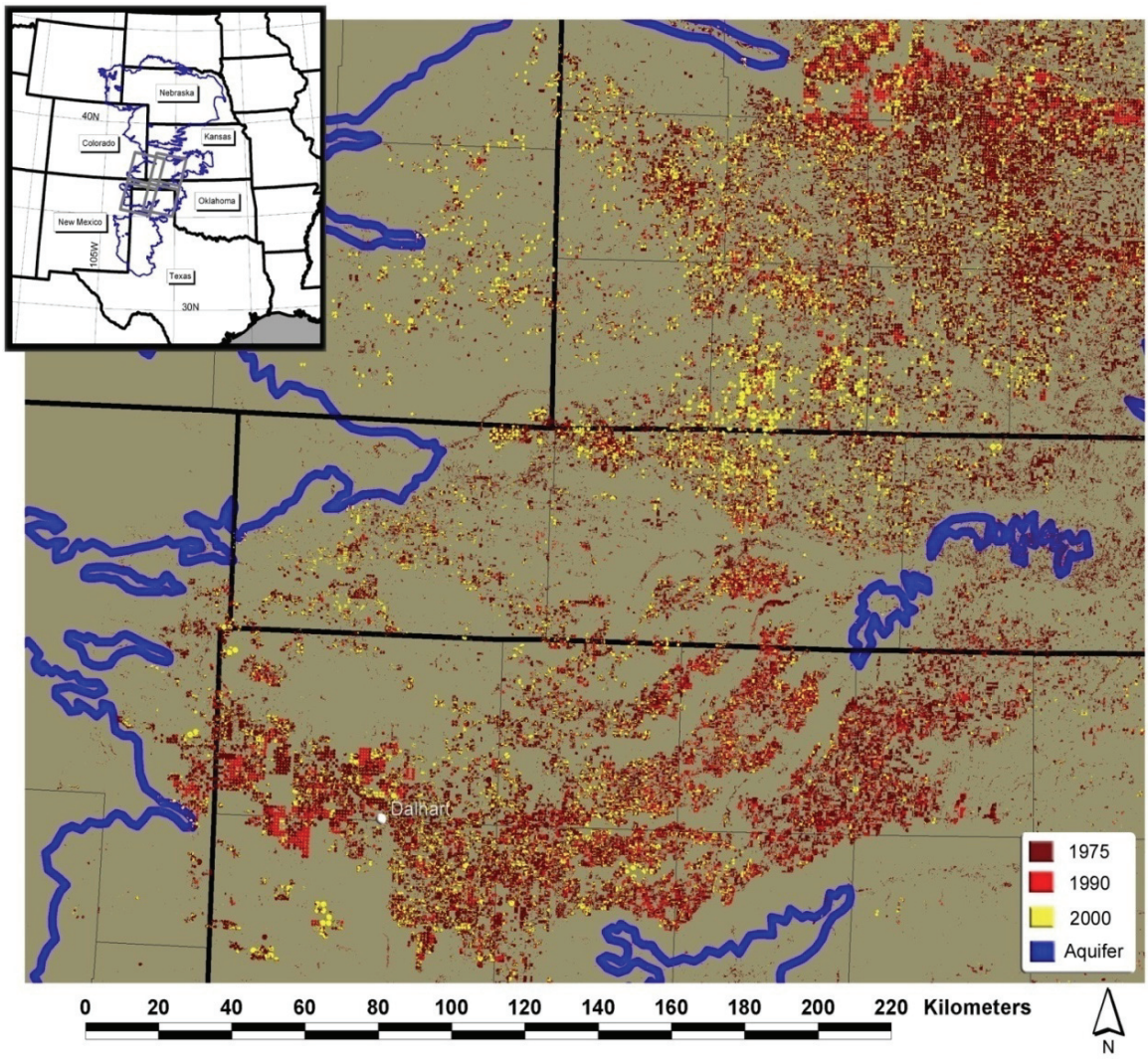

Figure 3.18 A land cover classification of the Oklahoma "Panhandle" and adjacent areas, shows the expansion of irrigated agriculture in this area from 1975 to 2000 based upon the analyses of Landsat data for these 3 time periods. Brown indicates agriculture land in 1975; red represents expansion in 1990, and yellow in 2000. Blue polygons represent the bounds of the Ogallala Aquifer. Investigation of Landsat time series revealed expansion of agriculture land within the bounds of the Ogallala Aquifer; this change in agriculture extent and intensity coincides with the trend in AVHRR NDVI.

3.3.4.2 Crop Data

To verify if abiotic changes were enhancing vegetation growth the NASS records were examined. Alterations in crop production were noted in the agricultural data and a trend similar to the Dakota region appeared to be the

case. Substitution of corn for grain, the dominant crop of the region, showed marked increases in production. From 1982 to 1997 in Dallam, Sherman, Hartley and Moore Counties located within the AVHRR NDVI anomaly region centered on Dalhart, Texas corn production had increased greater than > 200% (Figure 3.19, A). Counties located outside of the anomaly region experienced little to no growth in corn for grain production. NDVI seasonal profiles have been shown to aid in estimating crop performance and the observed anomaly trends appear to reflect this observation (Benedetti and Rossini 1993; Boissard et al. 1993; Doraiswamy and Cook 1995; Labus et al. 2002; Rasmussen 1992). This positive growth relationship between crop statistics and enhanced NDVI signature was apparent in the study.

Change from wheat to corn production appeared to be causing the marked increase in the AVHRR NDVI. Conversion to center pivot irrigators for corn production enhanced the observed AVHRR NDVI anomaly. Expansion of center pivot irrigated agriculture throughout this region had a marked impact on land cover in this region and was visible in Landsat (Figure 3.19, B and C). The coupled influence of change in crop type and more extensive irrigation networks resulted in the AVHRR NDVI anomaly.

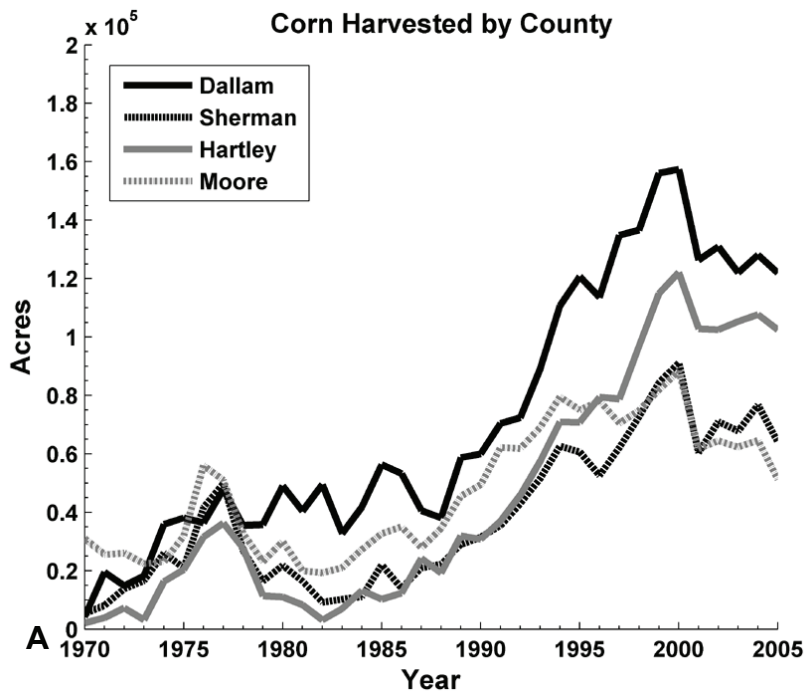

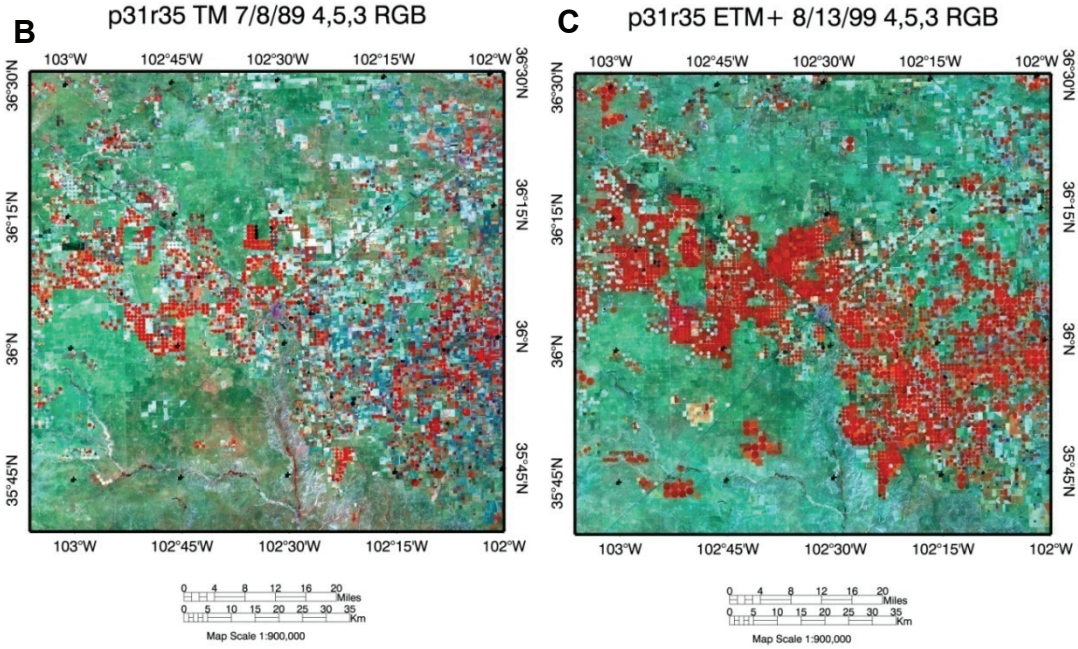

Figure 3.19 (A) Corn harvested by county increased markedly during observations. Expansion of center pivot irrigated agriculture throughout this region had a marked impact on land cover near infrared reflectance and was visible in Landsat (B, C). Conversion to center pivot irrigators for corn production enhanced the observed AVHRR NDVI anomaly. The coupled influence of change in crop type and more extensive irrigation networks resulted in the AVHRR NDVI anomaly.

3.3.5 Quebec

The Quebec study region encompasses a majority of the southern portion of the province, which is mixed boreal forest. The ecotone is very similar to Northern Saskatchewan as they are both considered to be a part of the North American Boreal Shield. Many of the same tree species also exist in this region and they have the same response and succesional sequences. Similar to Northern Saskatchewan, two species are very common: white spruce (*P. glauca*); and black spruce (*P. marinana*). Other species present include: eastern larch (*L. laricina*); balsam fir (*A. balsamea*); jack pine (*P. banksiana*); trembling aspen (*P. tremuloides*); and paper birch (*B. papyrifera*). The observed AVHRR NDVI anomalies are around the Lac Saint-Jean area in the East to the Reservoir Gouin to the West (Figure 3.20).

This region has experienced extensive logging and modifications to the forest cover were evident at Landsat resolution. Fire disturbance does not modify the land cover extensively in this region. The majority of fire events were observed further North, with one event in 1991 occurring to the Northeast of the study region. Population density occurs toward the East in the Saguenay Lac Saint-Jean region where over 300,000 inhabitants are distributed over 56 municipalities (Alma 2007).

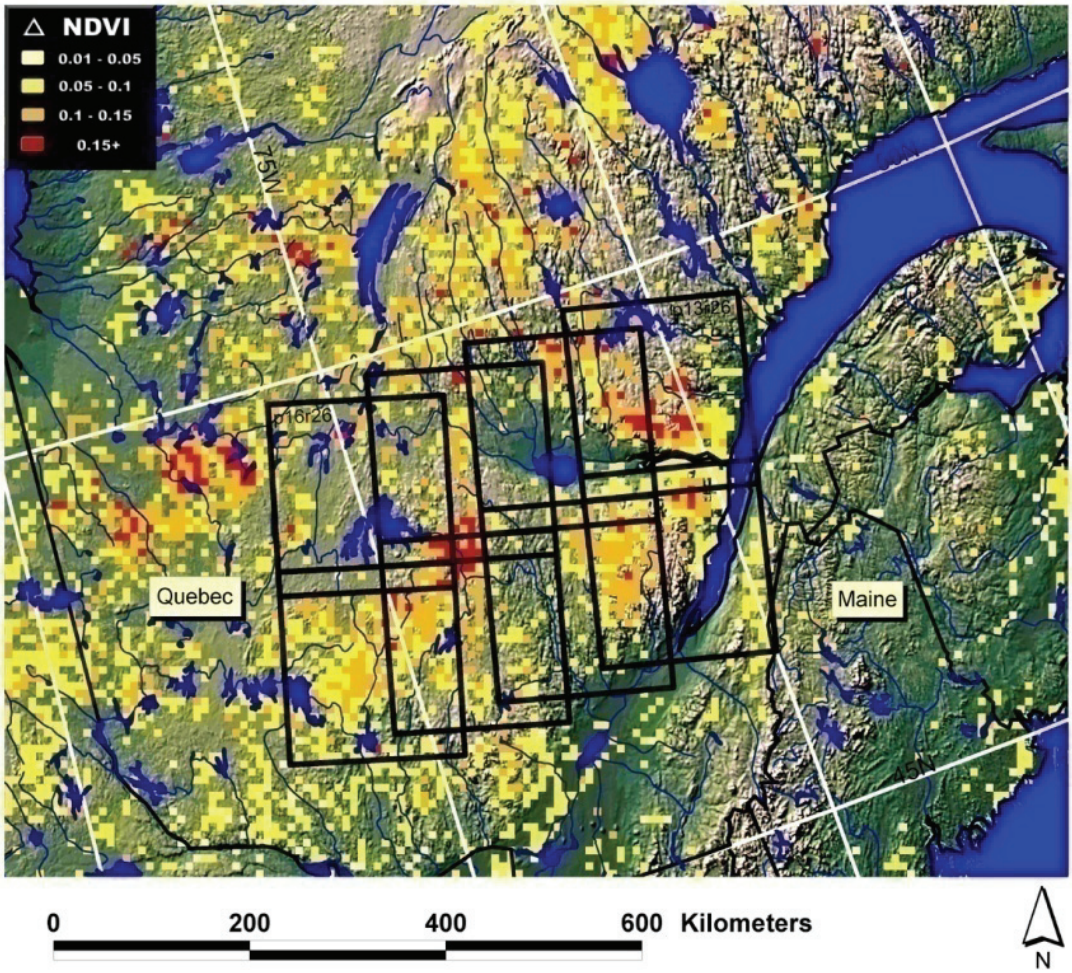

Figure 3.20 An area in Southern Quebec that had an increased NDVI trend from 1982-2005, with black polygons indicating area of Landsat analysis.

3.3.5.1 Land Cover

Land cover analysis for this region indicated marked changes in vegetation cover. ~170,000 km^2 were mapped, and during observations needle leaf evergreen forests declined by ~2,350 km^2 (-39% change in area), short vegetation grassland increased ~1310 km^2 (+37% change in area), broad leaf deciduous forests increased by ~5,580 km^2 (+15% change in area), and dwarf trees and shrubs extent changed by ~2,570 km^2 (+26% change in area) (Figure

3.21, A and B). Map accuracy ranged from 87% to 89% (Table 3.9). Logging and recovery from logging was common throughout this region.

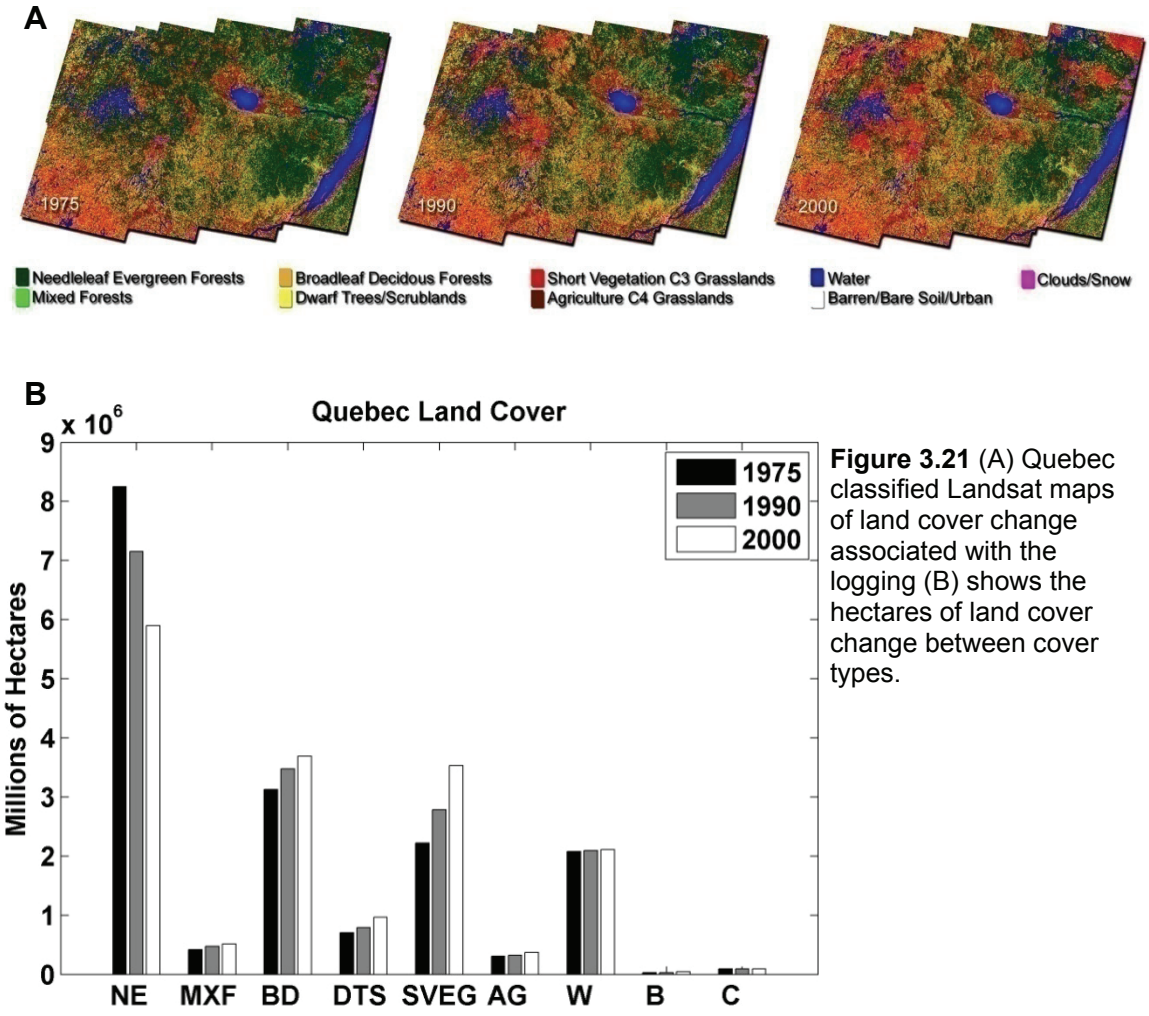

Figure 3.21 (A) Quebec classified Landsat maps of land cover change associated with the logging (B) shows the hectares of land cover change between cover types.

Landsat land cover trends were comparable to similar rates recorded from the Canadian Forest Service which both have recorded increasing rates of logging. Fire did not have a significant role in disturbance regime in this region as it did in Saskatchewan. Extensive salvage logging was initiated by a wide spread spruce budworm (*C. fumiferana*) outbreak during the mid 1970s. During the last century, Eastern North American forests have suffered increasing rates

of spruce budworm outbreaks rising to ~550,000 km^2 in 1975 (Kettela 1983). Blias et al. (1981, 1983), reported that a spruce budworm outbreak collapsed in 1975 in Southern Quebec, and extensive mortality up to 91% of balsam fir (*A. balsamea*), their preferred fare, occurred. Recovery of the understory was reported to be rapid of tree species that comprised the original stand because they did not suffer extensive infestation. This has been interpreted to be part of the successional system (Baskerville 1975; Blias 1985). The Canadian forest service permitted extensive salvage logging to take place as much of this region is utilized for cash crops in pulp and paper production. Recovering vegetation at logged sites was found to have an enhanced near infrared reflectance that would also enhance the AVHRR NDVI (Figure 3.22, A, B, and C).

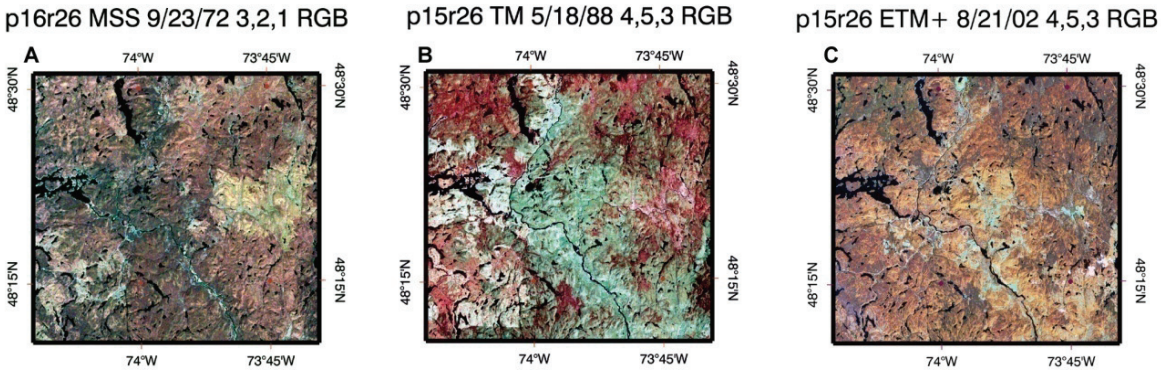

Figure 3.22 Unprocessed GeoCover Landsat examples of land cover change associated with logging near the reservoir Goin, Quebec; (A) shows undisturbed needle leaf evergreen forest (dark red); (B) shows the disturbance, and conversion to grasslands (pale green); (C) shows the recovery of vegetation (pale orange).

Table 3.9 Error Matrices for Quebec.

Air Photo & IKONOS Reference Data		*Ne*	*Mbn*	*Bd*	*Dts*	*Sveg*	*Ag*	*W*	*B*	*C*	Map %
MSS	*Ne*	4534	9	1	11	89	0	12	0	0	47.9
Mapped Data	*Mbn*	0	48	0	0	0	0	0	0	0	2.4
	Bd	17	36	671	0	0	0	0	0	0	18.2
	Dts	19	0	5	101	0	0	4	0	0	4.1
	Sveg		164	14	135	1	566	0	0	0	0 12.9
	Ag	12	0	0	0	0	0	0	0	0	1.8
	W	0	0	0	0	0	0	844	0	0	12.1
	B	0	0	0	0	0	0	0	0	0	0.2
	C	0	0	0	0	0	0	0	0	0	0.5
Producer's Accuracy		95.5	44.9	82.6	89.4	86.4	-	98.1	-	-	-
User's Accuracy		97.4	100.0	92.7	78.3	64.3	-	100.0	-	-	-
Sample %		67.0	0.7	9.9	1.5	8.4	-	12.5	-	-	-
Overall Accuracy 92.6%											
Kappa Statistic 86.8%											
TM	*Ne*	1520	0	84	70	34	0	12	0	0	41.6
Mapped Data	*Mbn*	8	24	18	0	11	0	0	0	0	2.7
	Bd	70	3	263	0	6	0	0	0	0	20.2
	Dts	4	0	0	138	0	0	4	0	0	4.6
	Sveg		3	3	0	10	742	0	0	0	0 16.2
	Ag	0	0	0	0	0	0	0	0	0	1.9
	W	0	0	0	0	0	0	1405	0	0	12.2
	B	0	0	1	0	0	0	0	0	0	0.2
	C	0	0	0	0	0	0	0	0	0	0.5
Producer's Accuracy		94.7	80.0	71.9	63.3	93.6	-	98.8	-	-	-
User's Accuracy		88.3	39.3	76.9	94.5	97.9	-	100.0	-	-	-
Sample %		37.2	0.6	6.4	3.4	18.1	-	34.3	-	-	-
Overall Accuracy 92.3%											
Kappa Statistic 89.3%											
ETM	*Ne*	1532	0	23	0	1	0	0	0	0	34.2
Mapped Data	*Mbn*	0	163	84	0	18	0	0	0	0	3.0
	Bd	114	33	558	0	7	0	0	0	0	21.4
	Dts	10	0	7	277	43	0	0	0	0	5.6
	Sveg		7	6	71	27	790	0	0	0	0 20.5
	Ag	0	0	0	0	0	0	0	0	0	2.2
	W	0	0	0	0	0	0	669	0	0	12.3
	B	0	0	0	1	0	0	0	0	0	0.3
	C	0	0	0	0	0	0	0	0	0	0.5
Producer's Accuracy		92.1	80.7	75.1	90.8	92.0	-	100.0	-	-	-
User's Accuracy		98.5	61.5	78.4	82.2	87.8	-	100.0	-	-	-
Sample %		38.4	4.1	14.0	6.9	19.8	-	16.8	-	-	-
Overall Accuracy 89.8%											
Kappa Statistic 86.8%											

3.3.5.2 Logging Rates

The Canadian Forest Service has reported substantial increases in logging rates throughout the province of Quebec. Total annual harvesting during the NDVI record has grown from 2,000 km^2 a year to greater than 3,500 km^2. It has been reported by (Sabol et al. 2002), that post-logging regrowth in Pacific Northwest U.S. conifer forests had a higher NDVI after 3-4 years than the mature conifer stands they replaced, which persisted for 10 to 30 years. Higher near infrared reflectance was observed in Quebec at disturbed sites, which increased NDVI. Forest age structures as suggested by (Caspersen et al. 2000), may be responsible for the observed trend increase in this region. The successional process of *P. glauca,* which are ubiquitous in this region, begins after logging with fast growing deciduous species. These deciduous species of paper birch (*B. papyrifera*) and trembling aspen (*P. tremuloides*) typically have a higher NDVI signature than the conifers that replace them. In this region regrowth following logging acted as a disturbance-driving element of the observed AVHRR NDVI anomaly.

3.3.6 Newfoundland and Labrador

The island of Newfoundland and the Labrador coast has a unique environment with a maritime boreal forest influenced by the confluence of two ocean currents, the cold Labrador and the warm Gulf Stream. Its maritime climate can change drastically depending on what current is dominating flow. The entire island over 100,000 km^2 has recorded a marked increase in NDVI

over the 1992-1999 period. Land use change is not a dominant factor in this region as it is sparsely populated and does not have productive soil for agriculture. Over half of the population resides in St. Johns, the capital of Newfoundland on the eastern coast. Newfoundland also has a fairly extensive logging operation in the West where large amounts of spruce and pine are harvested for pulp and paper production. The ecotone is very similar to that of the Quebec study region. The vegetation of Newfoundland consists of dense mixed forest of trembling aspen (*P. tremuloides*), paper birch (*B. papyrifera*), balsam fir (*A. balsamea*), white spruce (*P. glauca*) and black spruce (*P. marinana*) in the west. The central and eastern portions of the island are open lichen woodland where fertile soils have been removed and underlying rock has been exposed by ancient glaciers of the past (Figure 3.23).

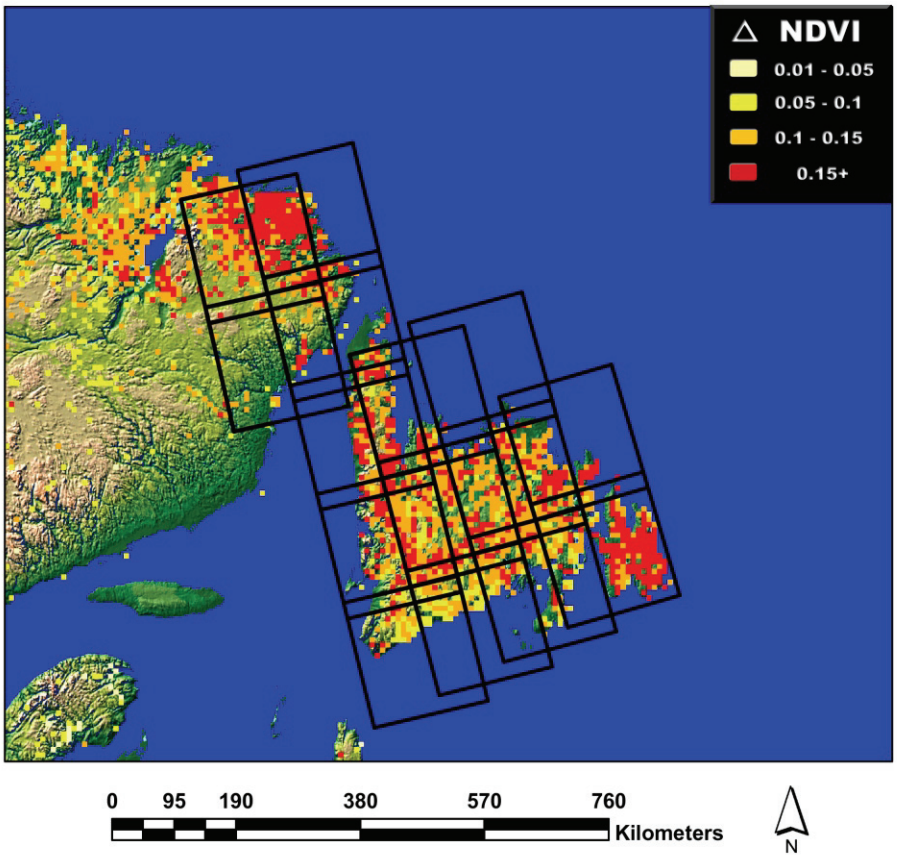

Figure 3.23 The Newfoundland and Labrador areas that experienced marked increases in NDVI from 1992 to 1999 with the Landsat images used for spatial understanding superimposed as an overlay.

3.3.6.1 Land Cover

Extensive logging was noted on the western coast of Newfoundland for pulp and paper production. From 1982 to 1999 an additional 100 km^2 were logged but this is insignificant compared to the 100,000 km^2 extent of the island (NFS 2007). Land cover results for this region indicate moderate changes in vegetation cover. ~170,000 km^2 were mapped including Labrador, and during observations needleleaf evergreen forests declined by ~6,650 km^2 (-10% change in cover type), short vegetation grassland increased ~3,920 km^2 (+7% change in cover type), broadleaf deciduous forests increased by ~350 km^2 (+12% change

in cover type), and barren extent changed by ~1,360 km^2 (+20% change in cover type) (Figure 3.24, A and B). Map accuracy ranged from 81% to 91% (Table 3.10). Logging and recovery from logging is pervasive throughout the western portion of Newfoundland.

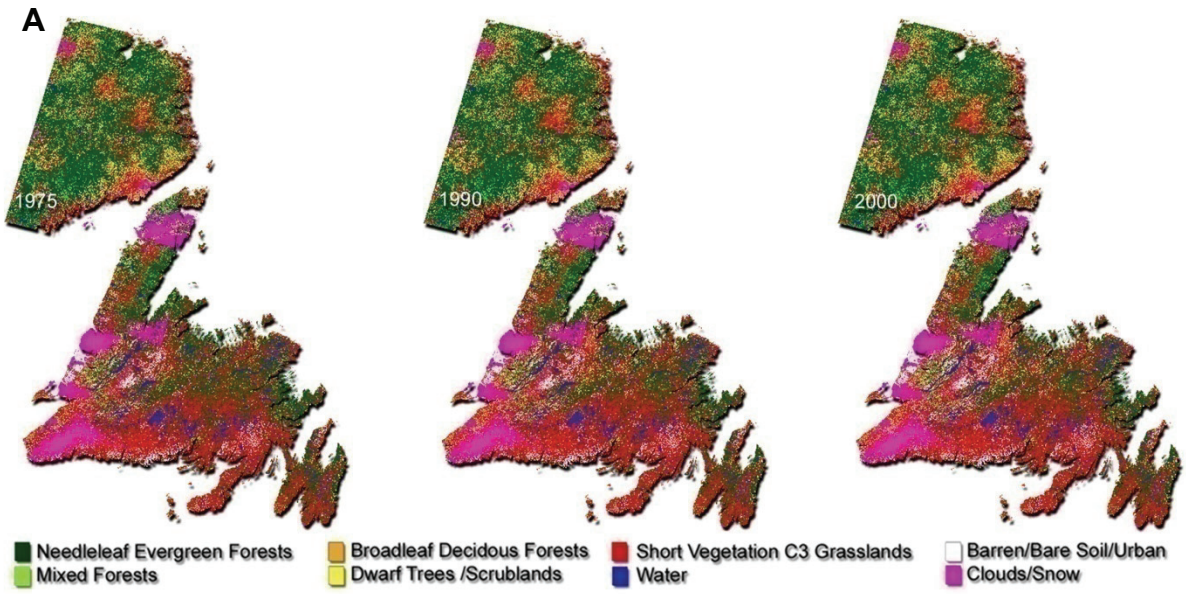

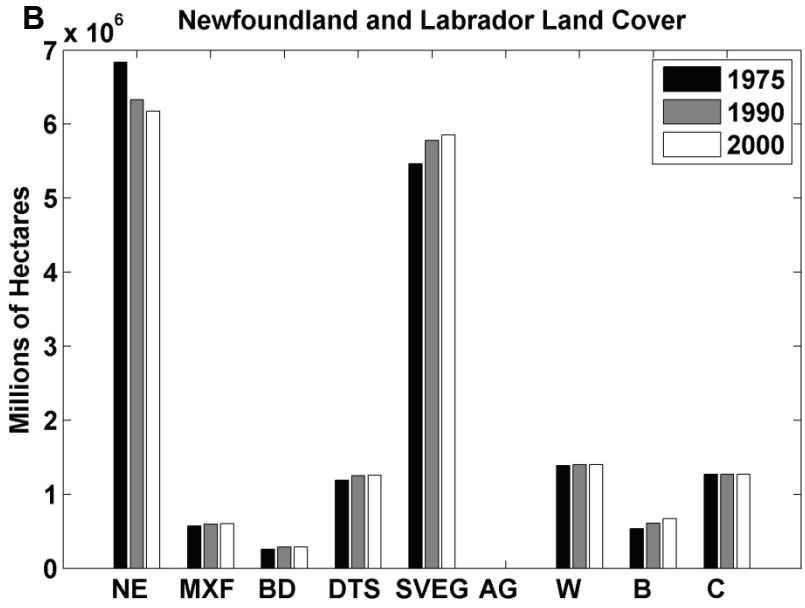

Figure 3.24 (A) Newfoundland classified land cover maps, (B) shows that few land cover changes have occurred.

Table 3.10 Error Matrices for Newfoundland.

Air Photo & IKONOS Reference Data		*Ne*	*Mbn*	*Bd*	*Dts*	*Sveg*	*Ag*	*W*	*B*	*C*	Map %
MSS	*Ne*	79	10	17	0	932	0	0	0	0	39.1
Mapped Data	*Mbn*	5	12	72	45	111	0	0	0	0	3.3
	Bd	0	0	74	144	8	0	0	1	0	1.5
	Dts	1	0	16	54	222	0	0	0	0	6.8
	Sveg	19	53	406	379	5617	0	0	2	0	31.2
	Ag	0	0	0	0	0	0	0	0	0	0
	W	0	0	0	2	17	0	5751	0	0	7.9
	B	0	4	0	9	53	0	0	0	0	3
	C	0	4	3	5	183	0	45	6	0	7.2
Producer's Accuracy		76.0	14.5	12.6	8.4	78.6	-	99.2	0.0	-	-
User's Accuracy		7.6	4.8	32.6	18.4	86.7	-	99.7	0.0	-	-
Sample %		0.7	0.1	0.6	0.5	48.5	-	49.6	0.0	-	-
Overall Accuracy 80.7%											
Kappa Statistic 68.4%											
TM	*Ne*	7289	361	76	13	385	0	11	12	0	36.1
Mapped Data	*Mbn*	444	1220	54	21	210	0	15	3	0	3.4
	Bd	8	151	351	65	49	0	3	2	0	1.6
	Dts	160	194	86	90	35	0	5	4	0	7.1
	Sveg	1648	256	361	252	6856	0	79	187	0	33
	Ag	0	0	0	0	0	0	0	0	0	0
	W	29	0	4	4	12	0	13116	4	0	8
	B	15	46	36	13	472	0	2	1235	0	3.5
	C	57	4	3	5	183	0	45	6	0	7.2
Producer's Accuracy		75.5	54.7	36.1	19.4	83.6	-	98.8	85.0	-	-
User's Accuracy		89.5	62.0	55.8	15.7	71.1	-	99.6	67.9	-	-
Sample %		24.8	4.1	1.2	0.3	22.7	-	43.5	4.1	-	-
Overall Accuracy 83.2%											
Kappa Statistic 77.3%											
ETM	*Ne*	1867	153	0	8	50	0	5	1	0	35.1
Mapped Data	*Mbn*	7	137	0	11	0	0	0	0	0	3.4
	Bd	0	0	0	0	0	0	0	0	0	1.7
	Dts	14	0	0	213	32	0	0	0	0	7.2
	Sveg	1	0	0	47	1700	0	0	11	0	33.4
	Ag	0	0	0	0	0	0	0	0	0	0.0
	W	0	0	0	0	0	0	451	0	0	8.0
	B	0	0	0	0	16	0	0	30	0	3.8
	C	0	0	0	0	0	0	0	0	0	7.2
Producer's Accuracy		98.8	47.2	-	76.3	94.5	-	98.9	71.4	-	-
User's Accuracy		89.6	88.4	-	82.2	96.6	-	100.0	65.2	-	-
Sample %		42.5	3.12	-	4.9	38.7	-	10.3	0.7	-	-
Overall Accuracy 92.5%											
Kappa Statistic 88.8%											

No other large-scale land cover trend was observed, as population density is sparse throughout the region. Emergence of more deciduous species of paper birch (*B. papyrifera*), and trembling aspen (*P. tremuloides*) in formally logged areas was noted from aerial over flights. However, these alterations in land cover are insignificant compared to the observed NDVI anomaly, which extends over the entire island. Land-cover land-use change is not a major factor in the observed NDVI trend; abiotic factors are the dominant cause. Annual surface temperature nearly doubled over the 1990's and it appears to have enhanced the NDVI record. The growing season has extended by 17 days and enabled more biomass to be produced (Figure 3.25, A and B). These marked climate changes over one decade have been reflected in the NDVI record as anomalies. The intense change in surface temperature is responsible for the observed anomaly in NDVI (Neigh et al. 2007).

3.3.6.2 Climate

Newfoundland has a temperature-constrained environment where precipitation is non-limiting. Muskegs are a common feature in the landscape held by ancient glacial rock and rejuvenated by frequent precipitation events. The climate of Newfoundland varies drastically because of its northern maritime exposure on all fronts. During the last decade, the Gulf Stream has dominated the Labrador Current allowing warm waters to reach Newfoundland's shores (Afanasyev et al. 2001). These warm currents are driving an observed increase of 3.5° C in 1992 to 7° C in 1999 in mean annual temperature.

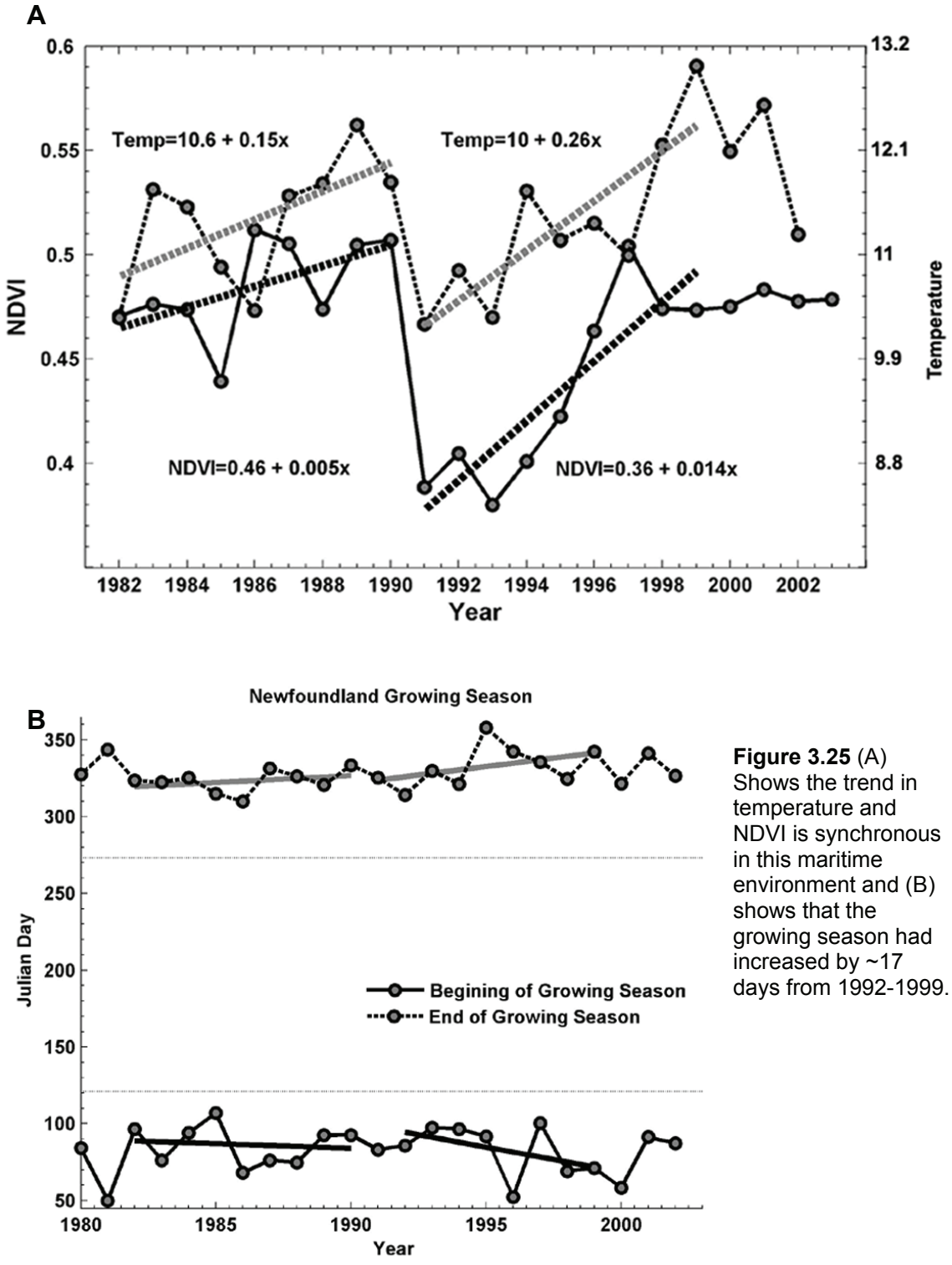

Figure 3.25 (A) Shows the trend in temperature and NDVI is synchronous in this maritime environment and (B) shows that the growing season had increased by ~17 days from 1992-1999.

A typical warm weather promotes growth and photosynthesis in this mixed boreal forest. The growing season has extended by over 17 days from 1982 to 1999, reducing snow cover and enabling more vegetation productivity (Neigh et al. 2007). Similar to the northern Saskatchewan study region, growth is often limited in coniferous forest by mineral poor soils with productivity controlled by nutrient cycling through litter fall and decomposition (Cole and Rapp 1981). Enhanced temperature accelerates decomposition enabling more nutrients to be released into the soil (vanCleve et al. 1983). Culminating with this fact, black spruce (*P. mariana*), the dominant stand species in this region, has an optimum temperature for photosynthesis of 15° C, with a 90% rate maintained between 9° C and 23° C (Vowinckel et al. 1975). The role of increasing temperature to vegetation productivity will be investigated with simulation modeling.

3.4 Synthesis

Six different areas displaying marked changes in NDVI values for the period from 1982 to the present have been examined using multi-temporal Landsat data and other ancillary data sources to provide attribution for the changes. These results indicate a complex interaction between anthropogenic changes and direct biophysical impacts. In some areas, especially in northern latitudes, the changes appear to be the result solely of biophysical impacts. In the Mackenzie Delta it appears that temperature increases are the prime drivers. In Newfoundland the immediate cause of increases in NDVI appears to be related to regional increases in water temperatures in the adjacent ocean. In

contrast in Northern Saskatchewan the proximate driver of increases in NDVI is forest regrowth following frequent large forest fires, though the latter may be affected by temperature increases associated with global warming superimposed on cyclical fluctuations in fire frequency.

In the other examined areas the impact of anthropogenic influences was more direct. In Quebec the anomalies arise from the regeneration of extensive logged areas of evergreen forests leading to forests dominated by deciduous species. In Southern Saskatchewan and the Dakotas, the increases in NDVI derive from increased agricultural activity following the increased precipitation after an extensive drought prior to 1992. But further south in the High Plains of the Oklahoma Panhandle, the area's increases in NDVI are related to large increases in pivot irrigation relying on ground water.

The pattern of NDVI anomalies over the time period considered therefore arises from a variety of interacting factors. Some of these changes appear to be driven by long-term climate change but most appear associated with climate variability on decadal and shorter time scales along with direct anthropogenic land cover conversions. Interactions between the three types of drivers of change demonstrate the difficulty of interpreting changes in NDVI. Furthermore, this indicates the complex nature of changes in the carbon cycle within North America. Coarse scale analysis of changes could well fail to identify the important local scale drivers controlling the carbon cycle and to identify the relative roles of disturbance and climate change.

3.5 Conclusion

North American vegetation dynamics driven by a number of different biophysical phenomena have been revealed in this research. Discrete events over the past two decades have induced change in ecosystem functioning that have been identified with multi-resolution satellite imagery. It was found that: (1) Multi-resolution data provides information critical to the state of knowledge of vegetation dynamics in North America; (2) land-cover land-use change driven by humans had a marked impact to North American photosynthetic capacity; (3) natural abiotic and anthropogenic events can modify vegetation dynamics in concert or singularly; (4) coupled processing of multi-resolution data can be performed efficiently to extract synoptic information of ecosystem state; and (5) information about vegetation dynamics enhances ecosystem models to emulate altered terrestrial biogeochemistry and land surface energy exchange.

Investigation through multi-scalar and multi-temporal data revealed land cover dynamics during the 1980s and 1990s. In correspondence to Hicke et al., (2002), Neigh *et al*., (2007), and Zhou *et al*., (2001), changes in temperature and precipitation have also been found to be marked contributors to vegetation change. Human activities were observed to have an impact to vegetation productivity altering the relationship between the biota and the physical environment. The unique contribution of this study is how regional land-cover land-use change altered vegetation dynamics at the continental scale in North

America. Continued investigation is needed to extrapolate how natural and anthropogenic changes impact the North American carbon cycle.

Chapter 4. Carbon Consequences of Regional Vegetation Productivity Increases in North America

4.1 Introduction

Approximately half of CO_2 released to the atmosphere from fossil fuel combustion and deforestation is sequestered in spatial-temporal dynamic biosphere reservoirs (CCSP 2007). Climate impacts rates of carbon exchange through photosynthesis and decomposition, while humans initiate land-cover land-use-change and other processes that alter net ecosystem carbon balance (Bousquet et al. 2000; DeFries et al. 1999; Houghton et al. 1991). Duration of inter-annual carbon repositories are difficult to measure due to inadequate accounting for the underlying processes (Baker et al. 2006; Deng et al. 2007). Typically investigations focus on climate drivers and preclude fine-scale human disturbances to ecosystem function (Cramer et al. 1999). This lack of accounting results in large discrepancies between estimates of mean sink status due to spatial-temporal uncertainties of vegetation dynamics relevant to the carbon cycle (Hall et al. 2006; Houghton 2007).

Global inversions and ecosystem process models at coarse resolutions are deficient in capturing disturbance dynamics that alter regional carbon balance of ecosystems, due to insufficient knowledge of land cover disturbance (Hall et al. 2006; Potter et al. 2003a). Limited knowledge increases uncertainties for carbon accounting, which hampers understanding of terrestrial ecosystem functioning. The means to explore regional disturbances exist and I contend it is important to understand past terrestrial processes which have altered

biogeochemistry of ecosystems that when aggregated may impact the global carbon balance.

North America has experienced marked land-cover land-use change due to human actions of mechanized agriculture and forestry management in the early 20th century (Houghton 2007). Agriculture production once dominated the East now has migrated to the Midwest, and portions of the eastern United States have experienced forest recovery (Caspersen et al. 2000). Midwest herbaceous regions receive water and nutrients to produce crops that contain more biomass than natural grasslands. The Canadian boreal region has increased standing biomass in forests (Blias 1983, 1985) from ongoing suppression of herbivorous insects; while fire regimes have increased in occurrence from climate warming, resulting in more emissions (Kasischke 1997; Stocks et al. 2003).

Two primary questions about ecosystem carbon sequestration have been proposed by research organizations (CCSP 2007; IPCC 2007): (1) what is the current state of the carbon cycle in North America; and (2) what mechanisms alter the regional balance. My hypothesis is that fine-scale understanding of carbon-disturbance processes will improve knowledge and reduce uncertainties of the regional carbon balance of ecosystems (Ogle et al. 2003; Robertson and Grace 2004; Six et al. 2004). The vegetation-atmosphere interface controls regional climate, and energy exchange (Bounoua et al. 2000; Dorman and Sellers 1989), while humans impede this coupling markedly impacting vegetation productivity. Conversion between forests to non-forested land cover alters

energy balance and carbon storage by removing pools that sequester carbon over long (>40 years) periods. Prior land cover change results (Neigh et al. 2008) were integrated in this investigation to simulate disturbance to carbon cycling of regional ecosystems. Satellite remote sensing data provide 30+ years of past characteristics of vegetation which could enhance understanding of carbon cycle process.

This investigation seeks to understand fine-scale ecosystem carbon pool disturbance in North America from 1982-2005 utilizing multi-temporal multi-spectral remote sensing observations implemented in biogeochemistry modeling. Fine-scale disturbance data were used in simulations to understand legacy land-use and balance of carbon in regions of increased plant productivity. Many aforementioned dynamics were not simulated in prior investigations with explicit fine-scale information on disturbance type or extent with inclusion of full carbon balance. Vegetation dynamics in North America are complex due to a combination of anthropogenic and climatic effects on vegetation productivity and heterotrophic respiration (Neigh et al. 2008). This work constrains disturbance to understand carbon cycle implications over a long-time period relative to satellite observations.

4.2 Methods and Data

Currently the only method to understand spatially distributed consequences of carbon disturbances across all of North America at 8 km^2 scale

is via a model, which simulates net ecosystem production (NEP) and estimates carbon exchange through biosphere reservoirs. The Carnegie-Ames-Stanford Approach (CASA) carbon cycle model discussed in detail by (Potter et al. 1993) and (Field et al. 1995) was used to calculate NEP as difference between net primary production (NPP) and heterotrophic respiration (R_h). In my version of CASA, plant functional types derived from multi-temporal fine-scale data (Neigh et al. 2008) were used to calculate NPP, and allocation rates, which in turn control trace gas fluxes (Bonan et al. 2002; Buchmann and Schulze 1999). Estimates of net biome productivity (NBP) or NEP minus biomass removed from land cover change (logging, fire, herbivory, crop harvest) were also simulated to account for perturbations to biophysical and biogeochemical processes providing comprehensive assessment of ecosystem productivity over 24-years (1982-2005) for North America regional study areas.

Many other models exist that are driven by NOAA/ AVHRR to calculate NPP for terrestrial ecosystems including the Global Production Efficiency Model (GLO-PEM) (Prince 1991), Simple Interactive Biosphere Model (SDBM) (Knoor and Heimann 1995), Terrestrial Uptake and Release of Carbon (TURC) (Ruimy et al. 1996), and Simple Interactive Biosphere Model (SIB2) (Sellers et al. 1996). However, CASA was selected due to its dependence on spatially explicit remote sensing data from vegetation plant functional types derived from prior Landsat classifications, FPAR, LAI and percent tree cover derived from AVHRR to drive biogeochemical processes (Cramer et al. 1999) and openly available source

code which could be modified to replicate regional carbon cycle processes in modules. CASA is a radiation-use efficiency model similar to TURC and SDBM with potential light-use efficiency reduced due to environmental constraints. CASA simulates multiple carbon pools with structured processes that transfer carbon between pools that enables replication of complex disturbance dynamics observed from multi-resolution satellite data with inclusion of climate (precipitation and temperature) stress upon NPP (Cramer et al. 1999). CASA was selected because it links production efficiency based on the Montieth (1977) approach with a robust representation of heterotrophic respiration based upon decomposition rates of different pools similar to the mechanistic approach used in CENTURY and DAYCENT (Parton et al. 1998) models.

Briefly, CASA is a production efficiency model (Carvalhais et al. 2008; Friedlingstein et al. 1999; Randerson et al. 1996; Ruimy et al. 1999) which estimates NEP as the difference between NPP minus R_h. CASA utilizes satellite data in the form of fraction of absorbed photosynthetically active radiation (fPAR) from normalized difference vegetation index (*NDVI*) and the simple ratio (*SR*), which are defined as:

$$NDVI = (NIR - VIS)/(NIR + VIS) \quad (4.1)$$

$$SR = (1 + NDVI)/(1 - NDVI) \quad (4.2)$$

using visible (*VIS*) and near-infrared (*NIR*) bands of the NOAA Advanced Very High Resolution Radiometer (AVHRR) provide direct time-series data on

changes in surface “photosynthetic capacity”, which is expressed in leaf area index (LAI) or (fPAR) (Los et al. 2000).

NPP was computed from multiplying maximum light use efficiency (ε^*) by (*fPAR*), photosynthetically active solar radiation (*PAR*), and down-regulators which represented plant stresses due to sub-optimal temperature (T_ε) and soil moisture (W_ε):

$$NPP = \varepsilon^* \cdot T_\varepsilon \cdot W_\varepsilon \cdot fAPAR \cdot PAR \quad (4.3)$$

NPP is mediated by heterotrophic respiration (R_h) produced by microbial organic decomposition of parent plant material and can generally be described as:

$$R_h = \sum_i^p C_i \cdot k_i \cdot W_s \cdot T_s \cdot (1 - M_\varepsilon) \quad (4.4)$$

Where: (p) is the number of pools; (C_i) is the carbon content of pool (i); (k_i) is maximum decay rate of constant pool (i); (W_s) is soil moisture effect on decomposition; (T_s) is temperature effect on decomposition; (M_ε) is the carbon assimilation efficiency of microbes. All simulations were first run to equilibrium (i.e., NPP $\cong$ R_h) with constant NPP to define ecosystem steady state before disturbance (Carvalhais et al. 2008). Climate anomalies were calculated during the 24-year period of observations to select a climate normal for simulation spin up. The impacts of climate on NEP were driven by observed climate and NDVI variability (Figure 4.1).

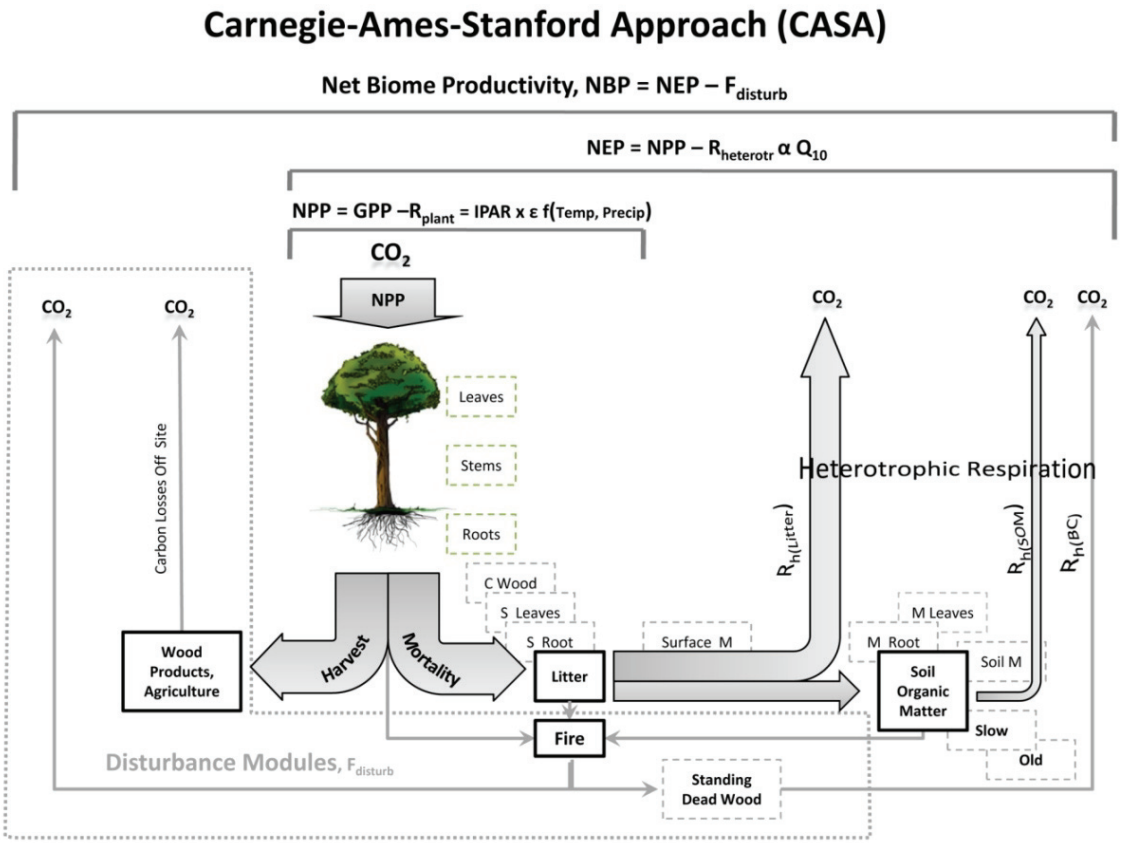

Figure 4.1 A conceptual carbon flow scheme through ecosystems with input through photosynthesis and balance between autotrophic and heterotrophic respiration calculated in the Carnegie-Ames-Stanford Approach (CASA) model. Disturbance is captured in modules of harvest (agriculture, logging) and mortality (fire, insect herbivory outbreaks). Inclusion disturbance to carbon cycle processes in ecosystems is referred to as net biome productivity (NBP). CASA captures changes through a mechanistic approach of NPP flowing through carbon pools (dashed boxes) on monthly intervals as prescribed by field observations. Conceptual carbon flow derived from Schulze et al. (2000).

Terrestrial NPP fluxes derived from CASA have been validated in specific sites against carbon dioxide sampling stations around the world (Denning 1994) and tree rings (Malmstrom et al. 1997). CASA has been used in numerous simulations to predict ecosystem carbon flux (Carvalhais et al. 2008; Gurney et al. 2004; McGuire et al. 2000; Murayama and Taguchi 2004; Potter et al. 2003a; Potter 1999; Randerson et al. 1997; Thompson and Randerson 1999; vanderWerf et al. 2004; vanderWerf et al. 2006). Carbon cycle processes in

CASA are similar to those in the CENTURY model (Parton et al. 1987) with multiple pools each with unique turn over intervals expected to replicate plausible dynamics allowing investigation of fine-scale disturbance to regional carbon cycling.

CASA is a global radiation use efficiency model which has limitations when used to replicate specific ecoregions and climate dynamics. Sub 8 km^2 pixel processes have not been extensively implemented within this model in prior investigations and known limitations pertaining to specific processes exist. Types of dynamics which need improvement include soil hydrology processes and arctic carbon soil processes. Limitations to changes in NPP are also acknowledged as it is derived from FPAR which is derived from 8 km^2 NDVI that contains a mixed pixel response from sub 8 km^2 pixel land cover changes as observed from Landsat and other high resolution remote sensing data.

4.2.1 Model Inputs

CASA required information on climate, plant functional type, forest cover, soil texture, and land-cover land-use change to carry out NEP simulations and/or logging, fire, and agriculture production data for NBP simulations. Model climate and soil inputs were selected based upon the ability to compare to prior coarse resolution simulations which had identical drivers. Climate was derived from Leemans & Cramer climatology (Leemans and Cramer 1991) and GISSTEMP anomalies (Hansen et al. 1999), solar radiation from the International Satellite

Cloud Climatology Project (ISCCP) (Bishop and Rossow 1991), and precipitation from the Global Precipitation Climatology Project version 2 (GPCP) (Adler et al. 2003) were used to derive NPP stressors (T_ε and W_ε). Forest cover density was derived from 1-km AVHRR (DeFries et al. 2000). Soil texture and depth data, from the Food and Agriculture Organization of the United Nations, United Nations Educational Scientific and Cultural Organization (FAO/UNESCO) soil map (FAO 1978) was used for soil hydrology calculations (Saxton et al. 1986).

Ancillary data was gathered to understand and prescribe model dynamics. Logged area was derived from Canadian Forest Service (NRC 2007), burned area extent from the large fire database for Canada developed by Stocks *et al*. (2003), and agriculture production statistics were analyzed from the United States Department of Agriculture (USDA) National Agriculture Statistics Service (NASS) records (www.usda.nass.gov). Coarse resolution global gridded climate datasets were bilinear interpolated from 0.5 – 2.5º to 8 km^2 to remove coarse grid foot print affects on regional simulations.

Table 4.1 CASA simulation inputs.

Dataset	Resolution	Description	References
NDVI	8 km^2	GIMMS 'g'	Tucker *et al.* (2005)
Solar Radiation	2.5°	ISCCP	Bishop and Rossow (1991)
Temperature	1°	Climatology mean plus GISS temperature anomalies	Leemans and Cramer (1991) Hansen *et al.* (1999)
Precipitation	2.5°	GPCP Mean monthly precipitation	Adler *et al.* (2003)
Vegetation map	30 m^2	9 Classes, derived from Landsat	Neigh *et al.* (2008)
Soil texture	1°	FAO/UNESCO soil texture groups	Zobler *et al.* (1986)
Burned area	2 km^2	Boreal North America	Stocks *et al.* (2003)
Vegetation Continuous fields	1 km^2	Percent tree cover	DeFries *et al.* (2000)

4.2.1.1 AVHRR Anomalies

Six regions in North America were previously selected to investigate vegetation dynamics based on positive AVHRR NDVI trends during four periods (Neigh et al. 2008). Regions meeting criteria found land cover dynamics associated to climate and land-cover land-use change include: (1) Yukon, Mackenzie River Delta (warming climate, extended growing season); (2) Northern Saskatchewan (fire disturbance and recovery); (3) Southern Saskatchewan (drought, rain fed agriculture recovery); (4) Oklahoma Panhandle (expansion of irrigated agriculture); (5) Southern Quebec (insect outbreak, salvage logging and forest recovery); and (6) Newfoundland (warming climate, extended growing season).

4.2.1.2 Landsat Land Cover Data

Thematic maps of Landsat GeoCover Ortho data were produced regionally during epochs 1975, 1990, 2000 totaling > 150 scenes and classified into plant functional types of evergreen needle leaf, mixed evergreen needle leaf and broadleaf deciduous, broadleaf deciduous, dwarf trees and shrubs, short vegetation C4 grasslands, agriculture C3 grasslands, water, barren, clouds, snow and ice. An unsupervised ISODATA classification was implemented, and change detection was performed based upon a multi-date linear tassel cap transformation followed by ISODATA (Neigh et al. 2008; Tou and Gonzales 1974). Map accuracy was validated with high-resolution (~0.5 – 2 m^2) archived digital aerial photography, IKONOS high resolution satellite imagery (1 – 4 m^2),

and in situ aerial Global Position System (GPS) referenced photography surveys. Study region extent ranged ~8 to ~18 million hectares, and map accuracies varied 80.7% to 97.6% (Neigh et al. 2008). Landsat land-cover change was incorporated to simulate fine-scale biomass distribution and cycling impacts to regional carbon balance.

4.2.2 CASA Disturbance Modules

To represent land-cover land-use change found in remote sensing data with simulations, CASA modules were implemented for agriculture, logging, insect herbivory outbreaks, and fire dynamics found in previous analysis. A similar approach to incorporate ecosystem dynamics was employed in mechanistic scalars from tabular records in the Century model for agriculture (Parton et al. 1998); however my approach herein is heavily dependent upon remote sensing inputs to understand spatial physiological dynamics of vegetation. My outputs estimated scenarios of human and natural perturbation in a variety of North American ecosystems, providing NBP fluxes of each disturbance regime.

4.2.2.1 Midwest Agriculture Module

Management of agroecosystems is undertaken to maximize productivity, and yield per unit area managed over large regions, which can impact carbon cycling. This required an agriculture module implementation due to intensive land-use of Midwest short and tall grass prairies. Lobell *et al.* (2002) estimated

that 0.62 Pg C yr $^{-1}$ or ~20% of total Conterminous US's NPP is contained in agriculture lands, and from 1982 to 1998 increased 63 Tg C. Hicke *et al.* (2004) estimated through United States Department of Agriculture (USDA) harvest data NPP had increased 40% over 1972 values from 0.37 Pg C yr $^{-1}$ to 0.53 Pg C yr $^{-1}$ in 2001. NDVI anomalies in agriculture regions may indicate increased productivity or yield produced and exported for consumption that could evolve into a NBP sink, which necessitated further investigation calculating ecosystem balanced heterotrophic respiration.

Amount of biomass harvested from each pixel per year (C_{crop}) is derived as annual crop carbon yield calculated as sum of net primary production (NPP) allocated to above ground vegetation pools that are harvested (Equation 4.5); where fraction of agricultural above ground biomass ($fAGB_c$) corresponds to NPP fraction allocated to above ground pools in agricultural herbaceous areas. Harvest index (HI) is the ratio between the yield mass and the above ground biomass from Hay (1995), and (t) the number of time steps per year. Crop biomass is assumed 45% carbon (Schlesinger 1997) and 80% of NPP is allocated to aboveground parts (Steingrobe et al. 2001) which is partitioned as the root shoot ratio. Crop productivity was simulated as:

$$C_{crop} = \sum_{i=1}^{t} NPP_i \cdot fAGB_c \cdot HI \qquad (4.5)$$

Carbon exported is translated by a constant NPP fraction removed each time step, consequently harvest is not simulated as an event but as a continuous

removal of carbon from above ground vegetation pools (Kroodsma and Feild 2006). This approach allowed common model structure of fluxes from vegetation soil pools to translate differences observed in agriculture: (i) reduced fluxes from the soil pools (Kroodsma and Feild 2006) and (ii) consequent decreased R_h throughout the year (Kroodsma and Feild 2006; Lobell et al. 2002) as well as to (iii) estimate annual crop yield based on harvest indexes supported by the literature (Hay 1995). Values for ($fAGB_c$) correspond to that presented by Prince *et al.* (2001), also used by Hicke *et al.* (2004).

In order to reflect tillage, turnover rates increased of microbial (25%), slow (50%) and passive (50%) carbon pools (Randerson et al. 1996). Irrigation is reproduced by eliminating water stress effect (W_ε) on both NPP and R_h and by setting the soil moisture sub-model to constant field capacity ($EET = PET$). Analogously, temperature resistance above optimum temperature is simulated by assuming a constant (= 1) temperature effect scalar. NPP allocation in agricultural herbaceous areas is controlled by fraction of agriculture above ground biomass ($fAGB_c$) and in forested areas follows a fixed allocation of 1/3 per pool (root, wood and leaf). Dynamics in productivity stress and allocation were prescribed to better replicate field observations.

4.2.2.2 Boreal Fire Module

Fire is a dominant disturbance agent to productivity of ecosystems throughout the world and a module was included to simulate this process in

North American boreal forests (Stocks et al. 2003). Fire directly removes carbon converting pools of wood, leaves, and litter to atmosphere emissions while adding roots to decay in woody detritus pools. Recovering post-burn vegetation initially has reduced NPP and litter/detritus input to depleted soil pools compared to old growth forest in which NPP exceeds R_h for ~150 years resulting in long-term sink (Odum 1969; Tompson et al. 1996).

Fire events were simulated by removing biomass based on combustion completeness and mortality, removal of forest carbon (wood, leaves) removed, and transferred carbon between pools to account for biomass killed but not removed (similar to van der Werf et al., 2006 for fire). The leaf pool was removed and transferred to atmosphere emissions while burned roots or stumps were added to a new standing dead wood pool not included in prior simulations. This pool was created for this module to mimic moderate fire severity where standing dead wood has a slower decay rate than surface coarse woody debris pool that will reduce and prolong carbon respired over a longer time interval as compared to other studies (different from van der Werf et al. 2006). Amount of biomass burned from each pixel per event ($C_{emissions}$) was derived as carbon yield calculated as sum (NPP) allocated to above ground vegetation and surface detritus pools that burned; where ($fFGB_c$) represented fraction of wood/leaves above ground biomass and corresponds to NPP fraction allocated to above ground pools in forested areas, (t) corresponds to time of forest productivity and is simulated as the following:

$$C_{emissions} = \sum_{i=1}^{t} NPP_i \cdot fFGB_c \quad (4.6)$$

Other terms such as losses of soil organic carbon by leaching, forest floor mosses, and herbivory, were ignored. Some post-fire ecosystem changes were not modeled, such as increased soil temperature associated to lower albedo affect on R_h. Instead, differences in NEP behavior resulting solely from including post fire carbon pool dynamics was the focus. Post-fire recovery of NPP was prescribed from ecoregions mean NDVI recovery from post-burn sites defined by the Large Fire Database allocating half of NPP carbon to leaf and root pools in locations with forest cover for the first nine years following fire.

4.2.2.3 Boreal Logging Module

Logging of North American forests is a dominant disturbance agent to ecosystem productivity which has resulted in a carbon sink (Caspersen et al. 2000; CCSP 2007). Agro forestry for wood/paper resources removes biomass and sequesters carbon for long periods of time in products needed to sustain human society. Similar to agriculture in carbon export or harvest, wood is removed from the ecosystem, reducing litter/detritus input into soil pools which reduce R_h creating a sink.

Harvest events were simulated, by satellite observations from Landsat, removal of carbon forest products (wood), and transferring carbon between pools to account for biomass killed but not removed (similar to van der Werf *et al.*, 2006 for fire). A fraction of leaves are transferred to the detritus pool and roots or

stumps are added to soil detritus pools and allowed to decay. Amount of biomass harvested from each pixel per disturbance event (C_{logged}) is derived as carbon yield calculated as sum of NPP allocated to above ground vegetation pools harvested; where ($fWGB_c$) represented fraction of wood above ground biomass and corresponds to fraction (NPP) allocated to above ground pools in forested areas, (t) corresponds to time of harvest. Forest productivity with logging is simulated as:

$$C_{logged} = \sum_{i=1}^{t} NPP_i * fWGB_c \quad (4.7)$$

Post logging recovery was prescribed from the observed dynamics of NDVI recovery. Some post-harvest ecosystem changes were not modeled, such as leaching, and increased soil temperature that affects decomposition (Burke et al. 1997). Instead differences in NBP behavior resulting solely from including post logging carbon pool dynamics were the focus.

4.2.2.4 Boreal Insect Herbivory Outbreak Module

Insect outbreaks are a natural disturbance to North American forests and one of the dominant agents to ecosystem productivity which has produced a carbon sink from regrowth. Numerous species of insects infest and defoliate forests throughout North America with impacts of constant reduction of productivity to intense outbreaks which decimate and kill specific forest species (USDA 2005). From previous work spruce budworm was found to have an extensive outbreak in eastern Canada (mid 1970s) decimating balsam fir (*A.*

balsamea) and white spruce (*P. glauca*) (Blias 1983). Spruce budworm (*C. fumiferana*) has the widest distribution of all budworm species extending from central Alaska to Newfoundland (NRC 2007). To account for impact of insect outbreaks, a module was created that removed leaf carbon and allowed regrowth to occur after leaf consumption, while allowing a portion of C to enter litter/detritus soil pools which altered R_h.

Outbreaks were simulated in a similar manner to continuous herbivore consumption presented in the literature by Randerson et al. (1996). However, in my simulation, an outbreak completely decimates the leaf pool. Empirical equations have been developed by McNaughton et al. (1989) and were the basis of my implementation to estimate impact of herbivory during the growing season on plant productivity where leaf biomass consumed by herbivores is related to net the annual sum of NPP. Randerson et al. (1996) calculated continuous herbivory consumption scaled to remaining annual sum of NPP from logarithmic scalars of herbivore consumption from McNaughton et al. (1989).

Maximum seasonal herbivore consumption (SHC) is calculated to replicate impact of insect herbivory on NPP. To prescribe outbreaks (SHC) is allowed to consume all available NPP and leaf pool at time of outbreak (t). Amount of leaf biomass consumed from each needle leaf evergreen forest pixel per disturbance event $(C_{outbreak})$ is derived as carbon yield calculated as sum of NPP allocated to above ground vegetation pools that are consumed; where $(fLGB_c)$ represents fraction of forest biomass and corresponds to (NPP) fraction allocated to above

ground pools in forested areas, (SHC) corresponds to maximum seasonal herbivore consumption. Forest productivity with spruce budworm outbreak in needle leaf forest is simulated as:

$$C_{outbreak} = \sum_{i=1}^{t} NPP_i * SHC * fLGB_c \quad (4.8)$$

Post outbreak recovery of NPP was prescribed from observed dynamics of NDVI recovery, consumption of leaf carbon and assimilation carbohydrates in the budworm, and transferring carbon between pools to account for biomass consumed (similar to Randerson et al. 1996 for herbivory). Assimilation of carbon consumed by spruce budworm was assumed to be 0.6 which is a rough approximation of all types of herbivores, invertebrates (LaMotte and Bourliere 1983) and mammals (Randerson et al. 1996). This value was implemented to enable calculation of pastureland herbivory in simulations. Future simulations could insert values specific to certain types of herbivores which would likely improve results. Differences in NEP (no herbivory) and NBP (herbivore outbreaks) behavior resulting from post outbreak carbon pool dynamics was the focus.

4.3 Results

Simulation results were grouped by disturbance type and modules utilized to alter carbon pools. All simulations were carried out for the period o 1982 to 2005, presented with and without fine-scale disturbance dynamics to understand implications in the regional carbon balance of ecosystems with increased NDVI.

4.3.1 Climate Warming in the High Latitudes

The Mackenzie River Delta and Newfoundland and Labrador study regions located in the higher northern latitudes had no marked change in vegetation cover. Prior ancillary analysis of meteorological stations found abiotic impacts of warming temperatures extended growing seasons and reduced snow cover (Neigh et al. 2008). Simulations in these regions did not require module modification to CASA due to lack of disturbance from land-cover change. Climate warming and enhancement of NPP was apparent in both High Latitude study regions.

4.3.1.1 Yukon, Mackenzie River Delta

The Mackenzie River Delta study region located in the Arctic Circle has extreme variations in temperature and solar insulation, with little to no direct influence of human alterations to land cover. Short growing season productivity is primarily limited to summer months of June, July and August, (JJA) and permafrost controls nutrient availability to vegetation cover which consists of dwarf trees/shrubs and grasslands (Pavelsky and Smith 2004). Previous work found increased photosynthetic capacity (duration and amplitude) of vegetation due to extended growing season from earlier onset of spring (Neigh et al. 2008). Warm periods with few periods of temperatures below -2 C° monthly climate normal have occurred in this region. The Mackenzie River Delta has a similar climate to the Arctic slope and previous studies neighboring this region have found responses to long term (50+ years) warming of increased shrub land cover

(Sturm et al. 2005; Tape et al. 2006). Previous investigation by Neigh et al. (2008) found no marked change in vegetation cover observed from Landsat and other high resolution remote sensing data over the past 30 years (i.e. NEP = NBP).

Simulations predicted increased NPP driven by temperature and NDVI. Soil respiration was limited due to cold periods which extend to -30 C° during winter and a minimum respiration threshold of -4 C° was placed due to inactive microbial respiration and decomposition (Monson et al. 2006). The region had inter-annual source sink variability with a moderate annual NEP (black filled circles) increase driven by increased NDVI and NPP with slow growth in R_h. The upper portion of the area plot indicates monthly NPP (sink) values with monthly negative R_h indicated on the lower portion of the upper plot as a source of atmospheric carbon. The lower portion of the plot indicates monthly average NDVI for the region (black curve) and monthly NDVI anomalies (black bars) (Figure 4.2). Monthly NDVI anomalies indicate early and sustained mid-growing season NDVI increases correspond to annual NEP sinks and below normal NDVI values for similar periods produce annual NEP sources.

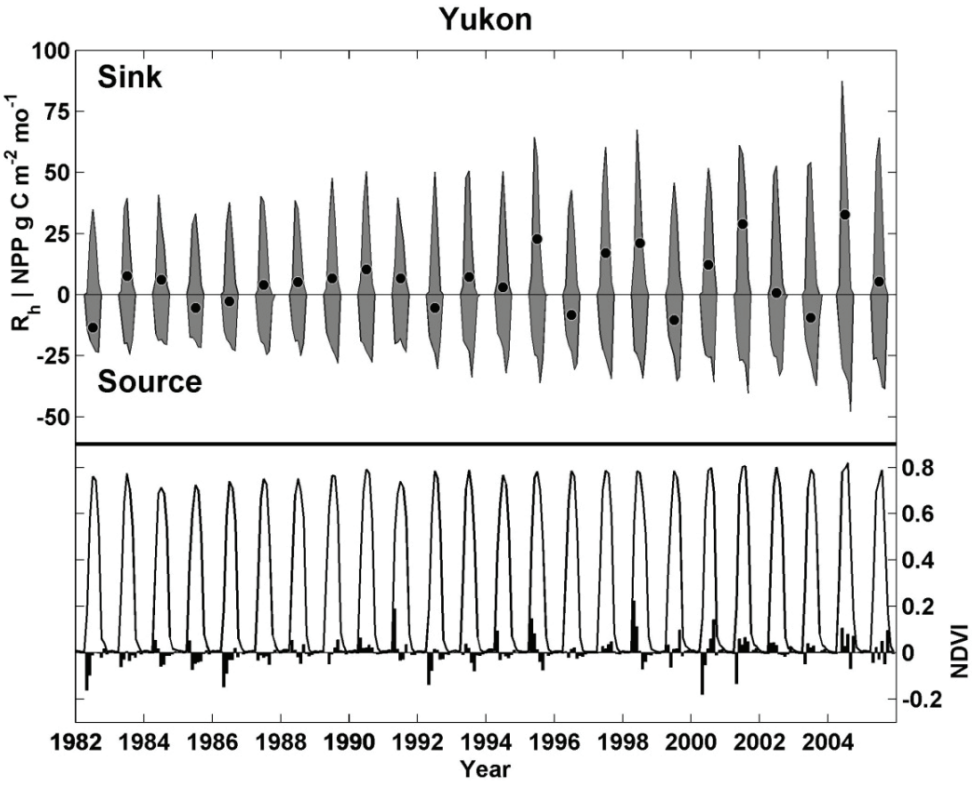

Figure 4.2 Annual mean time series of Yukon study region heterotrophic respiration (Rh), net primary production (NPP, grey curves), and annual net ecosystem production (NEP, black circles) from 1982 to 2005. Monthly regional average NDVI (black curves) and anomalies (black bars) show marked growing season anomalies impact annual NEP balance.

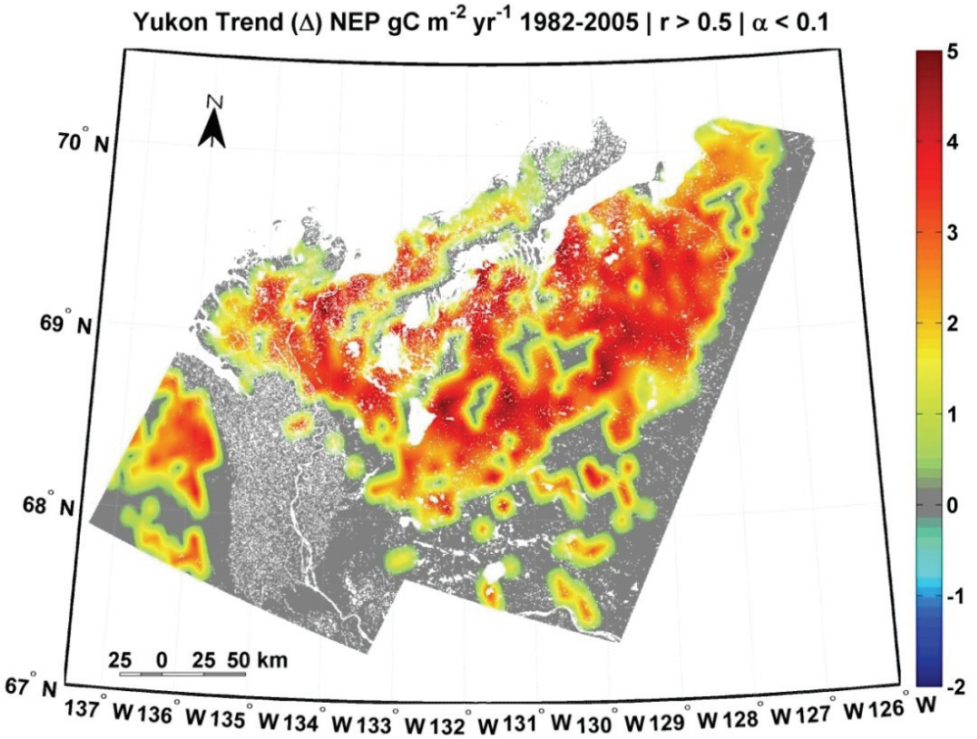

Figure 4.3 Yukon growing season (JJA) trend (Δ) of net ecosystem production (NEP) results. Trends retained if significance (α) < 0.1 and correlation (r) > 0.5.

Statistically significant JJA sequestration trends from 1982 to 2005 were found in short vegetation grasslands (0 - 5 g C m^{-2} yr^{-1}) surrounding the River Delta (Figure 4.3). Cold periods limit R_h which typically follows increased NPP in herbaceous vegetation cover types in non-temperature constrained systems. Climate warming with increased precipitation had a marked impact on NPP and R_h during the 1982-2005 period (Figure 4.4). Increased annual temperature and precipitation was found to drive increased NDVI which impacts simulated NPP and R_h, however growth in R_h lags NPP resulting in a sink.

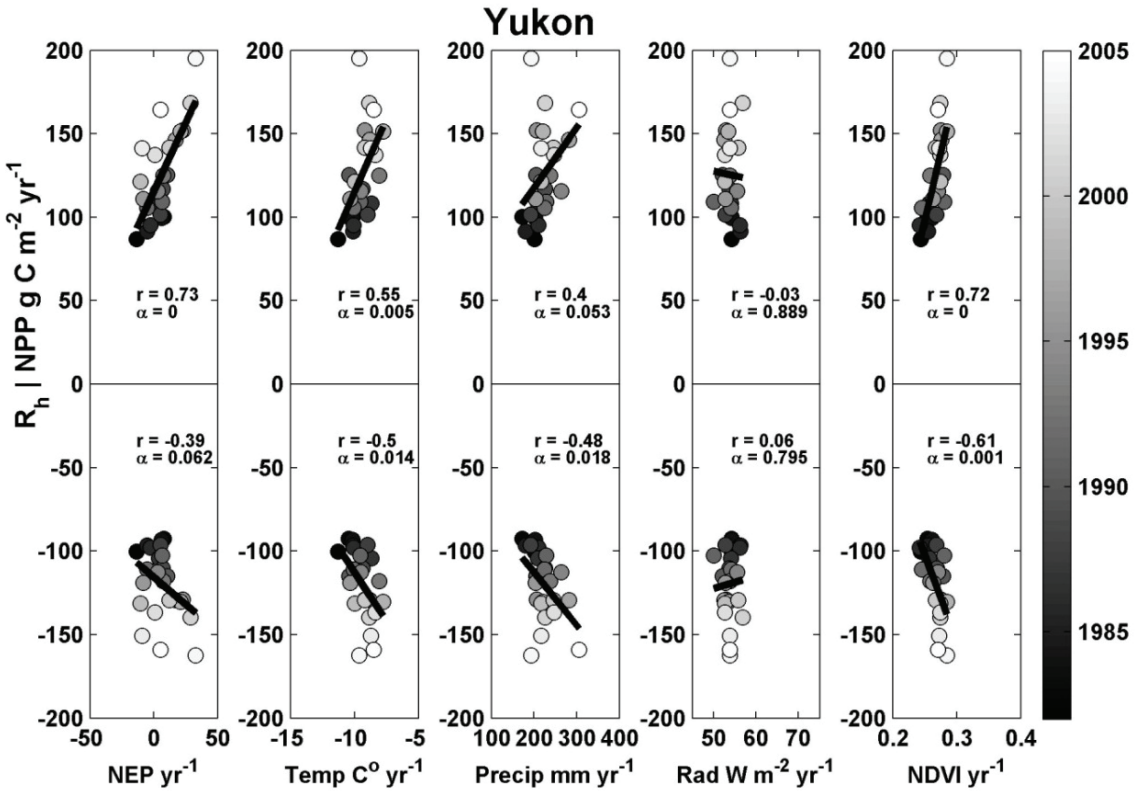

Figure 4.4 Scatter plots of Yukon mean annual sum NPP, R_h, NEP, NDVI, and climate, with correlation (r) and significance (α).

The Yukon, Mackenzie River Delta region is typical of an Arctic biome with grassland tundra vegetation intermixed with small dwarf trees and shrubs, that have long turnover intervals due to temperature constrained R_h. Sequestration in these biomes is associated to low respiration rates, reduced decomposition and accumulation of peat. Warming during winter months above -4 C° would reduce sinks predicted due to enhancement of soil respiration and decomposition of peat. This may be indicative of what has occurred in other Arctic regions, however once vegetation reaches production maxima constrained by net evapotranspiration balance, large stores of deep organic soil carbon could respire at enhanced rates from warming which would produce a net carbon source. A recent study has found loss in productivity and increased respiration in dwarf trees and shrubs vegetation cover near Inuvik due to thermal stress (Pisaric et al. 2007). Currently simulations of arctic and boreal ecosystems are limited due to lack of knowledge of soil hydrology, permafrost depth, vertical structure of organic matter, and biogeochemical processes of thawing permafrost. The Mackenzie River Delta study region from 1982-2005 was predicted to be a net carbon sink driven by earlier start of Spring, increased NPP and slow growth in R_h in herbaceous cover types, however these results do not include a number of processes due to a gap in knowledge of Arctic soil processes.

4.3.1.2 Newfoundland and Labrador

The island of Newfoundland and Labrador coast is a mixed maritime boreal forest influenced by the confluence of ocean currents of the cold Labrador and warm Gulf Stream. The vegetation cover consists of dense mixed boreal forest of trembling aspen (*P. tremuloides*), paper birch (*B. papyrifera*), white spruce (*P. glauca*) and black spruce (*P. marinana*) in the west and the central and eastern portions of the island are open lichen woodland. Maritime climate alters vegetation productivity depending on what current is dominating flow. The entire island (100,000 km^2) had a marked increase in NDVI over the 1992-1999 period associated to warming and lengthening of growing season, while land-cover land-use change is not a dominant factor (i.e. NEP = NBP) due to limited population density and poor agriculture soils (Neigh et al. 2008). Similar to Yukon warming, few periods of temperatures below -2 C° monthly climate normal have occurred.

Model predictions for the period of 1992 to 1999 had increased NPP driven by higher temperature. Newfoundland net annual NEP varied markedly as a net sink and source during the entire 1982 to 2005 record. A cold period from 1991 to 1994 reduced NPP while respiration persisted producing a moderate annual NEP source. Similar to the Yukon a minimum R_h threshold of – 4 C° was initialized due to inactive microbes (Monson et al. 2006), but Newfoundland and Labrador have a boreal climate where winter temperature minima reach -15 C° and shoulder seasons can influence R_h for longer annual cycles. Unlike the

Yukon, early season positive NDVI anomalies do not impact annual NEP; only sustained growing season increases produced NEP sinks while sustained growing season negative NDVI anomalies produced NEP sources. Temperature thus plays a critical role to productivity in this region as it drives increased NPP and alters heterotrophic respiration (Figure 4.5).

Statistically significant vegetation cover sequestration from 1992 to 1999 was focused in needle leaf evergreen forest (10 – 25 g C m^{-2} yr^{-1}) and mixed needle leaf evergreen forest, and shrubs/short vegetation grasslands (0 – 10 g C m^{-2} yr^{-1}) (Figure 4.6). Warming during winter months above -4 C° is critical to NEP balance in herbaceous cover due to lack of NPP and extension of R_h during shoulder seasons. Continued warming could reduce NEP predicted in this region and possibly throughout the Northern Latitudes due to enhancement of R_h. Vegetation cover types were predicted to have alternate responses to warming from 1992 to 1999. The NDVI anomaly observed has inter-annual variability transitioning from a NEP source during the 1991 to 1994 cool period with low NPP to a moderate sink as NPP recovered (Figure 4.7). However, interior herbaceous cover NEP did not contain statistically significant trends from warming while forests throughout the region have retained more carbon. Newfoundland and Labrador thus have a dynamic cover type dependent inter-annual NEP response to temperature shown in NDVI during the 1990s.

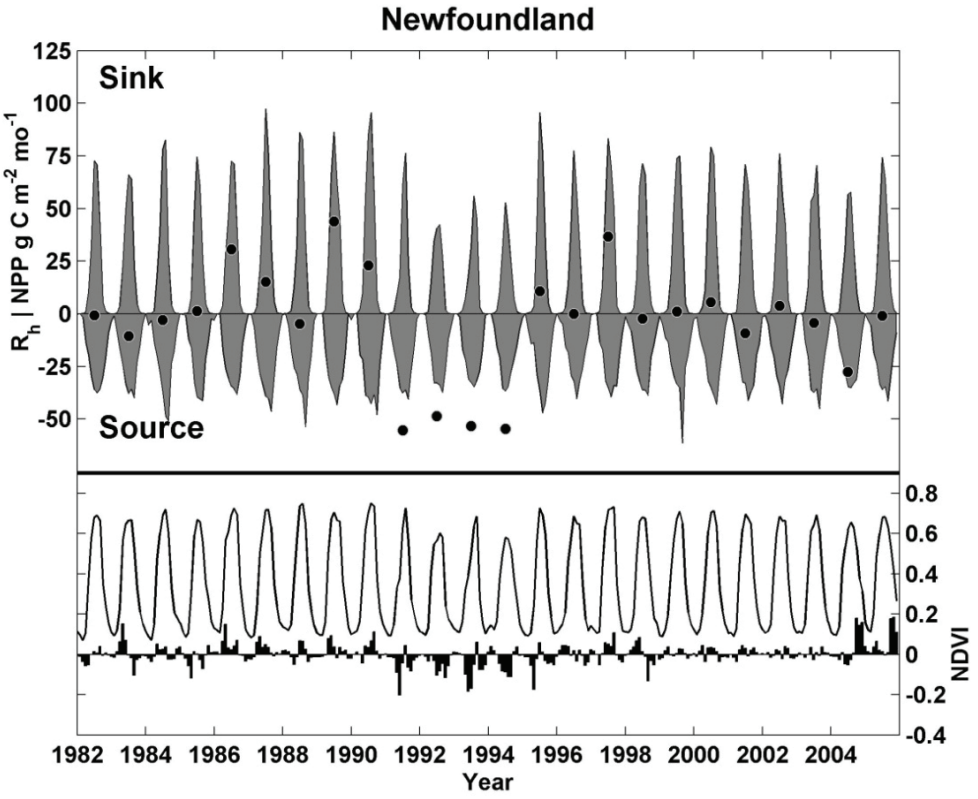

Figure 4.5 Time series of Newfoundland study region heterotrophic respiration (R_h), net primary production (NPP grey curves), and annual net ecosystem production (NEP, black circles) from 1982 to 2005. Monthly average NDVI (black curves, lower plot) and anomalies (black bars, lower plot) show marked (> −0.2) growing season anomalies from 1991 to 1994 impact annual NEP.

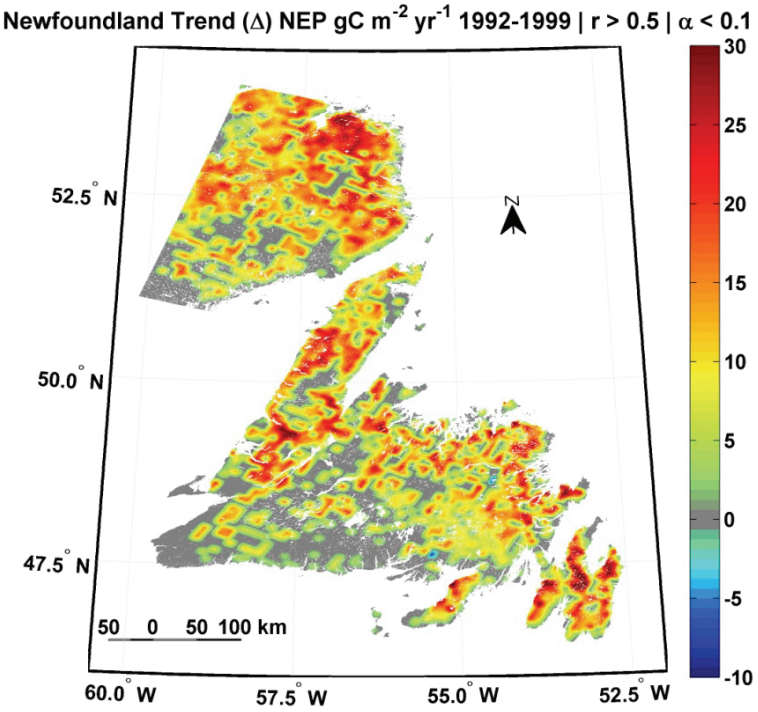

Figure 4.6 Newfoundland growing season (May-Sept) trend (Δ) net ecosystem production (NEP) results from 1992 to 1999. Trends retained if significance (α) < 0.1 and correlation (r) > 0.5.

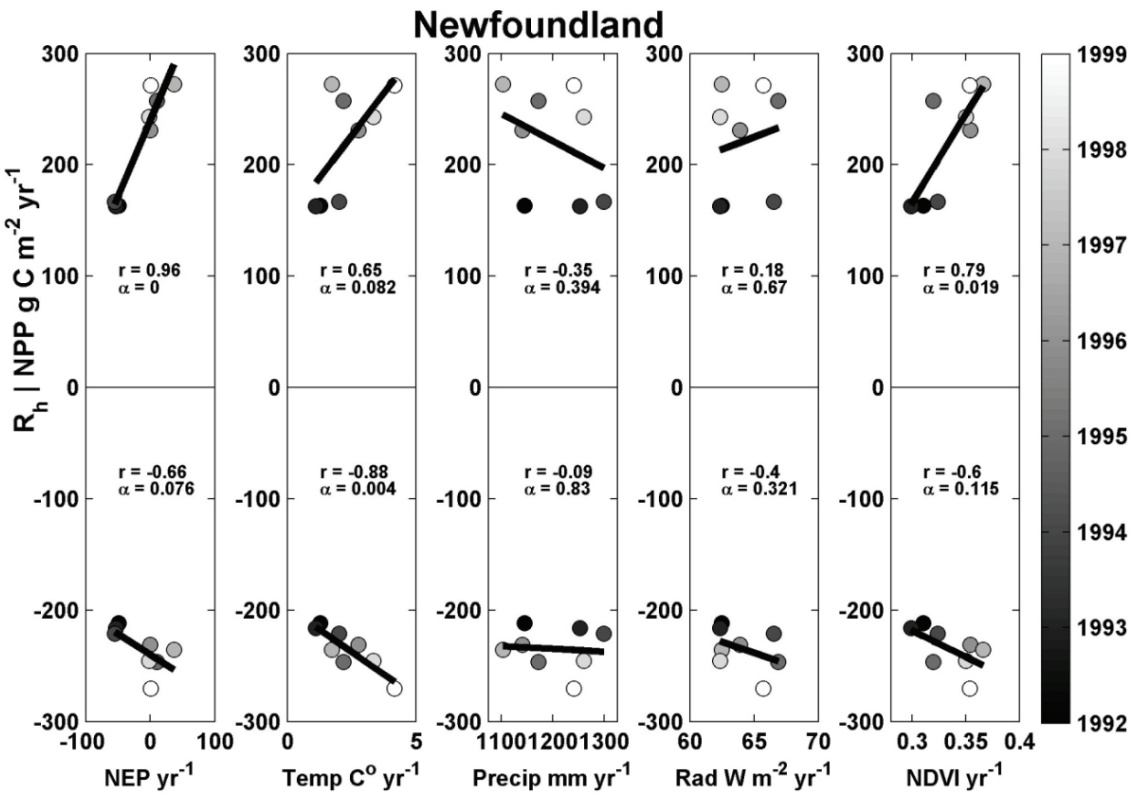

Figure 4.7 Scatter plots of 1992 to 1999 Newfoundland mean annual sum NPP, R_h, NEP, NDVI, and climate with correlation (r) and significance (α).

4.3.2 Fire Disturbance and Recovery in the Boreal Zone

The fire module which accounts for fire disturbance impacts to above ground biomass pools and simulated post-fire recovery was implemented in a region (Northern Saskatchewan) of the boreal zone where fire is the dominant disturbance agent to ecosystem productivity. Widespread fires in 1980 and 1981 burned over 3.5 million hectares in total throughout the province of Saskatchewan was found to drive the 1982 to 1991 NDVI trend (Neigh et al. 2008).

4.3.2.1 Northern Saskatchewan

The Northern Saskatchewan study region lies on boundaries of two ecoregions, the closed boreal forest and the open lichen woodland. Division between ecoregions is abrupt in northern boundaries of Manitoba and Saskatchewan with large differences in forest cover density and standing carbon. Two conifer species are nearly ubiquitous, white spruce (*P. glauca*) and black spruce (*P. marinana*) with other deciduous species of larch or tamarack (*L. laricina*), balsam fir (*A. balsamea*), balsam poplar (*P. banksiana*), trembling aspen (*P. tremuloides*) and white or paper birch (*B. papyrifera*) are intermixed depending on age of succession. Prior glacial periods produced peat bogs and muskegs that sporadically dot the landscape among dense forest stands.

Simulations had increased NPP driven by increased NDVI from post-fire recovery from the early-1980s and mid-1990s. Minor variability climate occurred during the 1980s allowing post-fire recovery. However, a mid-1990s dry period occurred which drove wide spread fires in 1995 throughout the Northern portion of the region. Fire dynamics were prescribed on a per pixel basis from fine-scale Landsat analysis and compared with the North American Large Fire database (LFDB) (Stocks et al. 2003). Large burn events were observed in MSS data during the 1970s which precluded using the Large Fire Database which spans 1980 to 1997. Burn events are common in this region and simulating recovery of vegetation and loss of carbon due to fire disturbance was imperative to this ecosystem.

To eliminate erroneous low values of NBP it is essential to select a year of a non-anomalous dynamics of fire and climate. Anomalies were calculated and extensive knowledge of fire disturbance periods were investigated to select a year with less than 100,000 hectares burned and > 10 years since large fire outbreaks (> 500,000 hectares). Recovering vegetation on a per pixel basis may contain NDVI recovery trajectories (Amiro et al. 2000; Goetz et al. 2006; Hicke et al. 2003) not desired in model spin-up. A year with minimal change in climate and fire disturbance was implemented.

Inclusion of fire disturbance had altered soil pool and recovery dynamics which produced differences in annual NEP and NBP calculations in regions with > 25% forest cover and > 50% 8km pixel burned (Figure 4.8). Differences become more pronounced through time as regeneration of soil pools and above ground wood pool took place in relation to forest density and burn extent. Fine-resolution Landsat was used to define fire disturbance as human settlements and roads are not a common feature of this landscape (Neigh et al. 2008). Approximations of time periods to apply fractional fire disturbance derived from Landsat in simulations were defined from imagery from the 1970s to late 1980s and 2000s time period as the LFDB was not available in polygon burned area extent before 1980. Burned area between the 1990s and 2000s was determined to be 1995 from the LFDB (Stocks et al. 2003).

Fire disturbance to vegetation productivity had a marked impact on NPP and respiration. NDVI anomalies found drove increased NPP during the 1980s

from post-fire recovery from large fire years in the late 1970s, 1980 and 1981. Large fire events before AVHRR measurements appeared as increased productivity with little soil respiration change. Difference between calculation of NEP and NBP accounting for fire disturbance, a dead wood pool, and altered allocation produced growing sinks of carbon through time.

NDVI captured disturbance and post-fire recovery and was simulated in NBP as a net sink with increased carbon storage. Upper portion of the area plot presents NPP for fire and no-fire module simulations, the lower negative portion of the plot indicates monthly soil respiration, with annual balance of NEP (no-fire) and NBP (fire) indicated in the lower plot (Figure 4.9). Sequestration rates from 1982 to 2005 ranged from > 20 g C m^{-2} yr^{-1} after disturbance to ~5 g C m^{-2} yr^{-1} for > 15 years after disturbance. Differences were due to above ground woody pools post fire recovery, surface structural and metabolic pools rebuilding with low R_h from small soil pools which are not fed by mortality of vegetation. Wood cover regional density increased from North to South, and sequestration follows a similar pattern even though fire disturbance is pervasive throughout the region. Mortality was exceptionally low in locations with forest cover density less than 50% which produced smaller than expected differences between simulations. Fire disturbance and post-fire recovery can have a marked impact altering carbon dynamics for long periods of time (>100 years). Regional understanding of post-fire vegetation dynamics was found to be an important component with differences between simulations of NEP (no fire) and NBP (fire).

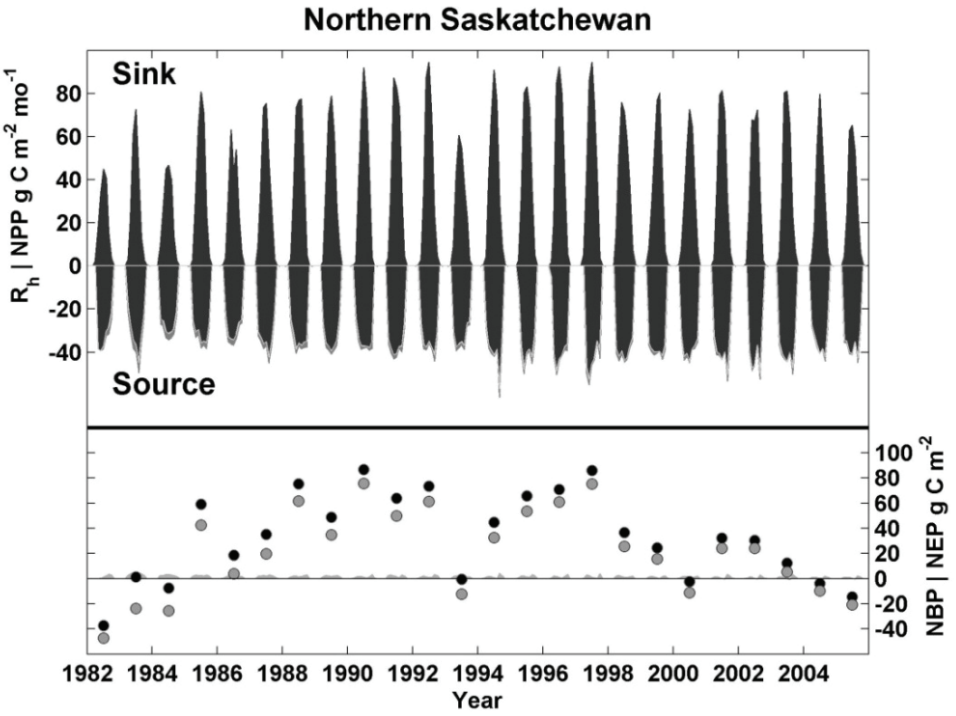

Figure 4.8 Northern Saskatchewan time series of NPP, R_h, NEP and NBP with fire, fractional and burned area extent change, indicated with dark grey (NPP) and (R_h) curves in regions with > 25% forest cover and > 50% of an 8km pixel burned. Monthly control runs with no fire dynamics indicated in dark grey curves (upper plot). Monthly model predictions of the difference in simulations are shown (light grey curves, lower plot) with black (NBP) and grey points (NEP) indicating annual simulation with no fire dynamics.

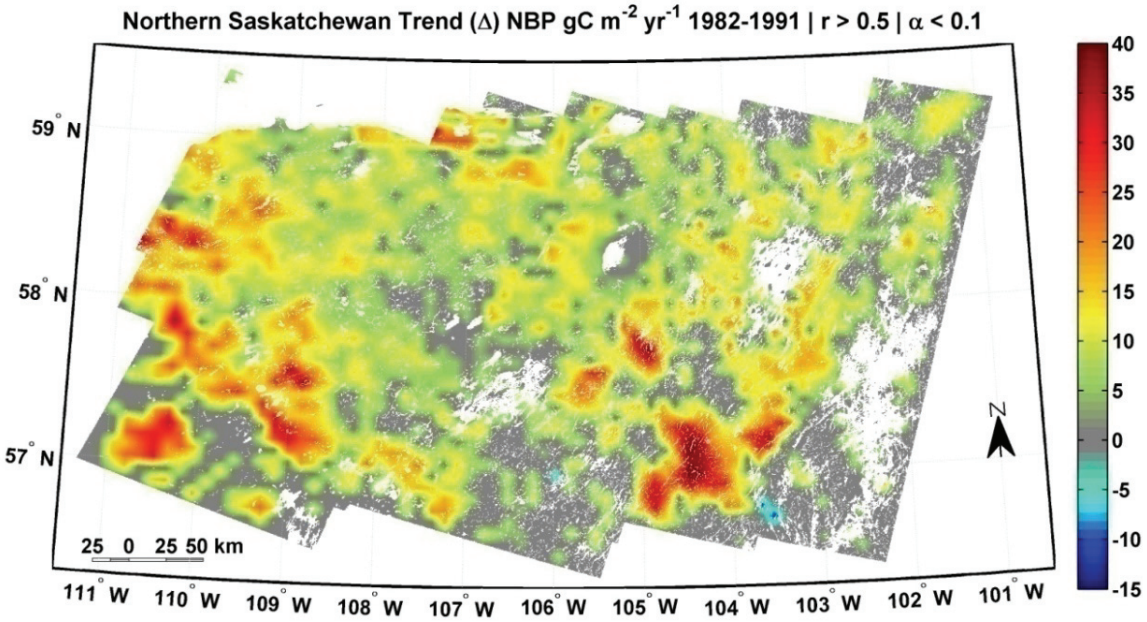

Figure 4.9 Northern Saskatchewan growing season sum (May-Sept) trend (Δ) net biome production (NBP) results with fire module on. Trends included if significance (α) < 0.1 and correlation (r) > 0.5. Note locations with the greatest increase were severely burned in 1980 and 1981 and had post fire NDVI recovery.

4.3.3 Changes in Agriculture Practices in the Midwest

The agriculture module accounted for harvest and was implemented to simulate Midwest agriculture production practices in two regions of irrigated (Oklahoma Panhandle) and non-irrigated (Southern Saskatchewan) croplands. Precipitation variability (Southern Saskatchewan) and land use change of expanded irrigated agriculture (Oklahoma Panhandle) were land cover dynamics found responsible for marked increases in NDVI. The agriculture module was developed to account for fine-scale NBP dynamics found in previous Landsat and ancillary data analysis (Neigh et al. 2008).

4.3.3.1 Southern Saskatchewan

The Southern Saskatchewan and Dakotas study region is primarily composed of agriculture and pasture land located in the Great Plains northern boundaries commonly referred to as the 'Prairie Pothole' region because of ancient glacial depressions of several hundred thousand small (< 100 ha), shallow (maximum depth < 5 m) pothole lakes which lie in depressions that extend over > ~750,000 km^2 of the American Midwest and Western Canada (Covich et al. 1997). Upland areas primarily produce sorghum, corn and wheat; precipitation limits growth. Droughts are common throughout the high plains and during simulations, a drought was noted during the mid-1980s which altered production of ~7,000 km^2 of agriculture land (Neigh et al. 2008). Drought subsided in 1992; and NDVI increase was due to recovery and marked increase in precipitation throughout the 1990s (Trenberth et al. 1988). Coarse gridded

climate datasets captured drought in this region, which persisted through growing season months from 1983 to 1988. Evaluation of anomalous climate enabled climate normal selection for implementation of model spin-up to avoid stressed light use efficiency (ε). Due to strong climate influence, variability in growing season annual anomalies of precipitation, temperature and solar radiation were calculated.

Simulations had increased NPP driven by NDVI and precipitation throughout the region during the 1990s. Minor solar radiation variation had occurred during the drought years from the early 1980s to 1992, while growing temperature varied less than 1.5 C°. Crop harvest during 1980s declined due to lack of rainfall, which produced low productivity and low amounts of carbon entering the soil detritus pools. The fast turnover rate of herbaceous vegetation throughout this region enabled respiration to closely follow NPP. Reduced biomass entering soil detritus in turn reduced heterotrophic respiration. This was observed in simulation results when comparing the amplitude of the 1980s to the 1990s in Southern Saskatchewan. Net biome productivity was negative during dry years from climate stress (Simulated T_ε and W_ε stress scalars reduction of calculated NPP from maximum light-use efficiency) while respiration which should have had low R_h remained constant due to poor replication of hydrological impacts on microbial respiration (Figure 4.10). After drought, productivity exceeded respiration and NBP turned into a sink. Difference between calculation of harvest and without harvest varied from 20 g C m^{-2} yr^{-1} during the 1980s to >

60 g C m^{-2} yr^{-1} during the 1990s with simulated agriculture area land-cover land-use change. Southern Saskatchewan had marked interannual NEP variability without calculation of agriculture dynamics and growth in NBP with simulation of dynamics. Maps of NBP indicated that agriculture sites had statistically significant increases in productivity when accounting for harvest (Figure 4.11). Increased productivity was more substantial in locations defined as agriculture from fine-scale Landsat data. Locations with the most sequestration occurred where agriculture persisted throughout the 1982 to 2005 period. Surrounding vegetation is used for pasture which had little change and stayed close to the carbon balance, however grazing was not simulated. During the 1990s precipitation increased, vegetation productivity increased and harvest increased, producing an NBP (Harvest) sink from 1982 to 2005 (Figure 4.12).

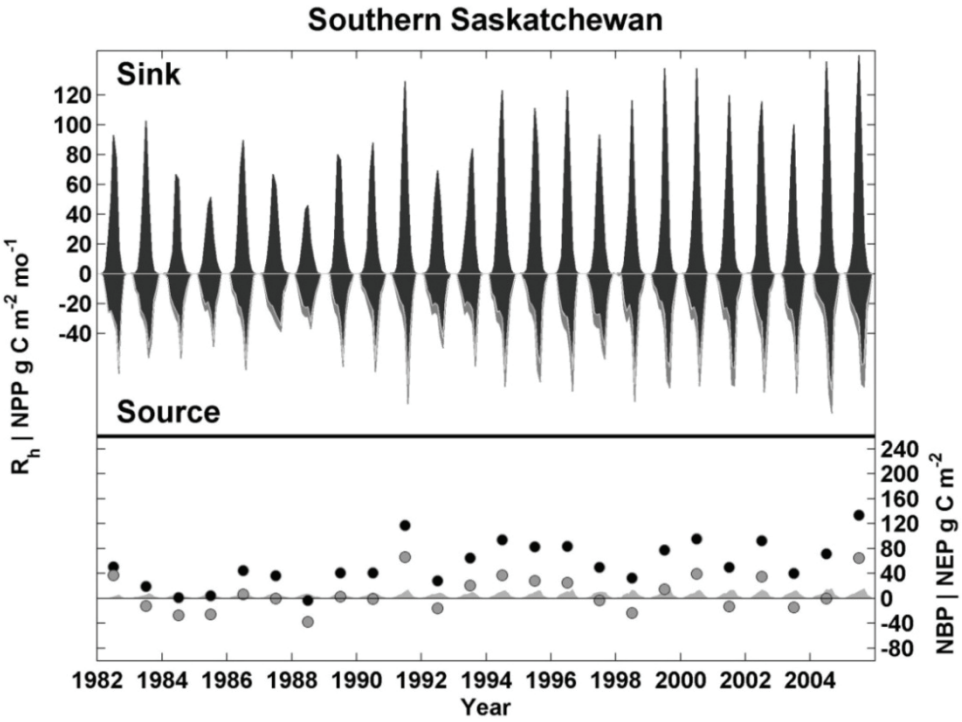

Figure 4.10 Southern Saskatchewan mean time series of NPP, Rh, NEP and NBP with agriculture harvest land cover change, and no soil tillage, indicated with black (NPP) and (Rh) curves. Monthly model predictions of the difference in simulations are shown (light grey curves, lower plot) with black (NBP) and grey points (NEP) indicating annual sum with and without agriculture dynamics.

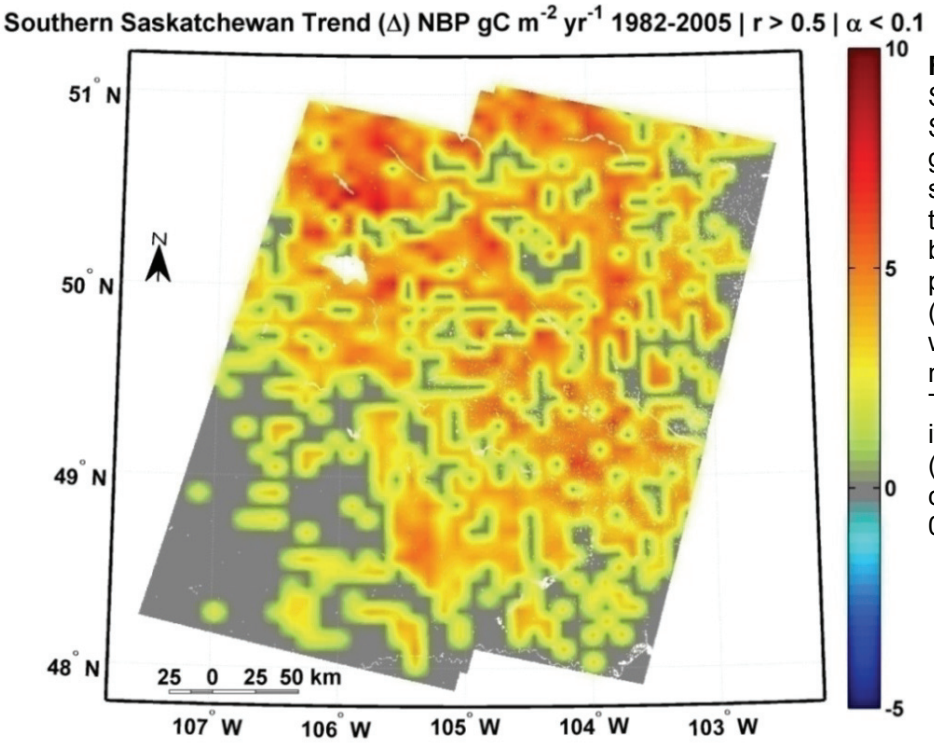

Figure 4.11 Southern Saskatchewan growing season sum (May-Sept) trend (Δ) net biome production (NBP) results with agriculture module on. Trends included if significance (α) < 0.1 and correlation (r) > 0.5.

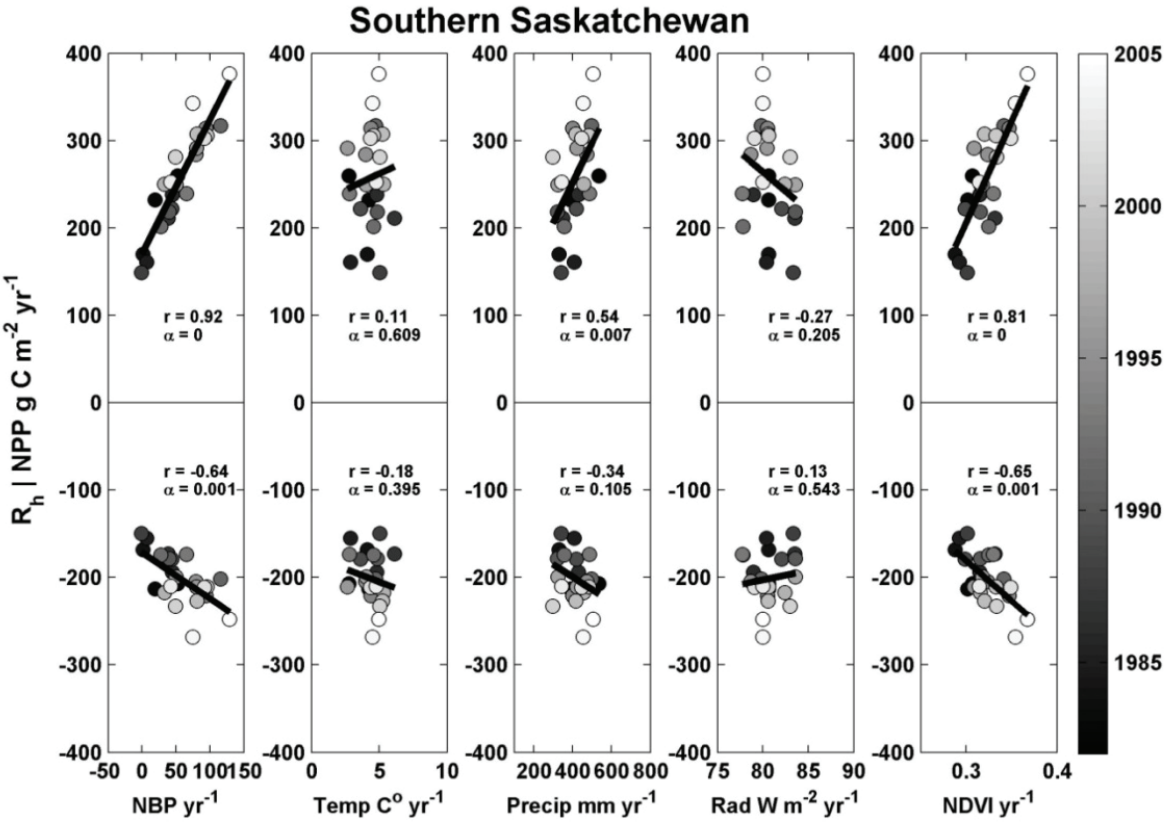

Figure 4.12 Scatter plots with agriculture module-on of annual regional sum NPP, R_h, NBP, NDVI, and climate with correlation (r) and significance (α).

4.3.3.2 Oklahoma Panhandle

The Oklahoma Panhandle study area is dominated by human land use of agriculture and pasture land. A similar agro ecosystem to the Southern Saskatchewan and Dakotas study region exists here, however, this landscape consists of flat to irregular plains where sedimentary bedrock is overlain by alluvial deposits. Precipitation has been found to spatially and temporally modulate NDVI in Kansas which neighbors this study region (Wang et al. 2001). The past 20 years had variations in crop type and production practices with increasing reliance on center pivot irrigation to eliminate drought stress and

increase yield. Irrigation practices and crop selection (conversion from wheat to corn) were found to explain the NDVI anomalies observed (Neigh et al. 2008). Water stress (W_ε) was removed from agriculture pixels and the effect of till and no-till on soil respiration was initialized reducing soil respiration.

Simulations revealed a dynamic system in which understanding land-cover land-use change is critical to the knowledge of a source or sink. A majority of this change was due to growing season productivity increases of non-stressed agriculture expansion into former pasture lands during the late 1980s and 1990s. Monthly increases in productivity can be observed as the difference between the monthly no-harvest (dark grey curve) and harvest (black curve) trends from 1982 to 2005 (Figure 4.13). Exclusion of harvest, irrigation and no tillage of the soil changed the region to a NEP source with increased NDVI due to the strong influence of climate and down regulation of NPP due to temperature (T_1) and precipitation stress scalars(W_ε) as found in the upper portion of the plot as the difference between black (Harvest, irrigation, and no-tillage) and grey (No Harvest) curves. Accounting for harvest (NBP), and excluding biomass from entering heterotrophic pools presented in the lower portion of the upper plot as the difference between black (NBP) and grey curves (NEP) is critical to classify the Oklahoma Panhandle region as a source or sink of atmospheric carbon.

Maps of NBP indicated that agriculture sites had marked increases in productivity when accounting for harvest than without harvest (Figure 4.14). Increased productivity was substantial in locations defined as agriculture from

Landsat due to expansion of harvest in former grasslands. Surrounding vegetation in this region is primarily short grass prairies which are used for pasture. Pasture lands had little change and stayed close to balance, however grazing was not simulated. Locations with the most carbon sequestered were regions that had agriculture throughout the 1982 – 2005 time period and the expansion of irrigated agriculture into pasture lands increased the overall regional carbon sink by enhancing NPP and reducing R_h. No statistically significant trends were found between climate and ecosystem productivity. Expansion of irrigated agriculture and inclusion of harvest produced marked differences in the annual trend of carbon sequestered. Locations which had simulation treatments of no-tillage, no climate stress, and harvest (NBP) sequestered carbon at a rate up to four times greater than no-harvest (NEP) simulations. NBP calculation in this region produced marked differences in estimates of carbon sink status.

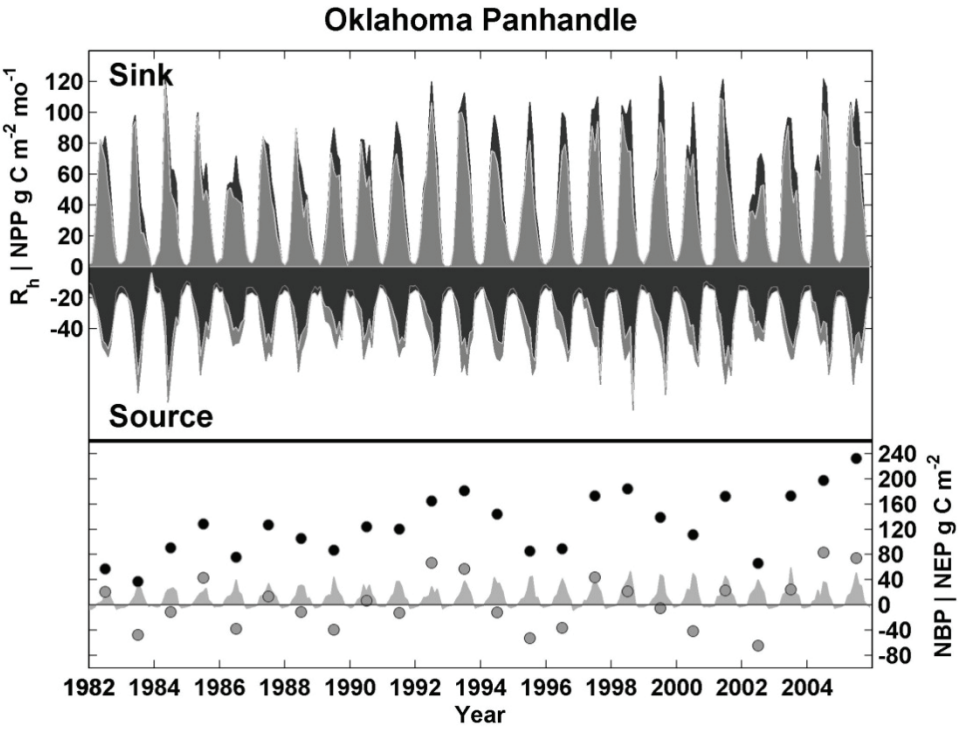

Figure 4.13 Time series of regional mean NPP, R_h, NEP and NBP with agriculture harvest land cover change, irrigation and no soil tillage, indicated with black (NPP) and (R_h) curves. Simulation with no agriculture module indicated in dark grey curves (upper plot). Monthly model predictions of the difference in simulations are shown (light grey curves, lower plot) with black (NBP) and grey points (NEP) indicating annual sum with and without agriculture dynamics.

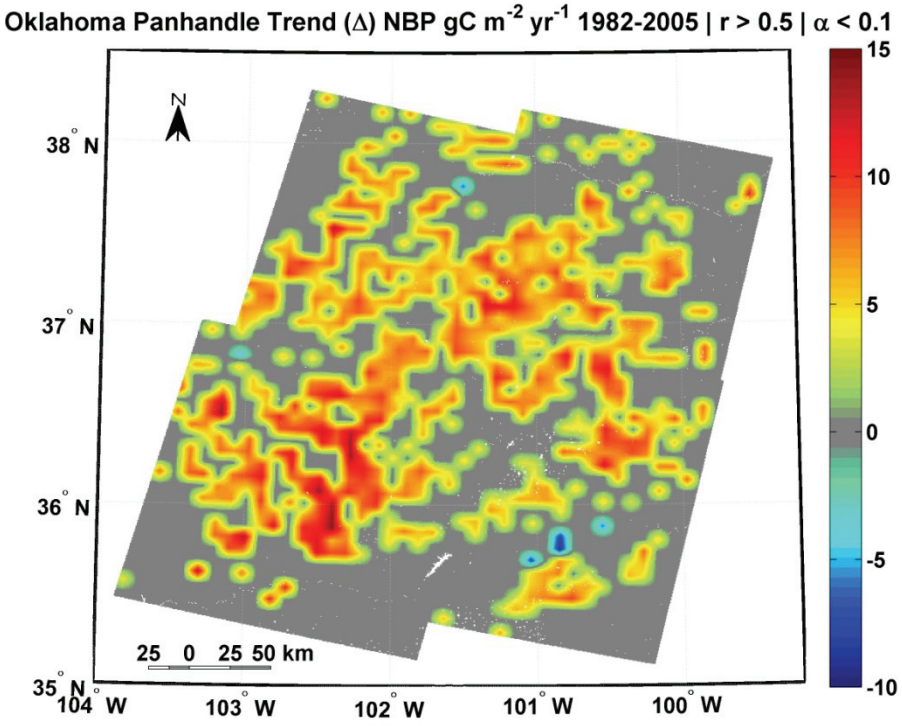

Figure 4.14 Oklahoma Panhandle growing season sum (May-Sept) trend (Δ) net biome production (NBP) with agriculture module on. Trends were included if the significance (α) < 0.1 and correlation (r) > 0.5.

4.3.4 Herbivory and Logging in the Boreal Zone

4.3.4.1 Southern Quebec

The southern Quebec study region is mixed boreal forest with common tree species including: white spruce (*P. glauca*); and black spruce (*P. marinana*); eastern larch (*L. laricina*); balsam fir (*A. balsamea*); jack pine (*P. banksiana*); trembling aspen (*P. tremuloides*); and paper birch (*B. papyrifera*). This region experienced an extensive outbreak of spruce budworm (*C. fumiferana*) during the mid 1970s and salvage logging took place into the early 1980s (Blias 1981, 1983). Fire disturbance does not modify the land cover extensively as regional climate is typically humid (Pham et al. 2004), and large fire events have only been observed further to the north (Stocks et al. 2003). Population density occurs toward the east in the Saguenay Lac Saint-Jean region where over 300,000 inhabitants are distributed over 56 municipalities(Alma 2007).

Simulation results for the period of 1982 to 2005 had increased NBP driven by forest harvest, and forest recovery in distinct locations experiencing marked increase in NDVI. Herbivory outbreak followed by logging drove increased NDVI, NPP, and NBP during the 1980s. No statistically significant trends in abiotic drivers had occurred or trends in NEP associated to land cover classes other than forest-regrowth. Calculation of NBP provided a marked difference in simulating herbivory outbreaks and logging as compared to simulations without logging on a monthly time step due to reduced dead material left behind after harvest (leaves, stumps and slash wood) which enter and

enhance the soil pools heterotrophic respiration (R_h). Simulated disturbance events from fine-scale Landsat are shown as monthly NEP - NBP difference (grey curves) in 1982 and 1988 in locations with > 25% forest cover and > 50% disturbed (Figure 4.15, lower). A long term small carbon sink is produced that occurs >15 years after the disturbance which is driven by the recovering woody pools and lack of litter input to the soil microbial pools resulting in reduced R_h. The annual difference between NEP and NBP was surprisingly small as continuous herbivory consumption reduced NPP offsetting the R_h sink from recovering carbon pools. The monthly difference (grey curves, lower plot) captures this dynamic which could be overlooked by only investigating the annual balance. Growth of this future sink is captured although the length of study excludes its integration in overall balance assessment as the sink will continue for +150 years.

Overall productivity differences between simulations of NEP (no logging) and NEP (logging and herbivory) found marked differences in statistically significant trends in sequestration (Figure 4.16). In all locations of sequestration indicated in yellow and red for both NEP and NBP, logging was found to have marked change in land cover and regeneration of forest cover is driving the carbon sink through NDVI increases in simulations as these locations correspond to the increased NDVI anomalies. Minor differences in productivity were due to leaves, and slash wood left behind to decompose and respire (R_h) after logging.

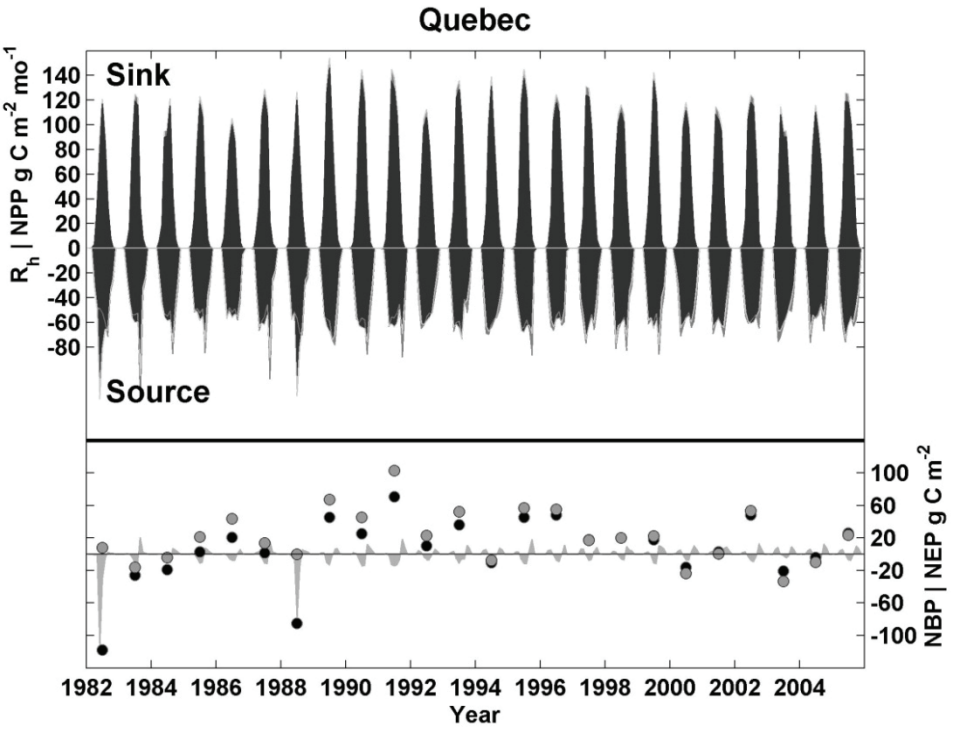

Figure 4.15 Time series of Quebec NPP, R_h, NEP and NBP with herbivory outbreaks and forest harvest, indicated with black (NPP) and (R_h) curves. Simulation with no disturbance or logged area indicated in dark grey curves (upper plot). Monthly model predictions of the difference in simulations are shown (light grey curves, lower plot) with black (NBP) and grey points (NEP) indicating annual sum with and without disturbance dynamics.

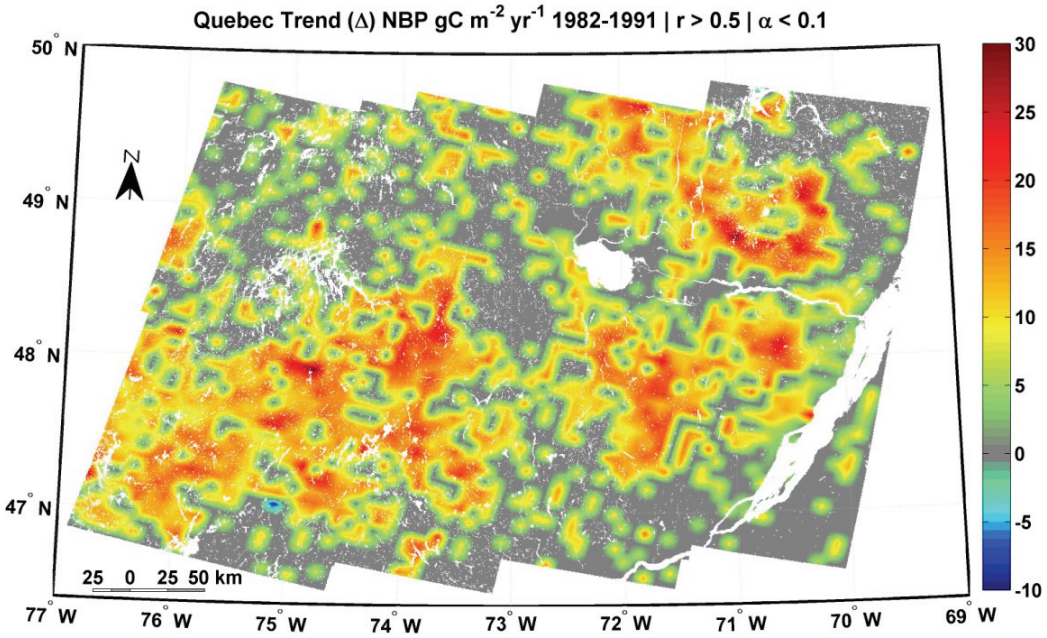

Figure 4.16 Quebec growing season sum (May-Sept) trend (Δ) net biome production (NBP) with herbivory outbreak and logging. Trends were included if the significance (α) < 0.1 and correlation (r) > 0.5.

4.3.5 Long-Term Regional Carbon Balance

Regional carbon sum had marked difference when accounting for fine-scale disturbance processes from 1982 to 2005. Carbon sinks were found in four of the six regions and sources existed in Newfoundland due to low NPP during anomalous mid 1990s cold years, and Quebec due to increased R_h in needle leaf evergreen forests from logging slash and insect outbreak mortality. Land cover change comprised ~13 – 26% of four study regions which drove marked difference between NEP and NBP (Table 2). Harvest of NPP from logging and agriculture removed large amounts of carbon (~115 – 320 Tg C) from entering soil pools.

Results suggest in regions of increased NDVI, it is critical to capture net ecosystem carbon balance (NECB) with agriculture harvest as they have marked difference due to continual removal and reduction of biomass entering soil detritus pools. To a lesser extent, disturbance events of insect outbreaks, logging, and fire are secondary in their impact to regional carbon balance. Although in simulations, calculation of mortality and R_h could be improved enhancing their importance. Capturing regional dynamics derived from fine-scale Landsat classified land-cover land-use change with ancillary data can produce teragrams (Tg, 10^{12} grams) of difference, changing accounting from a sink to a source (i.e. Quebec).

Table 4.2 Regional simulation totals (Σ) 1982-2005.

	Area m^2 10^6			Σ g C 10^{12}				
Region	Total	Dist.	% of Region	NBP	NEP	Fire	Mortality	Harvest
Yukon	78.3	-	-	-	11.2	-	-	-
Newfoundland	175.5	-	-	-	-17.9	-	-	-
N. Saskatchewan	162.3	27.2	16.8	54.6	47.5	15.7	1.8	-
S. Saskatchewan	92.9	24.1	25.9	125.3	18.9	-	-	124.6
Oklahoma Panh.	101.5	13.6	13.4	302.6	18.0	-	-	320.3
Quebec	172.0	23.0	13.4	-72.3	31.0	-	23.9	117.9
Study Σ	782.5	87.9		410.2	108.7	15.7	25.7	562.7

4.4 Discussion

A majority of regions with increased NDVI are net carbon sinks during periods of observation. NBP calculation is critical to capture fine-scale biophysical processes that alter the natural carbon cycle pathway of heterotrophic respiration. Bypassing decomposition and soil respiration through harvest can change a region annually from a net carbon source to a sink. The NBP calculation assumes that exported products do not immediately re-enter the carbon cycle, and it is acknowledged that carbon produced will eventually decompose and once again enter the active carbon cycle. For example, increases in corn for grain production in the Midwest could be a net carbon sink for a given year but the agriculture yield is fed to livestock which then convert it to waste which can partially be used as fertilizer, while another portion is released as methane. The utilization of agriculture yield has an impact on other biogeochemical cycles, which adds complexity in understanding the ecological dynamics of the system. Export of carbon for wood products (logging) can result in a long term carbon sink as wood products can last for over one-hundred years

in items such as construction building materials, and furniture. Due to the complexity of identifying the length and pathway of harvested carbon, understanding final endpoint or re-entry into the carbon cycle is beyond the scope of this work.

Spatially explicit information gathered from multiple data sources allowed calculation of NBP. In situ field measurements of the type of vegetation harvested from USDA NASS data in agriculture regions provided portrayal of the root/shoot ratio of carbon exported from the system. High resolution Landsat, IKONOS, and aerial photography provided understanding of spatial extent and time period of disturbance. Limitations to this analysis include identification of the exact time of disturbance in logged regions due to the limitation to Geocover time periods of mean 1975, 1990, and 2000 time periods. A record of Landsat data every three years would have enhanced this analysis however the cost (data classification time and effort) would not have substantially changed biogeochemistry knowledge of system dynamics. Overall accuracy in characterizing carbon export would have improved temporally, however marked difference between NEP and NBP has been captured and pools of carbon adjusted accordingly.

A number of model improvements were performed in this analysis to capture the vegetation dynamics observed in regions of increasing NDVI; however more improvements could be performed in future investigations. Problems found in this analysis that could be improved in future multi-resolution

simulations include: 1) the heterotrophic respiration scalar based on the relationship of soil moisture, and temperature impact to soil respiration does not account for permafrost and other Arctic soil processes. Future simulations could include a spatially dynamic function for rate of respiration (Q_{10}) with per pixel adaptation. In the analysis performed, this could potentially increase heterotrophic respiration (R_h) and reduce the annual NEP sink. 2) Recovery of NDVI and NPP after disturbance was not consistent with the literature with NPP recovering in a maximum of ten years while field measurements found much longer time periods to full recovery of NPP and biomass accumulation of thirty years or more. Allocation was extended in this assessment so that the pools of carbon replicated the dynamics of the system but the sum input of NPP post-disturbance was greater than field measurements reported in the literature. Future model simulations may consider this difference due to deficient remote sensing measurements of NDVI which have artificially high values of productivity after disturbance due to change in the spectral signatures. 3) Implementing multi-resolution satellite data to identify disturbance produced scale issues, Landsat at moderate resolution defined disturbed vegetation yet productivity observed by 8 km AVHRR did not change in the same pixels. Prescribing reduced NPP, as a fraction of the 8 km pixel disturbed associated to Landsat or use of moderate resolution MODIS data in future decade long assessments may alleviate this problem.

Defining steady state of ecosystems is a difficult and daunting task considering multiple processes that occur and interact continuously in ecosystems. In this modeling approach, steady state was assumed by evaluation of climate anomalies during the 1982 to 2005 time period. Early periods were selected for model spin up which did not have marked differences between later years as this would alter the change in productivity of the system once the simulation was initialized. Land cover steady state of study regions investigated was simulated as the 1975 vegetation cover. However, it is known that regions with land cover change had continual change prior to 1975. This limitation is acknowledged in this evaluation as a best approximation and could be improved with later evaluations of these regional ecosystems with additional high resolution data and selection of a per-pixel steady state assumption. This modeling effort was performed to capture explicit regional dynamics with the intention of understanding a number of different processes following disturbance which could possibly be scaled up and incorporated in global simulations of disturbance to ecosystem process. Adequate input data is an ongoing problem to accurately portray ecosystems carbon dynamics before and after disturbance.

4.5 Synthesis

Six regions in North America were simulated with multi-temporal multi-resolution satellite data to quantify if positive NDVI anomalies over various periods from 1982 to 2005 represented sinks of carbon sequestered in biomass. A complex interaction of processes was found to drive carbon sequestration in

five of the six ecosystems simulated. All regions during the same period had increased NDVI and simulated NPP. Enhancement of growth through warmer longer growing seasons appeared to be driving a carbon sink in the Northern High Latitudes in Newfoundland and Labrador, the Mackenzie River Delta had warming coupled with more precipitation, while post-disturbance recovery from fire in Northern Saskatchewan, spruce budworm outbreak followed by salvage logging in Quebec drove a sink of carbon in mid-latitudes. Agriculture land-use of the Mid-Continent grasslands produced marked sinks due to harvest and exclusion of detritus input to soil pools which was found through expansion of center pivot irrigation in the Oklahoma Panhandle and rain-fed agriculture post-drought recovery in Southern Saskatchewan.

Simulation modules were developed to enhance replication of ecosystem dynamics observed from fine-scale data. The fire module was derived from the literature and modified to reproduce regional dynamics in Northern Saskatchewan. The agriculture module was developed based upon the literature and modified for expanding irrigated agriculture observed in the Oklahoma Panhandle. The herbivory and logging modules were created to replicate a synergism of post-disturbance recovery of southern Quebec's Boreal forests. All modules included fractional land-cover land-use change derived from Landsat and ancillary data which has not been performed in known carbon cycle studies.

Results presented indicate a complex interaction of fine-scale land-cover land-use changes in the mid-latitudes can have a marked impact to regional

ecosystem carbon budgets that may not be accounted for in coarse scale simulations. Regions investigated represented a small portion ~3% or 0.017 Gt C yr^{-1} (assuming the sink is 0.5 Gt C yr^{-1}) of the net annual carbon sink 0.5 – 1.3 ± 0.6 Gt C yr^{-1} in North America due to the geographic extent of studies investigated which totaled less than one million hectares, equivalent to less than ~3% of North America. However, many of the processes reported that contribute to the sink were captured which indicated that scaling up regional investigations could confine more of the reported unknown sink while understanding the physical processes responsible for sequestration. Positive NDVI anomalies indicate hotspots of ecosystem carbon change when coupled with biogeochemistry simulations that account for dynamics to better constrain regional NECB.

4.6 Conclusion

This investigation presented approaches to identify and understand carbon consequences resultant from fine-scale land-cover land-use change in regions of increased NDVI trends. Modules were developed to replicate ecosystem processes observed from satellite data from 1982 to 2005 to predict biogeochemical processes that could be occurring within regional ecosystems that have experienced disturbance. This analysis brought a new perspective of understanding fine-scale sensitivity of ecosystems to perturbations that altered the regional carbon cycle which has not been done in prior investigations. Detailed knowledge of regional systems coupled with modified simulations

resulted in a more complex conceptual understanding of ecosystem dynamics in regions of increased NDVI which produced marked differences in accounting for carbon. Coarse scale simulations could well fail to identify important processes that alter the carbon balance of regions.

Primary points revealed in this research include: 1) Spatial and temporal fine-scale data are critical to understand state of an ecosystem under countenance of change; 2) Satellite data provide a brief understanding of dynamics in relation to time scale of disturbance, however they are spatially robust; 3) Regional detailed investigations of ecosystems can foster development of explicit knowledge of a system which then enables modeling sensitivity to perturbations; 4) Knowledge gained from regional assessment improves understanding complex carbon cycle dynamics associated to disturbance; and 5) a majority of NDVI anomalies evaluated in this investigation are net carbon sinks of ~10 – 250 terragrams of carbon, (Table 4.2) when fine-scale disturbance dynamics are accounted over long time intervals.

Continued investigation of disturbance utilizing the bottom up approach of calculation of carbon flux through mechanistic simulations derived from satellite based radiation use efficiency models will enable comparison to atmospheric meso-scale inversion studies. The coupled approach of top-down inversions with bottom up disturbance simulations would enable characterization and understanding of systems with disturbance while increasing accuracy of estimated carbon flux. Integration of improved understanding of regional carbon

balances through multi-spatial analysis with simulation modeling and inversion studies would improve our understanding and knowledge of transient pools of carbon which are perturbed by humans and climate.

Chapter 5. Significance of Results, Implications to Carbon Simulations, Summary, and Future Applications

5.1 Significance of Results

The North American terrestrial biosphere has been estimated to offset a formidable amount (25% of the global sink) of carbon annually emitted to the atmosphere from fossil fuel emissions and deforestation (CCSP 2007; Houghton 2007; IPCC 2007). Spatial-temporal knowledge of how this sink has operated on a regional basis will be critical to potentially manage the future sustainability of our climate system. Carbon is an important trace greenhouse gas, and processes that currently control the sink may not extend into the future, which could have drastic detrimental consequences to the well being and biodiversity of the planet (Canadell et al. 2007; Parmesan et al. 1999).

To understand increased threat of climate change and ecosystem carbon cycle mitigated processes, prior investigations focused on large scale phenomena while discounting regional fine-scale ecosystem dynamics in carbon simulations (Nemani et al. 2003; Potter et al. 2003b). This dissertation has shown that long-term fine-scale processes can be significant, and may impact large-scale ecosystem carbon cycle dynamics when aggregated. My work has sought to understand if these processes would be important to continental scale carbon accounting in simulations. Regional hotspots of increased vegetation production observed by NOAA/AVHRR data were investigated with multi-resolution data to ascertain dynamics that were thought to be primarily attributed

to climate warming, extension of growing season, and carbon sequestration through enhancement of vegetation growth (Myneni et al. 1997; Zhou 2003). Sources and/or sinks of carbon within these hotspot regions could potentially be indicators of how terrestrial ecosystem carbon changes. Complex dynamics were simulated to improve knowledge of terrestrial carbon cycle processes beyond only investigating climate impacts to NPP.

I found higher northern latitude regions of the Mackenzie River Delta, and the island of Newfoundland and Labrador coast had climate warming enhanced NDVI as reported in other studies (Bunn and Goetz 2006; Zhou et al. 2001). It was found through a radiation use efficiency model, not all NDVI increases propagated into simulated carbon storage. For example, Newfoundland and the Labrador coast had increased NDVI during the 1992 – 1999 period that drove an increase in NPP through warmer longer growing seasons. Although, NPP and NDVI growth during this period were a result of maritime climate system reset from the eruption of Pinatubo in 1991 (Neigh et al. 2007), soil pools respired at greater rates than NPP increase due to more detritus being fed to mortality pools from prior 1980s higher levels of NPP and NDVI.

Unlike the higher northern latitudes, the mid-latitudes had marked regional changes in post disturbance vegetation recovery driven by a number of complex processes. For example: southern Quebec had post-disturbance needle-leaf evergreen forest recovery from insect outbreaks followed by salvage logging; northern Saskatchewan had post-fire needle-leaf forest recovery in 1980 and

1981 and open lichen woodland post-fire recovery during the early 1990s; southern Saskatchewan had post-drought rain-fed agriculture recovery; and the Oklahoma Panhandle had expansion and intensification of agriculture increasing the standing stock of carbon resulting in a harvest sink. These processes would not have been accurately replicated in simulation modules or captured at a fine-scale without the multi-resolution satellite data approach performed herein.

Land-cover and land-use changes found in my investigation that have been reported to be an important contributor to the North American sink include higher yielding cultivars and shifts to more productive crop types (Hicke et al. 2002; Hicke et al. 2004; Lobell et al. 2002), and reduced tillage of agriculture lands (Ogle et al. 2003; Pacala et al. 2001; Paustian et al. 2000; Randerson et al. 1997; Six et al. 2004) (southern Saskatchewan, Oklahoma Panhandle), changes in pest management (Ayres and Lombardero 2000) (Quebec), and fire management practices (Dixon et al. 1994; Houghton 1999) (northern Saskatchewan). Processes not captured in this multi-resolution investigation, yet reported in the literature to be important include agroforestry (Ciais et al. 1995; Dixon et al. 1994; Houghton 2003), woody encroachment (Pacala et al. 2001), and forest regrowth from agriculture abandonment (CCSP 2007). I found processes not reported in the terrestrial carbon cycle ecosystem simulation literature through my specific approach. Synergistic effects were found in post-disturbance recovery in Quebec, which had insect outbreak followed by salvage logging, while the Oklahoma Panhandle had expansion of center-pivot irrigated

agriculture. This integrated approach brought about a new perspective to capture multiple regional ecosystem processes within hotspots of vegetation change identified from coarse resolution continental data.

Simulations were performed with and without observed dynamics to assess the importance of enhanced biophysical process knowledge which found harvest from agriculture and logging to be a critical component for understanding net ecosystem carbon balance followed by insect outbreaks and fire. Some processes found through this approach were noted in the literature although they had not been explicitly quantified at a fine-scale throughout North America from 1982 – 2005 in locations of increased NDVI. This is the first assessment which has integrated long-term fine-scale land-cover and land-use change information in regionally specific carbon modeling modules. My approach has quantified multiple processes in net ecosystem carbon balance (NECB) and found dynamics to account for marked difference in carbon accounting (~10 – 250 Tg C).

5.2 Implications for Multi-Resolution Carbon Simulations

This investigation sought to explain AVHRR NDVI anomalies that drive ecosystem carbon simulations by examining other data sets including Landsat, IKONOS, aerial photography, and climate data. To further explore what NDVI trends mean to simulated ecosystem productivity, modeling experiments were implemented to understand from a numerical perspective what a coarse 8 km^2

measurement represents during a 24+ year period. Simulations took into account disturbance, land-cover change derived from fine-scale Landsat measurements, and ancillary data to alter pools of carbon to complement empirical observation of ecosystem dynamics.

It is critical to understand what is being measured when using long-time series coarse-resolution satellite data. AVHRR NDVI data were created to investigate changes in photosynthetic capacity of vegetation using a sensor designed for other purposes; many artifacts impact the surface signal from atmospheric contaminants (e.g. clouds, haze, smoke) to land surface characteristics (e.g. canopy density, background soil color, snow) during periods of observation. NDVI data contain a mixed signal of the land's surface often obstructed by atmosphere constituents, yet they are used to understand specific aspects of vegetation productivity, more explicitly light interception by vegetation canopies. It was acknowledged that AVHRR NDVI derived NPP from a light use efficiency model can overestimate recovery after disturbance due to rapid recovery (less than 10 years) of near-infrared reflectance. However, carbon cycle pool processes are correctly portrayed providing understanding of disturbance sensitivity during the 24-year period of study.

Disturbance to vegetation typically alters NDVI data producing values that are not comparable to prior measurements of vegetation photosynthetic capacity. If disturbance changes composition of vegetation structure, function, and density within an 8 km grid cell, red and near-infrared reflectances are not recording

measurements that are comparable to previous ecosystem state. When using these data over long time intervals, it is necessary to use ancillary data to determine what is being measured so that ecosystem processes can be accurately simulated.

In my analysis, I removed NDVI trends less than 0.1 which excluded spatially extensive northern latitudes measurements of NDVI. Climate warming induced increased NDVI throughout the northern latitudes with values less than 0.1 NDVI units from 1982 to 2005. Much of the literature that discusses climate phenomena that influences plant productivity does not match NDVI statistical requirements used in my analysis. In addition, a focus of my work was to study perturbations marked change to photosynthetic capacity, ecosystem function, and carbon storage.

Spatial and temporal changes in plant productivity observed through remote sensing and simulation modeling on a monthly time step revealed a number of interacting human and climate impacts to ecosystem productivity. Integration of multiple datasets to identify and understand ecosystem process driven by multiple agents is complex through time and space. Often these dynamics are excluded from analyses due to satellite sensor data acquisition limitations. However, I contend through this analysis they are important to understand ecosystem process on a regional basis.

5.2.1 Spatial-Temporal Aspects of Satellite Driven Carbon Simulations

The time scale of remote sensing observations (~30 years) in relation to ecosystem dynamics is brief, yet remote sensing measurements are the best solution to understand and identify ecosystem perturbations spatially. Selection of decadal time periods while removing low statistically significant trends limited my study to specific kinds of disturbances and biomes. By only looking at NDVI increases greater than 0.1 at 8 x 8 km effectively removed small scale and short duration disturbances in specific types of biomes. For example, forest harvest on small plots which return to pre-disturbance NDVI values within three years and fires in North America's taiga that is dominated by herbaceous vegetation both have post disturbance NDVI recovery within four years which are too brief to be captured in my decadal trend analysis.

The 8 x 8 km spatial scale of observations dictated a mixed pixel response of climate and anthropogenic change to vegetation for areas studied. Most studies of continental vegetation productivity sacrifice knowledge of mechanisms operating in the local system, for large scale processes which may never capture all dynamics of the system. Integration of multiple satellite sensors over a relatively long time period, with different spatial-temporal data, enabled thorough evaluation of ecosystem dynamics on a regional basis that can be used to understand and integrate with continental phenomena (Figure 5.1).

Even though satellite based measurements only capture a ~30 year time span, they are spatially robust, and encompass the entire terrestrial biosphere.

This knowledge of the ecosystem can then be simulated through mechanistic understanding of ecosystem process to calculate human and/or climate impacts to the carbon cycle. Integration of multiple data sources in a modeling framework enabled the investigation and understanding of multiple dynamics to ecosystem functioning from a regional and continental perspective from abiotic climate impacts to LCLUC processes of agriculture, logging, insect outbreaks, and fire enhancing simulation of NBP which provided a basis for understanding regional NECB.

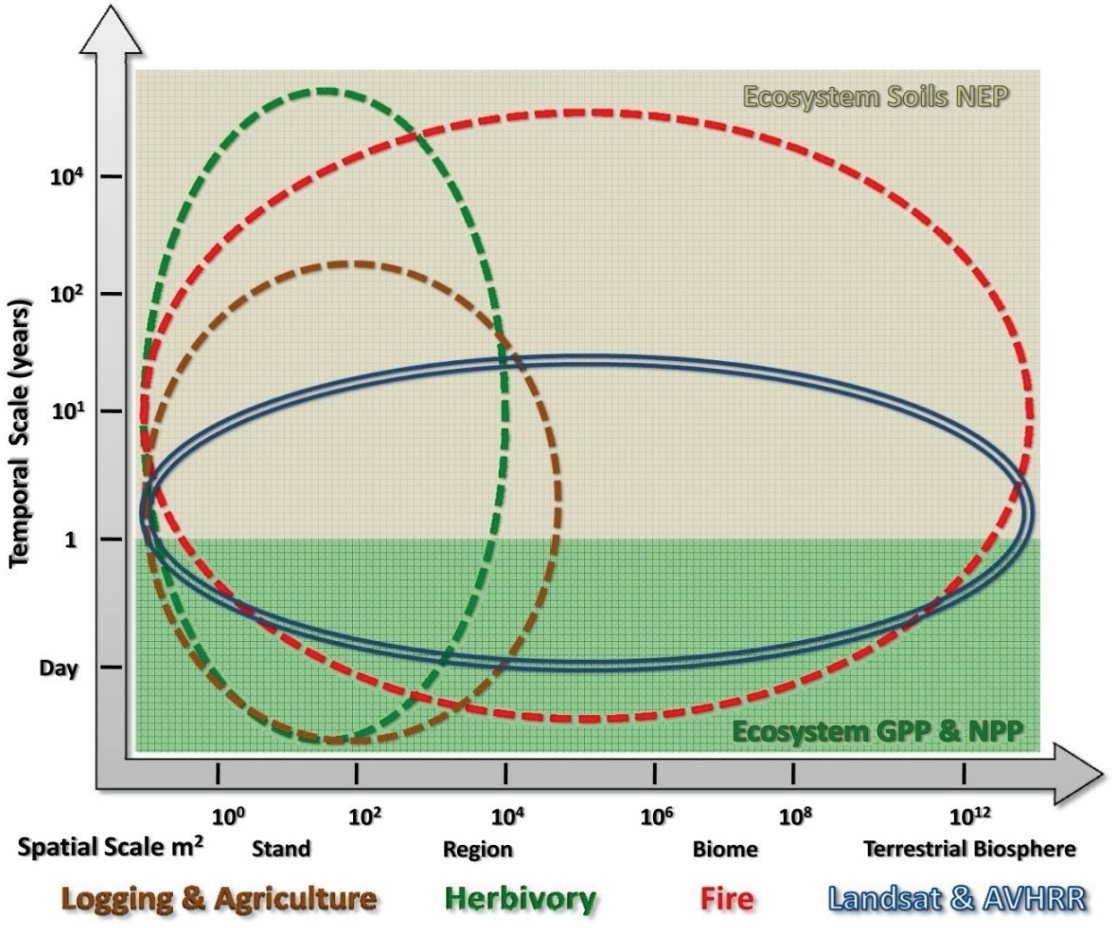

Figure 5.1 Spatial and temporal aspects of investigating and understanding disturbances to ecosystem functioning with multi-resolution remote sensing and modeling in North America.

5.3 Summary

Fine scale variability, associated with land-cover change observed at Landsat 30 m resolution, can be a significant factor when aggregated across North America in carbon balance assessments. Understanding transient pools of the flux of carbon in terrestrial ecosystems is a fundamental question of geography associated with temporal and spatial scales of disturbance and ecosystem dynamics. This investigation combined two positive attributes of Landsat (30 m spatial resolution) and AVHRR data to understand regional scale disturbances from fire, insect outbreaks, and harvest from logging and agriculture in carbon flux from 1982 to 2005. The merged analysis of both satellite-derived measurements into a model driven by NDVI produced quantitative predictions of carbon released or stored due to natural and anthropogenic disturbance(s) at large scales > 8 km^2. Improved understanding of human and climate induced impacts from AVHRR, Landsat, IKONOS, aerial photography, meteorological station data and ancillary datasets to simulate net biome productivity resulted and allowed for detailed analysis of change from biophysical disturbances to change of carbon pools in biogeochemistry simulations. The hypothesis put forth in this investigation that increased vegetation production shown by remote sensing data represented sinks of atmospheric carbon sequestered in biomass was found to be true in all study regions. However, periods of time that indicated the hypothesis was null occurred when soil respiration exceeded increases in net primary production in Newfoundland and Labrador coast. The carbon cycle accounting difference between net ecosystem production and net biome

production was found to be critical in systems experiencing “flush” losses of standing carbon, such as fire, logging, insect herbivory outbreaks and agriculture harvest.

The following specific research objectives were substantiated:

1. NDVI trends (anomalies) on decadal periods identified marked change in vegetation productivity over the period of 1982 to 2005, 1982 to 1991, 1992 to 1999, and 1992 to 2005 due to climate change and land-cover land-use change (Chapter 3);
2. In North American Mid-Latitudes, human induced land-cover land-use change had a marked impact in regions of increased AVHRR NDVI (Chapter 3);
3. A complex interaction of disturbance to vegetation productivity occurs whether driven by climate or humans in regions of increased NDVI (Chapter 3);
4. Simulations that replicated carbon cycle dynamics found land-cover land-use change analysis can have marked differences in accounting for carbon compared to assessments that do not include all the dynamics found in a regional ecosystem (Chapter 4);
5. Simulating net biome productivity of ecosystems with perturbations in North America improves understanding of mechanistic processes that occur in carbon cycle dynamics (Chapter 4).

5.4 Future Applications

Regional analysis at Landsat resolution from 1982 to 2005 found a number of perturbations to ecosystem productivity that drove changes in net biome productivity (NBP). Understanding regional carbon cycle processes using this approach revealed a number of studies that could be performed in the future. Spatially extending modules developed for CASA would be the natural next step to understand and quantify continental scale NBP. Currently, information on land-use at 8 x 8 km spatial resolution is scarce. Once these data become available, logging and agriculture modules could be implemented across the continent. Burned area extent data is currently available from the large fire database for all of Canada and Alaska (Stocks et al. 2003), which could be used with the fire module to understand carbon cycle dynamics in the higher northern latitudes with enhanced replication of fire dynamics in the boreal zone.

Integration of new data sets which do not offer the 24-year period of observation but have enhanced temporal, spatial, and radiometric resolution of NDVI and climate data would enhance simulations of NBP. Moderate Resolution Imaging Spectrometer (MODIS) data could be used as a surrogate for AVHRR NDVI, and utilization of MODIS FPAR and LAI products to drive NPP would provide an enhanced spatial (< 1 km) resolution of ecosystem simulations. For the contiguous United States, the Daymet (daymet.org) daily precipitation and temperature dataset would enhance simulations of climate disturbances. Currently CASA is run with coarse resolution (1° - 2.5°) monthly climate data

which may dampen or suppress regional climate variability. Considering the highly variable nature of precipitation in space and time, the soil hydrology component of simulations could be greatly improved. Higher resolution data in time, space, and radiometric accuracy would enhance production and flow of carbon through simulated ecosystems. This could resolve other phenomena that could not be observed with current simulations.

The primary motivation of research performed was quantification of carbon in regions of enhanced NDVI, advance future applications, and execute simulations globally with enhanced ecosystem dynamics to potentially reduce uncertainties. Future research could explore simulated NEP dynamics with NDVI anomalies, to understand changes in productivity due to climate from stress scalars (T_ε and W_ε) on NPP and R_h, while isolating regions with changes in NEP not associated with climate, which may be driven by land-cover land-use change. To illustrate the potential of identifying regions of change due to climate while potentially including land-cover change, CASA was run for all of North America calculating the trend with a significance (α) less than 0.1 and correlation (r) greater than 0.5, of NEP from 1982 to 2005 at 8 km^2 resolution (Figure 5.2). Note patterns of NPP are similar to NDVI. However, in regions with marked R_h, the resultant balance NEP (NPP – R_h) in Midwest grasslands and northern Arctic slope is close to the carbon balance. Continued investigation is needed to validate R_h predictions under climate change with LCLUC disturbances utilizing meso-scale inversions and regional flux tower measurements.

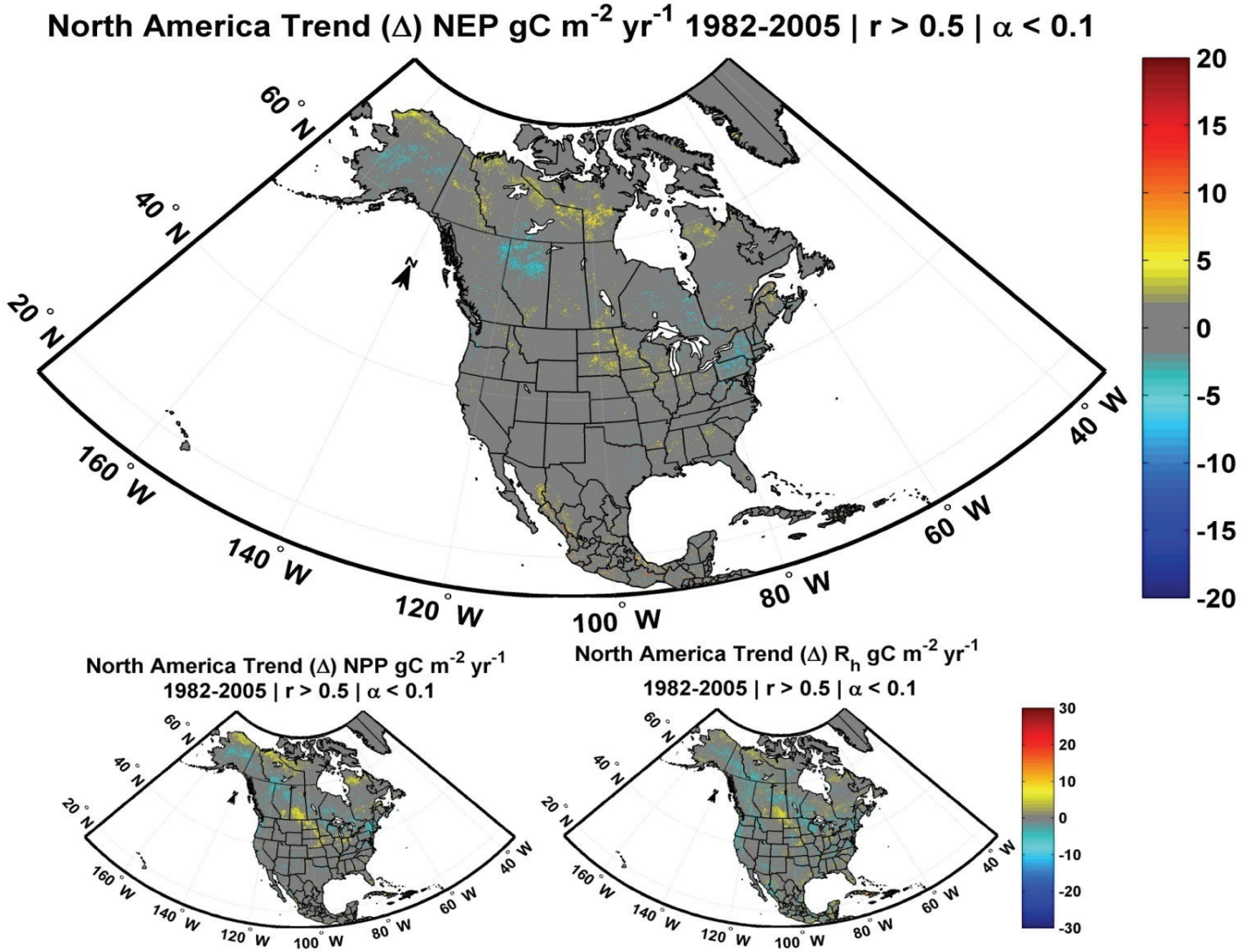

Figure 5.2 North America trend (Δ) of net ecosystem production (NPP- R_h) from 1982 to 2005.

Simulated NEP provided an alternative means to investigate changes in carbon as compared to NDVI anomalies. Future modeling activities could simulate NEP or NBP and synthetically prescribe human disturbances at larger scales to understand carbon balance across larger portions of North America which could have a greater impact to global carbon balance. Available global land cover datasets could represent the spatial bounds and scenarios or assumptions of amount of logged forest or agricultural land could be prescribed from available statistical datasets. This analysis could provide boundary values for these types of changes in their impact to global terrestrial carbon dynamics.

Future investigation could focus on negative trends in NDVI and integrate positive trend results to compare to recent meso-scale inversion studies to generate a full understanding of carbon balance for North America over the past 24+ years with the assumption NDVI anomalies capture hotspots of vegetation change. Comparison to meso-scale inversions could possibly reduce disparity in measurements while providing validation and optimization of parameters for carbon change accounted for in this investigation. Integration of complex regional scale dynamics in simulations of carbon flux must be compared to coarse resolution estimates (> 1°) to understand accounting implications for exclusion of regional scale dynamics at the human scale (< 250 m). Coarse scale investigations could fail to accurately identify sources and sinks of carbon which could contribute to the unknowns associated to the size of the missing carbon sink.

Glossary of Terms

Atmosphere: Earth's atmosphere is a layer of gasses surrounding the planet and retained by the Earth's gravity.

Biogeochemical cycle: In ecology and Earth Science, a biogeochemical cycle is a circuit or pathway by which a chemical element or molecule moves through both biotic and abiotic compartments of an ecosystem. In effect, the element is recycled, although in some such cycles there may be places (called "sinks") where the element is accumulated or held for a long period of time.

Biosphere: Coined by geologist Eduard Suess in 1875, defined as the place on Earth's surface where life dwells.

Carbon cycle: The carbon cycle is the biogeochemical cycle by which carbon is exchanged between the biosphere, Geosphere, hydrosphere, and atmosphere of the Earth.

CASA: Carnegie Ames Stanford Approach, radiation use efficiency biogeochemistry simulation model.

Disturbance: Any relatively discrete event in time that disrupts population, community, or ecosystem, structure and changes resources, substrate availability, or the physical environment (Pickett and White 1985).

Disturbance Frequency: The temporal frequency of number of events per unit time, and recurrence interval, which is the time expected to elapse before a disturbance reoccurs.

Disturbance Magnitude: Can include the size or spatial distribution while also including the intensity or force of the event itself.

Disturbance Regime Descriptors: Used to distinguish if a disturbance to an ecosystem is notably different from the background of natural variability. Regime descriptors include the magnitude, frequency, and synergism of the occurrence of disturbances within a select location.

Disturbance Severity: Defined in terms of consequences to ecosystem properties.

Disturbance Synergism: Interactions with other disturbances to promote or enhance one another.

Geomatics: The science and technology of gathering, analyzing, interpreting, distributing and using geographical information.

Geosphere: The densest parts of the Earth, which consist mostly of rock and regolith.

GPP: Gross Primary Productivity, CO_2 assimilation (assuming that respiration in the light equals dark respiration, measured as mass of carbon per unit area (g C m^{-2}).

Hydrosphere: In physical geography describes the collective mass of water found on, under, and over the surface of the planet.

LCLUC: Land-Cover Land-Use Change, common phrase used to describe change in terrestrial vegetation cover driven by humans, climate, or disturbance.

Lithosphere: is the solid outermost shell of a rocky planet. On the Earth, the lithosphere includes the crust and uppermost mantle.

NDVI: Normalized Difference Vegetation Index, measures the photosynthetic capacity of vegetation (Tucker 1979).

NPP: Net Primary Productivity, equals Gross Primary Productivity minus Autotrophic Respiration of the plant, measured as mass of carbon per unit area (g C m^{-2}).

NEP: Net Ecosystem Productivity, equals Net Primary Productivity minus Heterotrophic respiration in the rihzosphere, and microbes, measured as mass of carbon per unit area (g C m^{-2}).

NECB: Net Ecosystem Carbon Balance, Net rate of carbon accumulation in or loss from (negative sign). NECB represents the overall ecosystem carbon balance from all sources and sinks – physical, biological, and anthropogenic (Chapin et al. 2006).

NBP: Net biome productivity, equals Net Ecosystem Productivity minus non-respiratory fluxes often driven by disturbance to the ecosystem, measured as mass of carbon per unit area (g C m^{-2}).

Perturbation: Differing from the relative “normal” of the whole system orientation occurs when parameters or behaviors that define a system have been explicitly defined and a given disturbance is known to be new to the system at hand (Pickett and White 1985).

Appendix

A. Landsat Classification Procedure

The land cover classification procedure included two software packages and code to automatically generate unsupervised classified maps to interpret and recode to seven International Geosphere Biosphere classes of plant functional types for implementation in the Carnegie Ames Stanford Approach (CASA) (Potter et al. 1993). Geocover Landsat images were first downloaded from the global land cover facility (GLCF) and ingested with all bands.

An IDL-ENVI script was created that layer stacked all bands into one file and exported a Geomatica PCI file with bands three (red), four (near-infrared), and five (short-wave infrared) for unsupervised ISODATA clustering. ISODATA (Tou and Gonzales 1974) was performed utilizing the following parameters: Desired number of cluster (50); Minimum number of clusters (50); Maximum number of clusters (50); Maximum number of Iterations (20); Movement threshold (0.01); Signature generation (No); Standard deviation (1); and Maximum number of pairs (5). This analysis was first carried out on a number of scenes in different regions to test reliability of capturing the desired class clusters. If any cloud or haze atmospheric contaminants were present, up to three classification iterations were performed as they typically alter the class distribution structure. Successive iterations enabled the ability to cluster and exclude atmospheric contaminants, as well as snow and ice from change analysis.

Classification of class clusters is an individual interpretive procedure which is an acquired skill from thorough experience of classifying and validating numerous Landsat images. Image interpretation based only on Landsat images can result in multiple interpretations of cluster-class associations between expert interpreters. To reduce confusion between cluster-class associations Google Earth (www.earth.google.com) was used to aid in identification of cluster types as it contains imagery with resolutions from 15 m^2 to less than 1 m^2. Google Earth utilizes the same Orthorectified GeoCover Landsat data used in classifications herein with inset high resolution imagery from IKONOS, Quickbird and other high-resolution datasets. All six study regions investigated had very-high resolution (1 m^2 or less) data available from Google Earth to aid in selection of class-clusters. It was acknowledged that error terms were introduced by Google Earth very-high resolution imagery because dates of acquisition were unknown which limited the ability to assess if change happened between training and classified Landsat. The objective was to understand vegetation type within Landsat resolution pixels. Errors associated to map and classification accuracies were assessed utilizing separate high-resolution data compiled for validation.

Change classification was performed by utilizing an IDL/ENVI script to create a multi-date tassel cap image by first ingesting data layers stacking all reflective bands for a tassel cap transformation. Development of a script resulted in a semi-automated approach to classify >150 scenes used in this analysis. The

tassel cap was performed to reduce multiple band image redundancy, in which neighboring bands in spectral space contain similar data constituents. The IDL/ENVI software package was automated to generate multi-date 1990-2000 and 1975-1990 images for Geomatica PCI ISODATA unsupervised clustering with similar parameters previously mentioned.

The IDL/ENVI software operates with coefficients that are commonly used throughout the Landsat classification literature. Huang *et al.* (2002), coefficients were used for Landsat 7 data radiance, the Crist and Cicone (1984), coefficients were implemented for Landsat 4 and 5 data radiance data, and coefficients for Multispectral Scanner data were utilized on digital numbers from Kauth *et al.* (1978), (Table A.1). Transforming imagery to tasseled cap space aides in normalization of images because weighted components are sensor specific and not scene dependent (Guild et al. 2004). Often the third component of the tassel cap transformation is referred to as wetness, when actually it is associated to the soil moisture content of the target. The first iteration from Multispectral Scanner (MSS) Tassel Cap transformation referred to the third component as 'yellow stuff' or 'yellowness' because MSS does not include shortwave infrared measurements. In this analysis, the third component is considered a measure orthogonal to brightness or greenness of the target similar to principle component analysis. When multi-date tassel cap images are input into an ISODATA unsupervised transformation clusters result in change vector classes that have distinct characteristics associated to change in brightness and greenness within

the tasseled cap space and vegetation cover change. These change clusters were identified and overlaid upon the 2000 classified image to derive change maps for carbon simulations.

Table A.1 Tasseled Cap Coefficients

	Feature	Band 1	Band 2	Band 3	Band 4	Band 5	Band 7
MSS (Kauth et al. 1978)							
	Brightness		0.332	0.603	0.675	0.262	
	Greenness		−0.283	−0.660	0.577	0.388	
	Yellowness		−0.899	0.428	0.076	−0.041	
	“Non-such”		−0.016	0.131	−0.452	0.882	
TM (Christ and Cicone 1984)							
	Brightness	0.33183	0.33121	0.55177	0.42514	0.48087	0.25252
	Greenness	−0.24717	−0.16263	−0.40639	0.85468	0.05493	−0.11749
	Wetness	0.13929	0.22490	0.40359	0.25178	−0.70133	−0.45732
	Fourth	−0.83104	0.07447	0.42144	−0.07579	0.23819	−0.25247
	Fifth	−0.32530	0.05361	0.11485	0.11140	−0.46571	0.80549
	Sixth	0.11381	−0.89714	0.42038	0.06686	−0.01629	0.02706
ETM+ (Huang et al. 2002)							
	Brightness	0.3561	0.3972	0.3904	0.6966	0.2286	0.1596
	Greenness	−0.3344	−0.3544	−0.4556	0.6966	−0.0242	−0.2630
	Wetness	0.2626	0.2141	0.0926	0.0656	−0.7629	−0.5388
	Fourth	0.0805	−0.0498	0.1950	−0.1327	0.5752	−0.7775
	Fifth	−0.7252	−0.0202	0.6683	0.0631	−0.1494	−0.0274
	Sixth	0.4000	−0.8172	0.3832	0.0602	−0.1095	0.0985

B. Parameterization of Satellite Data for CASA

To adequately simulate carbon cycle dynamics, a number of preprocessing procedures were applied to account for data discrepancies (spatial and statistical adjustments) which could impact simulation results. Integration of multi-resolution data over a long 24-year period required a number of pre-simulation corrections to datasets and adjustments to model parameters. A combination of procedures was carried out on Landsat moderate resolution data, AVHRR and coarse gridded climate data to integrate in simulation modeling. All

procedures were performed in MATLAB, ENVI, and ArcMAP, utilizing a combination of software packages and design specific code.

B.1 Climate Data

Inadequate coverage of coarse gridded temperature data (1°) in study regions existed with extensive coastal areas. Yukon, Newfoundland, and Quebec study regions required preprocessing. All monthly coarse gridded temperature data from the Leemans and Crammer mean 1930 to 1960 climatology (Leemans and Cramer 1991), had land pixels with neighboring water expanded spatially in both Latitude and Longitude dimensions to extend values by the neighboring pixel value to cover coastal areas. A MATLAB routine was created, to expand data values then climatology means were added to the Goddard Institute for Space Studies (GISS) temperature anomalies. The coarse resolution climate data was then input into ENVI and bilinear interpolated to 8 km using the nearest neighbor approach. All climate datasets were interpolated in this fashion for simulations.

B.2 AVHRR NDVI GIMMS 'g' Scaled FPAR

In CASA simulations, normalized difference vegetation index (NDVI) is converted into fraction of photosynthetically active radiation (FPAR) absorbed by the green parts of vegetation which is a value needed to multiply times photosynthetically active radiation (PAR) to generate intercepted photosynthetically active radiation (IPAR) to multiply times climate stressors of

temperature (T_ε) and precipitation (W_ε) multiplied times light use efficiency (ε) to calculate net primary productivity (NPP).

$$NPP = \varepsilon \cdot T_\varepsilon \cdot W_\varepsilon \cdot FPAR \cdot PAR$$

To have correct calculations for FPAR and leaf area index (LAI) in model simulations the AVHRR NDVI 'g' dataset has been rescaled based upon the methods described by (Los et al. 2000). Often FAPAR and FPAR are used interchangeably in the literature both meaning fraction of absorbed photosynthetically active radiation. This calculation assumes that plant functional types have a minimum FPAR (open canopy, < 0.02 percentile) and maximum (closed canopy, 0.98 percentile) by land cover type. Minimum and maximum FPAR scalars were generated for each study region to accurately simulate NPP (Figures B.2.1 to B.2.6).

$$SR = {(1 + NDVI)}/{(1 - NDVI)}$$

$$FPARMAX = 0.95$$

$$FPARMIN = 0.0010$$

$$FPAR = \left(\left({SR - SRMIN}/{SRMAX - SRMIN}\right) \cdot (FPARMAX - FPARMIN)\right) + FPARMIN$$

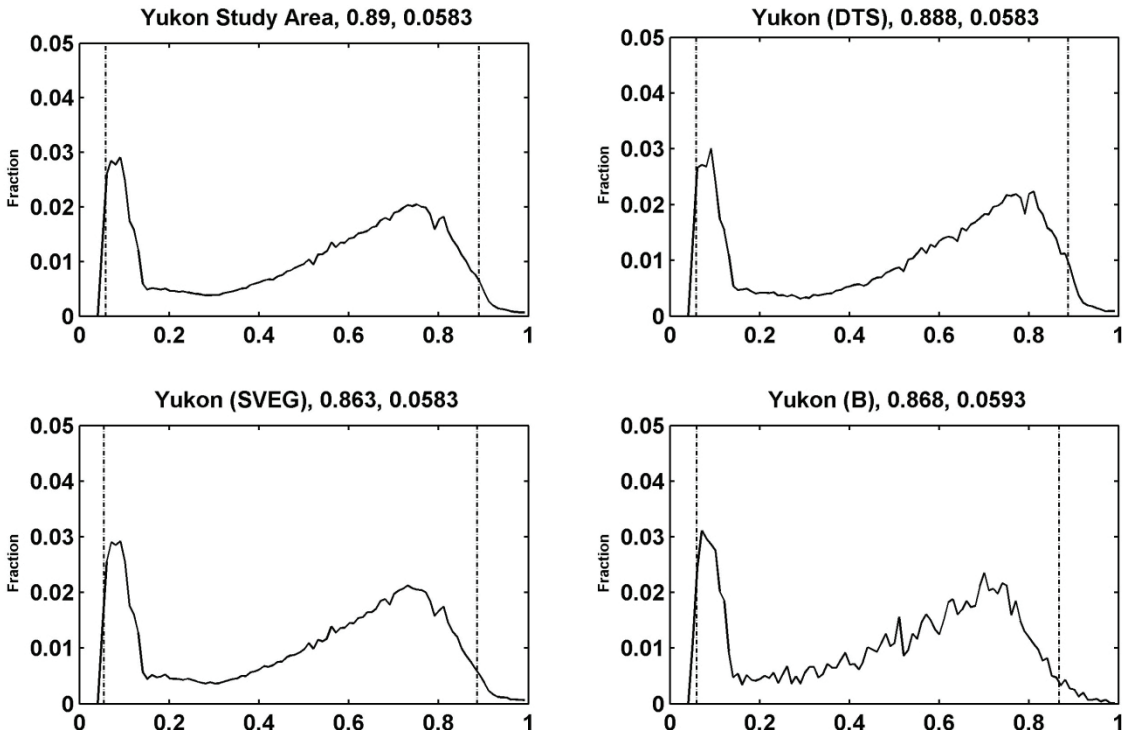

Figure B.2.1 FPAR NDVI scalars for the Yukon by land cover type, dashed vertical lines indicate the 2nd and 98th percentile utilized in scaling FPAR. Vertical axis (y-dimension) is the fraction of NDVI by land cover type and the horizontal axis (x-dimension) is the NDVI value.

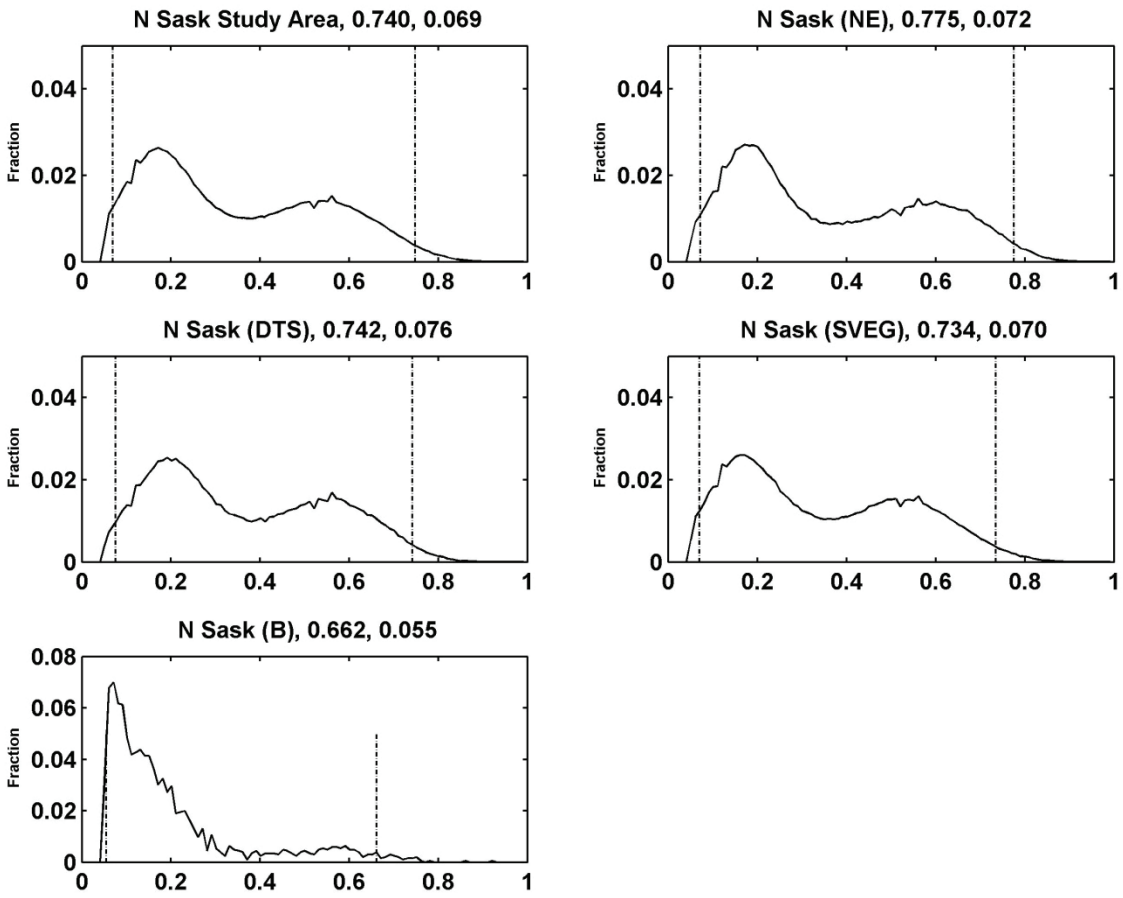

Figure B.2.2 FPAR NDVI scalars for the Northern Saskatchewan by land cover type, dashed vertical lines indicate the 2nd and 98th percentile of NDVI utilized in scaling FPAR. Vertical axis (y-dimension) is the fraction of NDVI by land cover type and the horizontal axis (x-dimension) is the NDVI value.

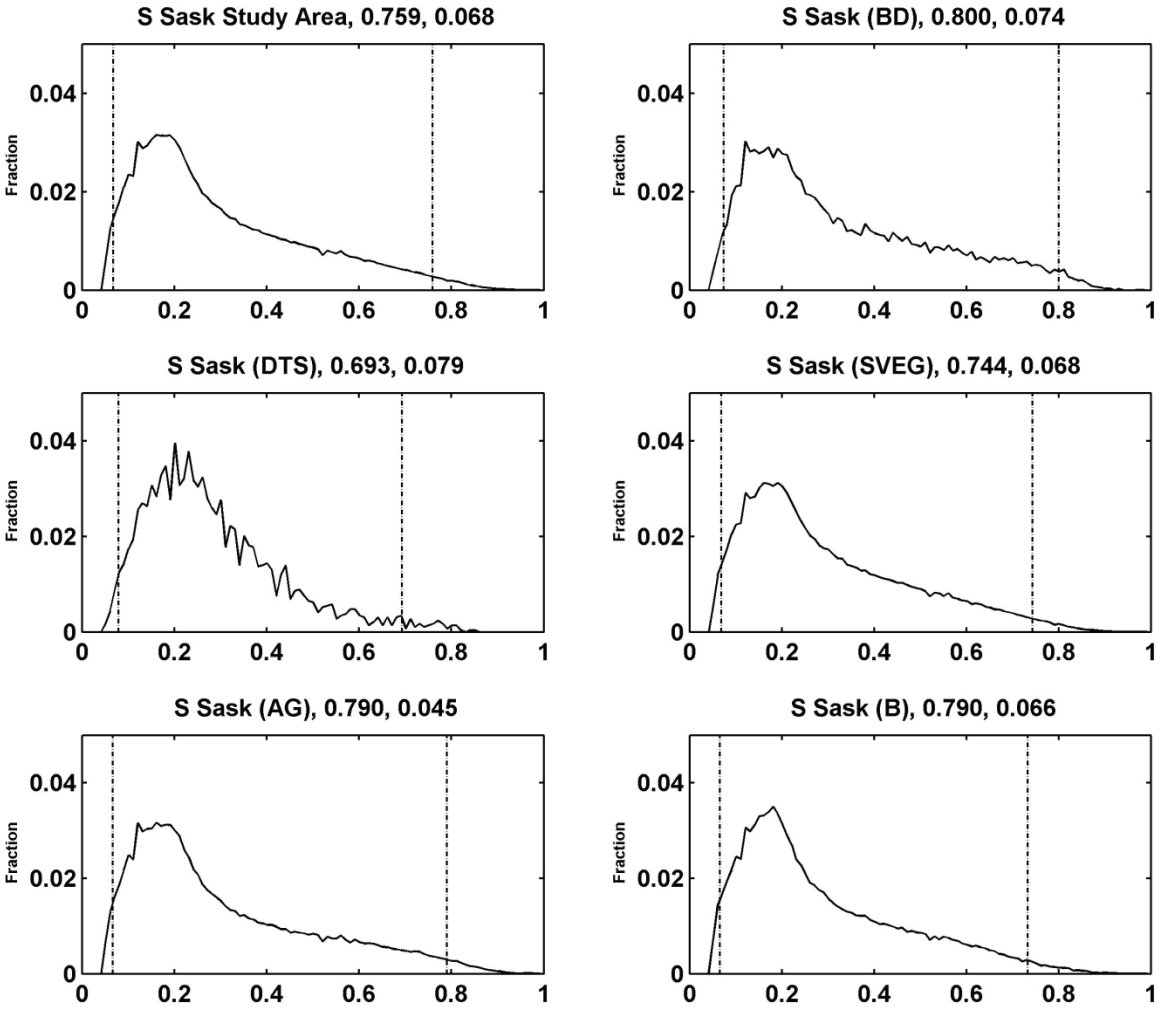

Figure B.2.3 FPAR NDVI scalars for Southern Saskatchewan by land cover type, dashed vertical lines indicate the 2nd and 98th percentile utilized in scaling FPAR. Vertical axis (y-dimension) is the fraction of NDVI by land cover type and the horizontal axis (x-dimension) is the NDVI value.

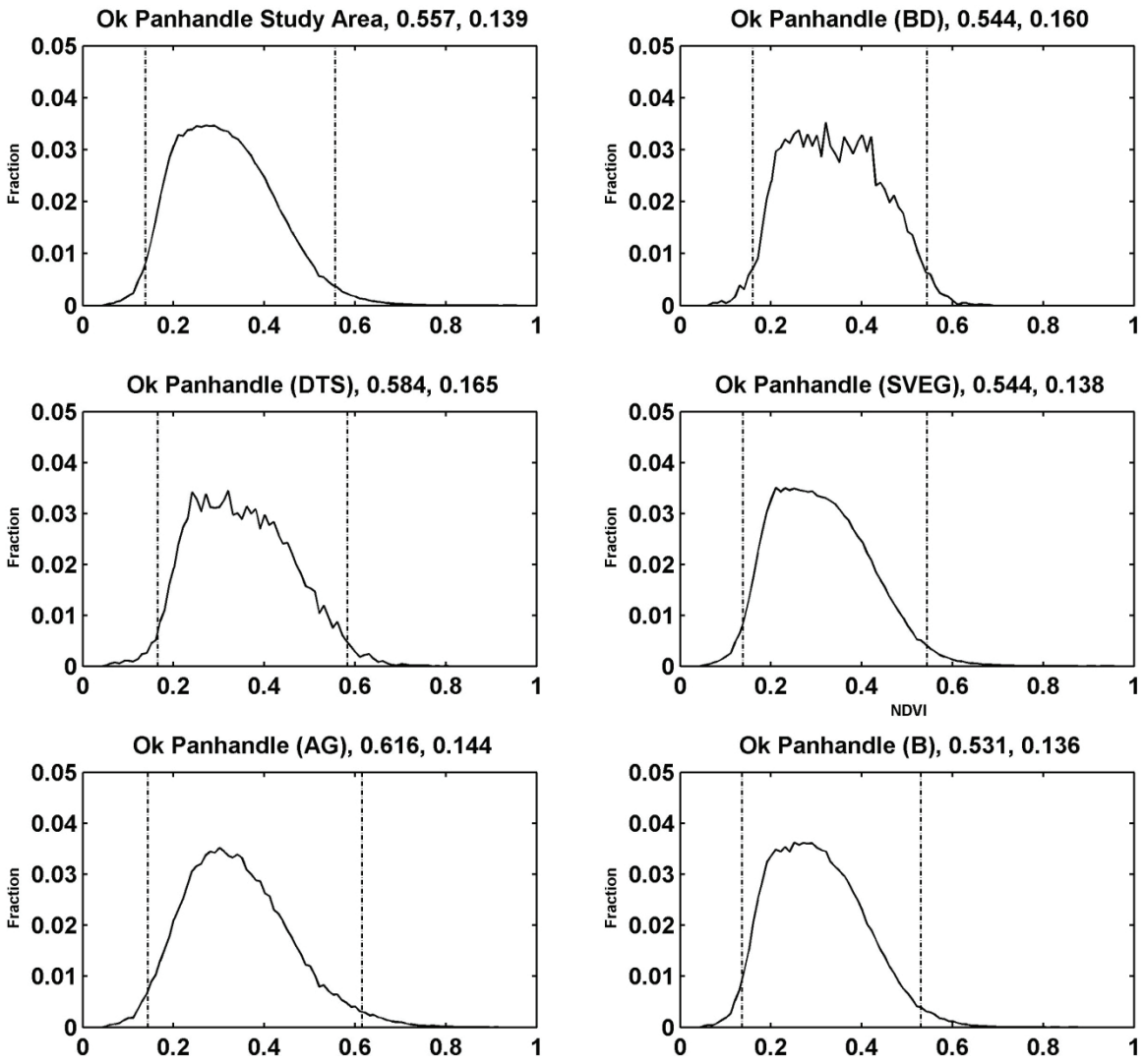

Figure B.2.4 FPAR NDVI scalars for the Oklahoma Panhandle by land cover type, dashed vertical lines indicate the 2nd and 98th percentile utilized in scaling FPAR. Vertical axis (y-dimension) is the fraction of NDVI by land cover type and the horizontal axis (x-dimension) is the NDVI value.

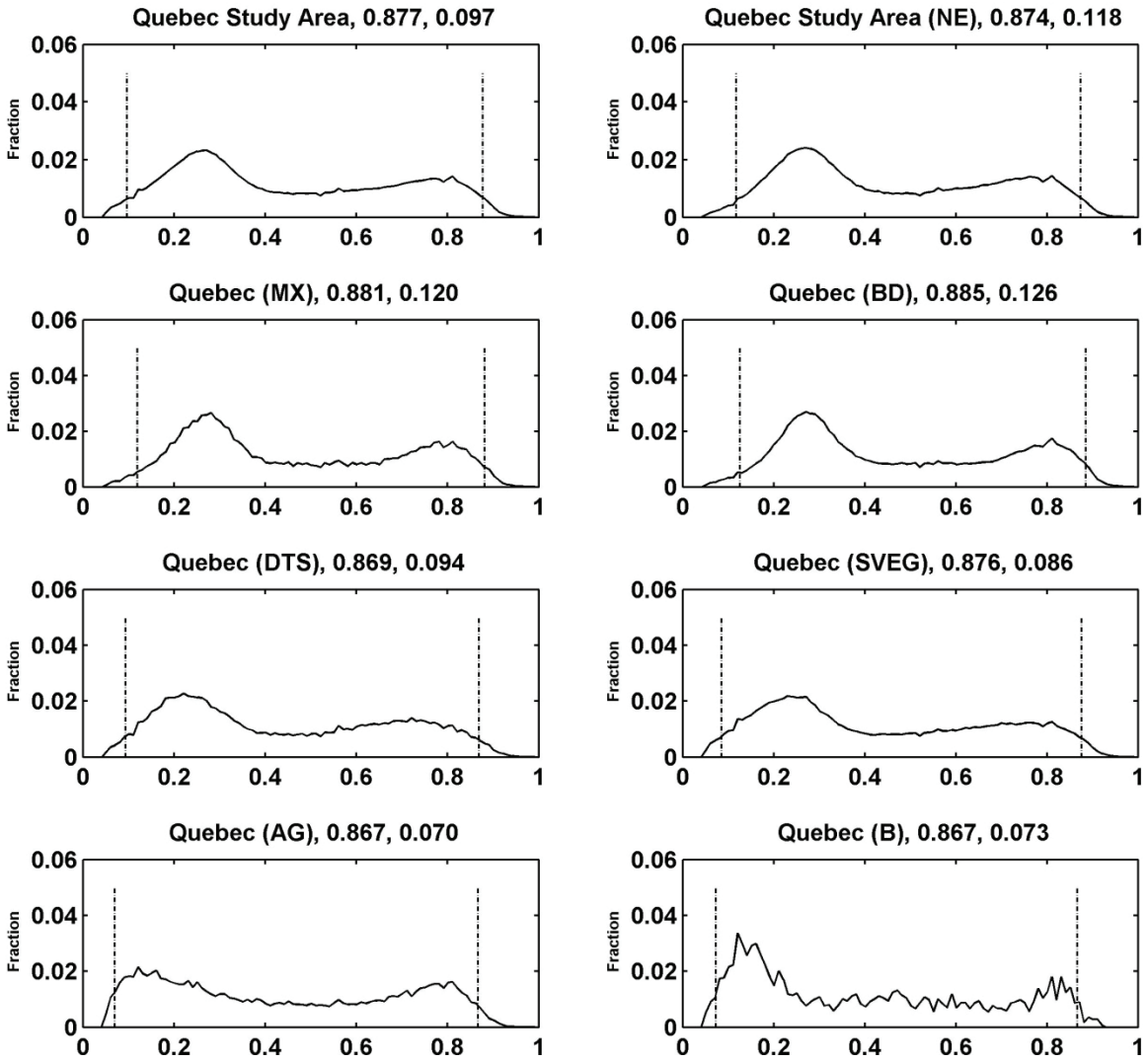

Figure B.2.5 FPAR NDVI scalars for Quebec by land cover type, dashed vertical lines indicate the 2nd and 98th percentile utilized in scaling FPAR. Vertical axis (y-dimension) is the fraction of NDVI by land cover type and the horizontal axis (x-dimension) is the NDVI value.

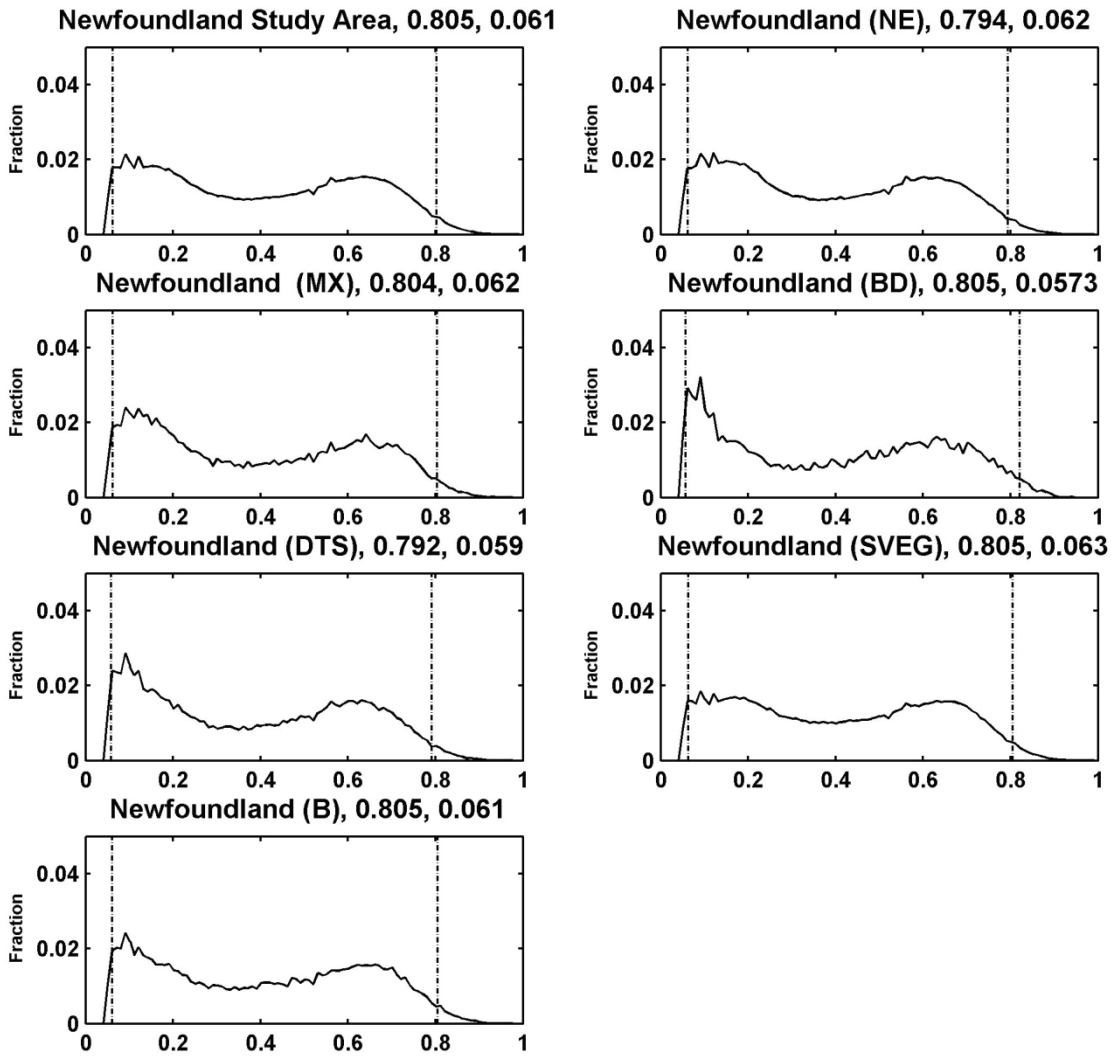

Figure B.2.6 FPAR NDVI scalars for Newfoundland and Labrador, dashed vertical lines indicate the 2nd and 98th percentile utilized in scaling FPAR. Vertical axis (y-dimension) is the fraction of NDVI by land cover type and the horizontal axis (x-dimension) is the NDVI value.

B.3 LAI Calculation from FPAR

In model simulations, Leaf Area Index (LAI) was generated from FPAR to simulate NPP in above-ground live leaf carbon pool and amount of carbon transferred to structural leaf surface litter pools, as well as the amount of available biomass for herbivory consumption. LAI was calculated from FPAR based upon homogeneous and heterogeneous plant functional types derived from Landsat land cover maps and International Geosphere Biosphere Program (IGBP) land cover classes(Vg). All derived calculations are from Los et al. (2000). Values for FPARMAX and LAIMAX are provided below.

Table B.3.1 Values used for maximum canopy closure by vegetation type.

Class (Vg)	LAIMAX
(NE) Needle leaf Evergreen Forests	8.0
(MXF) Mixed Forests	7.5
(BD) Broadleaf Deciduous Forests	7.0
(DTS) Dwarf Trees/Scrublands	5.0
(SVEG) Short Vegetation C3 Grasslands	5.0
(AG) Agriculture C4 Grasslands	6.0
(W) Water	0.0
(B) Barren/Bare Soil/Urban	5.0
(C) Clouds/Snow	0.0

For homogeneous vegetation (Vg) types (BD, DTS, SVEG, AG, and B) Leaf area index (LAI) is the exponential relation between FPAR and LAI calculated as:

$$LAI(Vg) = LAIMAX\ (Vg)\ \cdot \left({log\big(1 - FPAR(Vg)\big)} \Big/ {log(1 - FPARMAX)} \right)$$

For clustered vegetation (Vg) types (NE) LAI is an exponential relation between FPAR and LAI calculated as:

$$LAI(Vg) = LAIMAX(Vg) \cdot \left({}^{FPAR(Vg)}/_{FPARMAX}\right)$$

For clustered and evenly distributed vegetation types (MXD) LAI is a weighted combination of exponential and linear functions between FPAR and LAI calculated as:

$$LAI(Vg) = \left(LAIMAX(Vg) \cdot \left(\frac{log\left(1 - FPAR(Vg)\right)}{log(1 - FPARMAX)}\right) + \left(\frac{FPAR(Vg)}{FPARMAX}\right)\right)\Big/2$$

B.4 Climate Anomalies Generated to Determine Model Spin Up

The model was allowed to reach steady state based on year selection with low growing season anomalous variability in temperature, precipitation, and solar radiation. Mean climate from 1982 to 2005 was not assumed to be adequate for simulations due to climate warming trends in Yukon and Newfoundland and change in precipitation in Southern Saskatchewan study regions. Solar radiation data was only available from July of 1983 to December of 2004 when simulations were performed. To extend the record for full 1982 to 2005 time period, data beginning and end series were replicated by pixel location. To select a year of climate data for model for 2000 years of spin up, growing season (May to September) annual anomalies were generated by study region (Figure B.4.1 to B.4.6).

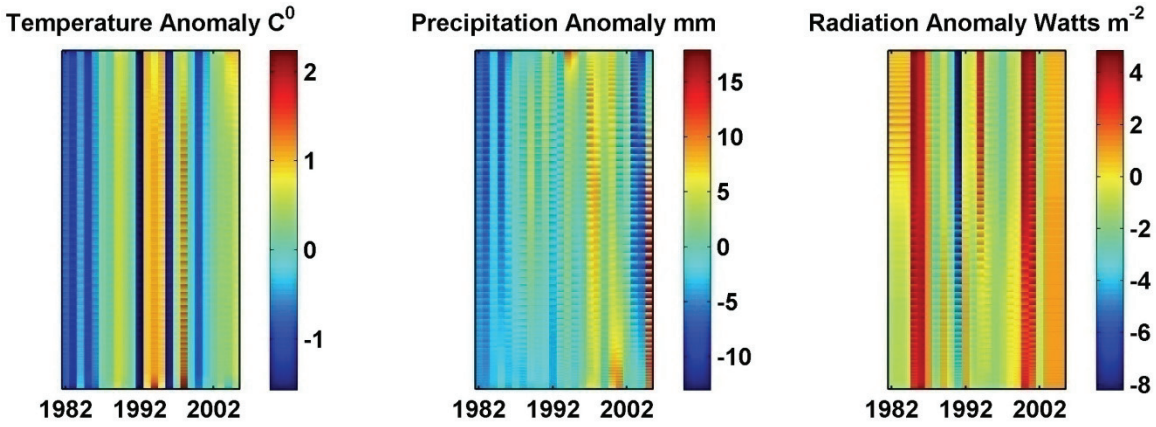

Figure B.4.1 Yukon growing season climate anomalies generated to determine model spin-up year. Data presented as location in the vertical and year in the horizontal dimension. Climate data from 1984 was used due to low variance relative to the 24-year anomaly.

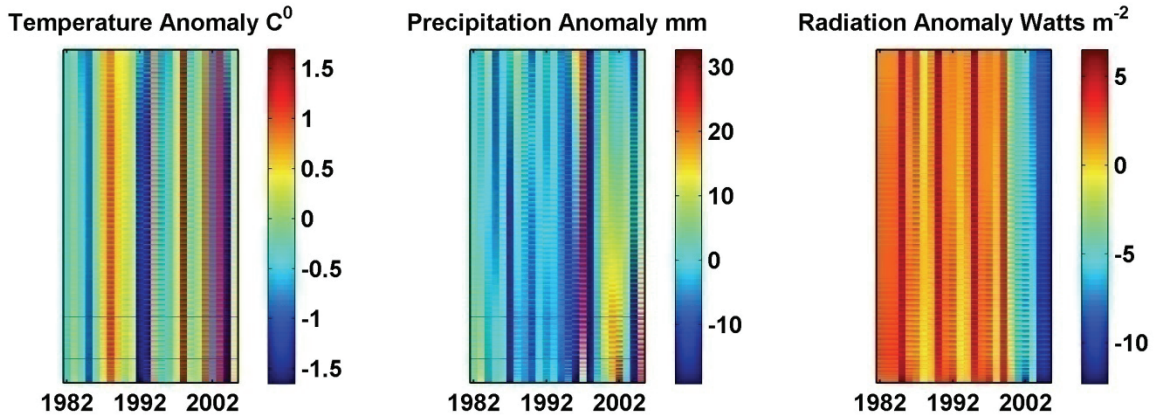

Figure B.4.2 Northern Saskatchewan growing season climate anomalies generated to determine model spin-up year. Data presented as location in the vertical and year in the horizontal dimension. Climate data from 1993 was used due to low variance relative to the 24-year anomaly and 10-years after 1980 and 1981 large fire years which impact NDVI.

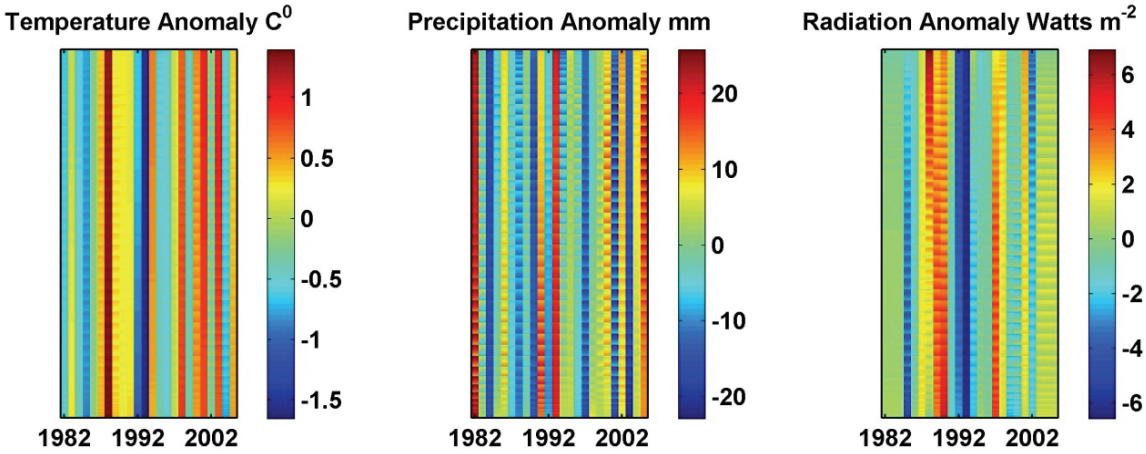

Figure B.4.3 Southern Saskatchewan growing season climate anomalies generated to determine model spin-up year. Data presented as location in the vertical and year in the horizontal dimension. Climate data from 1984 was used due to low variance relative to the 24-year anomaly.

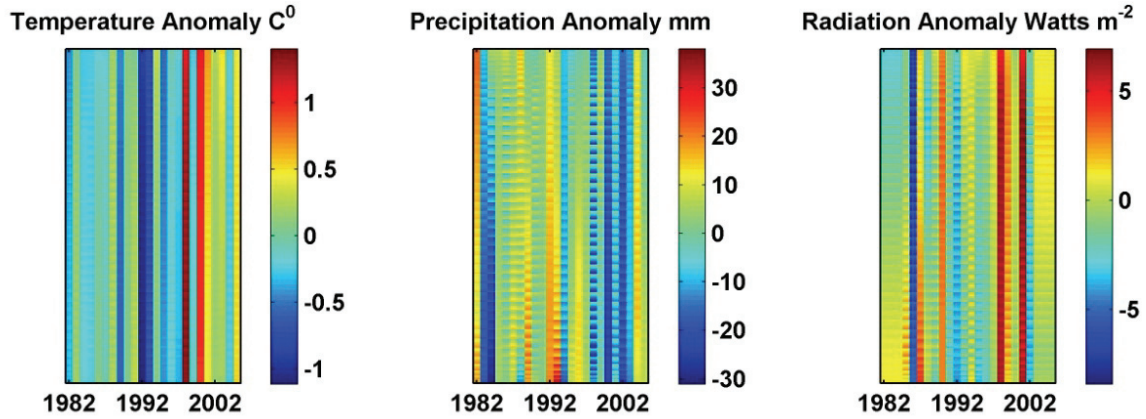

Figure B.4.4 Oklahoma Panhandle growing season climate anomalies generated to determine model spin-up year. Data presented as location in the vertical dimension and year in the horizontal dimension. Climate data from 1984 was used due to low variance relative to the 24-year anomaly.

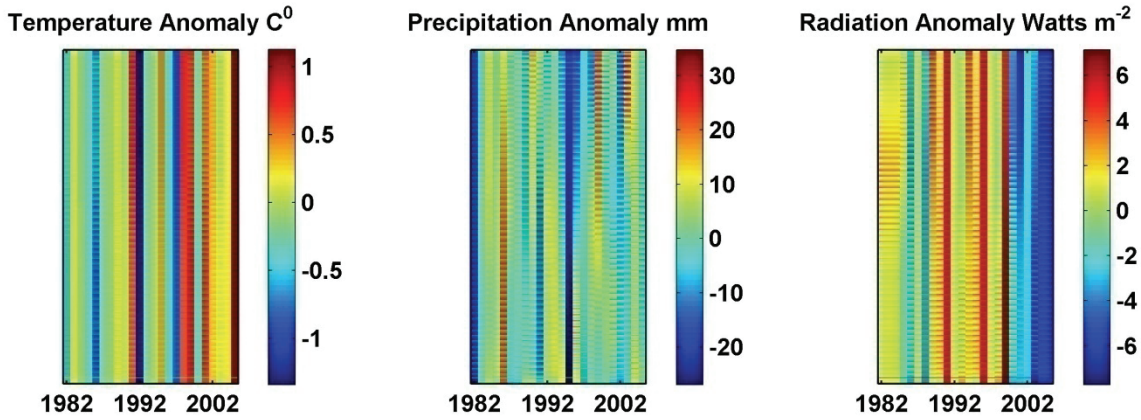

Figure B.4.5 Quebec growing season climate anomalies generated to determine model spin-up year. Data presented as location in the vertical and year in the horizontal dimension. Climate data from 1993 was used due to low variance relative to the 24-year anomaly and 10-years after spruce budworm outbreak and salvage logging which impact NDVI.

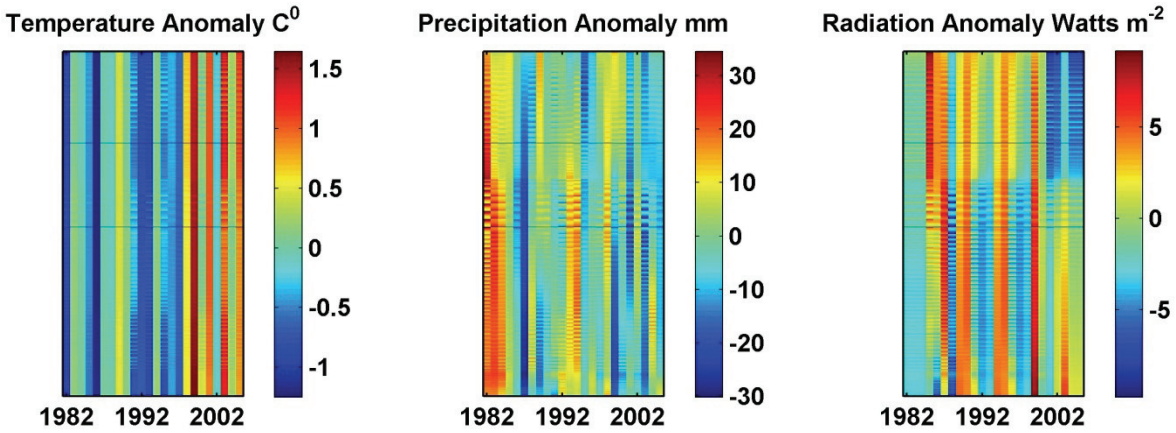

Figure B.4.6 Newfoundland growing season climate anomalies generated to determine model spin-up year. Data presented as location in the vertical dimension and year in the horizontal dimension. Climate data from 1984 was used due to low variance relative to the 24-year anomaly.

References:

Adler, R.F., Huffman, G.J., Chang, A., Ferraro, R., Xie, P.P., Janwiak, J., Ruddle, B., Schneider, U., Curtis, S., Bolvin, D., Gruber, A., Susskind, J., Arkin, P., & Nelkin, E. (2003). The Version-2 Global Precipitation Climatology Project (GPCP) Monthly Precipitation Analysis (1979-Present). *Journal of Hydrometeorology, 4*, 1147-1167

Afanasyev, Y.D., Nezlin, N.P., & Kostianoy, A.G. (2001). Patterns of seasonal dynamics of remotely sensed chlorophyll and physical environment in the Newfoundland region. *Remote Sensing of Environment, 76*, 268-282

Allen, T.F.H., & Starr, T.B. (1982). *"Hierarchy:Perspectives for Ecological Complexity."* Chicago: University of Chicago Press

Alma (2007). A Growing Population. Available Online at: http://www.ville.alma.qc.ca/anglais/investisseur/profil-population.html (accessed 07-29-07)

Amiro, B.D., Chen, J.M., & Liu, J. (2000). Net primary productivity following forest fire for Canadian ecoregions. *Canadian Journal of Forest Research - Revue Canadienne De Recherche Forestiere, 30*, 939-947

Amiro, B.D., Todd, J.B., Wotton, B.M., Logan, K.A., Flannigan, M.D., Stocks, B.J., Mason, J.A., Martell, D.L., & Hirsch, K.G. (2001). Direct carbon emissions from Canadian forest fires, 1959-1999. *Canadian Journal of Forest Research - Revue Canadienne De Recherche Forestiere, 31*, 512-525

Angert, A., Biraud, S., & Bonfils, C. (2005). Drier summers cancel out the CO2 uptake enhancement induced by warmer springs. *Proceedings of the National Academy of Sciences of the United States of America, 102*, 10823-10827

Archibold, O.W. (1995). *Ecology of World Vegetation*. London: Chapman & Hall

Auclair, A.N.D., Bouchard, A., & Pajaczkowski, J. (1976). Concentration, mass and distribution of nutrients in a subarctic Picea mariana-Cladonia alpestris ecosystem. *Canadian Journal of Forest Research - Revue Canadienne De Recherche Forestiere, 12*, 947-968

Ayres, M.P., & Lombardero, M.J. (2000). Assessing the consequences of global change for forest disturbance from herbivores and pathogens. *The Science of the Total Environment 262*, 263-286

Baker, D.F., Law, R.M., Gurney, K.R., Rayner, P., Peylin, P., Denning, A.S., Bousquet, P., Bruhwiler, L., Chen, Y.H., Cias, P., Fung, I.Y., Heimann, M., John, J., Maki, T., Maksyutov, S., Massaric, K., Prather, M., Pak, B., Taguchi, S., & Zhu, Z. (2006). TransCom 3 inversion intercomparison: impact of transport model errors

on the interannual variability of regional CO_2 fluxes, 1988-2003. *Global Biogeochemical Cycles, 20*, GB1002

Baldocchi, D.D., & Amthor, J.S. (2001). Canopy Photosynthesis: History Measurements, and Models. In J. Roy, B. Saugier & H.A. Mooney (Eds.), *Terrestrial Global Productivity* (p. 573). San Diego: Academic Press

Barber, V., Juday, G., & Finney, B. (2000). Reduced growth of Alaskan white spruce in the twentieth century from temperature-induced drought stress. *Nature, 405*, 668-673

Baskerville, G.L. (1975). Spruce budworm: The answer is forest management: or is it? *Forest Chronologies, 51*, 157-160

Benedetti, R., & Rossini, P. (1993). On the use of NDVI profiles as a tool for agriculture statistics: The case study of wheat yield estimate and forecast in Emilia Romagna. *Remote Sensing of Environment, 45*, 311-326

Bishop, J.K.B., & Rossow, W.B. (1991). Spatial and temporal variability of global surface solar irradiance. *Journal of Geophysical Research, 287*, 2467-2470

Blias, J.R. (1981). Mortality of balsam fir and white spruce following a spruce budworm outbreak in the Ottawa River watershed in Quebec. *Canadian Journal of Forest Research, 11*, 620-629

Blias, J.R. (1983). Trends in the frequency, extent and severity of spruce budworm outbreaks in eastern Canada. *Canadian Journal of Forest Research, 13*, 539-547

Blias, J.R. (1985). The ecology of the eastern spruce budworm: A review and discussion. In C.F. Service (Ed.) (pp. 49-59)

Boissard, P., Pointel, J.G., & Huet, P. (1993). Reflectance, green leaf area index and ear hydric status of wheat from anthesis until maturity. *International Journal of Remote Sensing, 14*, 2713-2729

Bonan, G.B., Levis, S., Kergoat, L., & Oleson, K.W. (2002). Landscapes as patches of plant functional types: An integrating concept for climate and ecosystem models. *Global Biogeochemical Cycles, 16*, 5-1,5-18

Bounoua, L., Collatz, G.J., Los, S.O., Sellers, P.J., Dazlich, D.A., Tucker, C.J., & Randall, D.A. (2000). Sensitivity of climate to changes in NDVI. *Journal of Climate, 13*, 2277-2292

Bousquet, P., Cias, P., Peylin, P., Ramonet, M., & Monfray, P. (1999). Inverse modeling of annual atmopsheric CO_2 sources and sinks 1. Method and control inversion. *Journal of Geophisical Research, 104*, 26161-26178

Bousquet, P., Peylin, P., Ciais, P., Quere, C.L., Friedlingstein, P., & Tans, P.P. (2000). Regional Changes in Carbon Dioxide Fluxes of Land and Oceans Since 1980. *Science, 290*, 1342-1346

Breshears, D.D., Cobb, N.S., Rich, P.M., Price, K.P., & Allen, C.D. (2005). Regional vegetation die-off in response to global-change type drought. *Proceedings of the National Academy of Sciences USA, 102*, 15144-15148

Brovokin, V., Sitch, S., Bloh, W.v., Claussen, M., Bauer, E., & Cramer, W. (2004). Role of land cover changes for atmospheric CO_2 increase and climate change during the last 150 years. *Global Change Biology, 10*, 1253-1266

Brown, M.E., Pinzon, J.E., & Tucker, C.J. (2004). New Vegetation Index Data Set Available to Monitor Global Change. *EOS Transactions, 85*, 565-569

Buchmann, N., & Schulze, E.-D. (1999). Net CO_2 and H_20 fluxes of terrestrial ecosystems. *Global Biogeochemical Cycles, 13*, 751-760

Bunn, A.G., & Goetz, S.J. (2006). Trends in satellite-observed circumpolar photosynthetic activity from 1982 to 2003: The influence of seasonality, cover type, and vegetation density. *Earth Interactions, 10*, 1-19

Burke, R.A., Zepp, R.G., Tarr, M.A., Miller, W.L., & Stocks, B.J. (1997). Effect of fire on soil-atmosphere exchange of methane and carbon dioxide in Canadian boreal forest sites. *Journal of Geophysical Research-Atmospheres, 102*, 29289-29300

Caldeira, K., Morgan, M.G., Baldocchi, D., Brewer, P.G., Chen, C.T.A., Nabuurs, G.J., Nakicenovic, N., & Robertson, G.P. (2004). A portfolio of carbon management options. In C.B. Field & M.R. Raupach (Eds.), *The Global Carbon Cycle: Integrating Humans, Climate, and the Natural World* (pp. 103-129). Washington, D.C.: Island Press

Canadell, J.G., Pataki, D., Gifford, R., Houghton, R.A., Lou, Y., Raupach, M.R., Smith, P., & Steffen, W. (2007). Saturation of the terrestrial carbon sink. In J.G. Canadell, D. Pataki & L. Pitelka (Eds.), *The IGBP Series* (pp. 59-78). Berlin: Springer-Verlag

Candell, J.G., Mooney, H.A., Baldocchi, D.D., Berry, J.A., Ehleringer, J.R., Feild, C.B., Gower, S.T., Hollinger, D.Y., Hunt, J.E., Jackson, R.B., Running, S.W., Shaver, G.R., Steffen, W., Trumbore, S.E., Valentini, R., & Bond, B.Y. (2000). Carbon Metabolism of the Terrestrial Biosphere: A Multi-technique Approach for Improved Understanding. *Ecosystems, 3*, 115-130

Carvalhais, N., Reichstein, M., Seixas, J., Collatz, G.J., Pereira, J.S., Berbigier, P., Carrara, A., Granier, A., Montagnani, L., Papale, D., Rambal, S., Sanz, M.J., & Valentini, R. (2008). Implications of Carbon Cycle Steady State Assumptions for Biogeochemical Modeling Performance and Inverse Parameter Retrieval. *Global Biogeochemical Cycles, in press*

Caspersen, J.P., Pacala, S.W., Jenkins, J.C., Hurtt, G.C., Moorcroft, P.R., & Birdsey, R.A. (2000). Contributions of Land-Use History to Carbon Accumulation in U.S. Forests. *Science, 290*, 1148-1151

CCSP (2007). *The First State of the Carbon Cycle Report (SOCCR): The North American Carbon Budget and Implications for the Global Carbon Cycle*: U.S. Climate Change Science Program and the Subcommittee on Global Change Research, US Government

Chapin, F.S., McGuire, A.D., Randerson, J., Pielke, R., Baldocchi, D., Hobbie, S.E., Roulet, N., Eugster, W., Kasischke, E., Rastetter, E.B., Zimov, S.A., & Running, S.W. (2000). Arctic and boreal ecosystems of western North America as components of the climate system. *Global Change Biology, 6*, 211-223

Chapin, F.S., Woodwell, G.M., Randerson, J.T., Rastetter, E.B., Lovett, G.M., Boldocchi, D.D., Clark, D.A., Harmon, M.E., Schimel, D.S., Valentini, R., Wirth, C., Aber, J.D., Cole, J.J., Goulden, M.L., Harden, J.W., Heimann, M., Howarth, R.W., Matson, P.A., McGuire, A.D., Melillo, J.M., Mooney, H.A., Neff, J.C., Houghton, R.A., Pace, M.L., Ryan, M.G., Running, S.W., Sala, O.E., Shlesinger, W.H., & Schulze, E.D. (2006). Reconciling Carbon-cycle Concepts Terminology, and Methods. *Ecosystems, 9*, 1041-1050

Chen, J.M., Chen, B., Higuchi, K., Liu, J., & Chan, D. (2006). Boreal ecosystems sequestered more carbon in warmer years. *Geophysical Research Letters, 33*, doi:10.1029/2006GL025919

Ciais, P., Reichstein, M., Viovy, N., Granier, A., Ogee, J., Allard, V., Aubinet, M., Buchmann, N., Bernhofer, C., Carrara, A., Chevallier, F., Noblet, N.D., Friend, A.D., Freidlingstein, P., Grunwald, T., Heinesch, B., Keronen, P., Knohl, A., Krinner, G., Loustau, D., Manca, G., Matteucci, G., Miglietta, F., Ourcival, J.M., Papale, D., Pilegaard, K., Rambal, S., Seufert, G., Soussana, J.F., Sanz, M.J., Schulze, E.D., Vesala, T., & Valentini, R. (2005). Europe-wide reduction in primary productivity caused by the heat and drought in 2003. *Nature, 437*, 529-533

Ciais, P., Tans, P.P., Trolier, M., White, J.W.C., & Francey, R.J. (1995). A Large Northern Hemisphere Terrestrial CO_2 Sink Indicated by the $^{13}C/^{12}C$ Ratio of Atmospheric CO_2. *Science, 269*, 1098-1102

Ciais, P., Tans, P.P., White, J.W.C., Trolier, M., Francey, R.J., Berry, J.A., Randall, D.R., Sellers, P.J., Collatz, J.G., and Schimel, D.S. (1995). Partitioning of ocean and land uptake of CO_2 as infered by C^{13} measurements from NOAA Climate Monitoring and Diagnostics Laboratory Global Air Sampling Newtwork. *Journal of Geophysical Research, 100*, 5051-5070

Clein, J.S., Kwiatkowski, B., McGuire, A.D., Hobbie, J.E., Rastetter, E.B., Melillo, J.M., & Kicklighter, D.W. (2000). Modeling carbon responses of tundra ecosystems to historical and projected climate: a comparison of a plot-and a global-scale

ecosystem model to identify process-based uncertainties. *Global Change Biology, 6*, 127-140

Cole, D.W., & Rapp, M. (1981). Elemental cycling in forest ecosystems. In D.E. Reichle (Ed.), *Dynamic Properties for Forest Ecosystems* (pp. 341-409). Cambridge: Cambridge University Press

Covich, A.P., Fritz, S.C., Lamb, P.J., Marzolf, R.D., Matthews, W.J., Poiani, K.A., Prepas, E.E., Richman, M.B., & Winter, T.C. (1997). Potential Effects of Climate Change on Aquatic Ecosystems of the Great Plains of North America. *Hydrological Processes, 11*, 993-1021

Cramer, W., Kicklighter, D.W., Bondeau, A., III, B.M., Churkina, G., Nemry, B., Ruimy, A., & Schloss, A.L. (1999). Comparing global models of terrestrial net primary productivity (NPP): overview and key results. *Global Change Biology, 5*, 1-15

Crist, E.P., & Cicone, R.C. (1984). Application of the Tasseled Cap concept to simulated Thematic Mapper data. *Photogrammetric Engineering and Remote Sensing, 50*, 343-352

Dai, A., Trenberth, K.E., & Qian, T. (2004). A Global Dataset of Palmer Drought Severity Index for 1870-2002: Relationship with Soil Moisture and Effects of Surface Warming. *Journal of Hydrometerology, 5*, 1117-1130

DeFries, R., Field, C.B., Fung, I., Collatz, G.J., & Bounoua, L. (1999). Combining satellite data and biogeochemical models to estimate global effects of human-induced land cover change on carbon emissions and primary productivity. *Global Biogeochemical Cycles, 13*, 803-815

DeFries, R.S., Hansen, M.C., Townshend, J.R.G., Jenetos, A.C., & Loveland, T.R. (2000). A new global 1-km dataset of percentage tree cover derived from remote sensing. *Global Change Biology, 6*, 247-254

Deng, F., Chen, J., Ishizawa, M., Yuen, C., Mo, G., Higuchi, K., Chan, D., & Maksyutov, S. (2007). Global monthly CO_2 flux inversions with a focus over North America. *Tellus, 59B*, 179-190

Denning, A.S. (1994). Investigations of the transport, sources, and sinks of atmospheric CO_2 using a general circulation model. In. Fort Collins: Colorado State

Dixon, R.K., Brown, S., Houghton, R.A., Solomon, A.M., Trexler, M.C., & Wisniewski, J. (1994). Carbon Pools of Global Forest Ecosystems. *Science, 263*, 185-190

Domenikiotis, C., Dalezios, N.R., Loukas, A., & Karteris, M. (2002). Agreement assessment of NOAA/AVHRR NDVI with Landsat TM NDVI for mapping burned forested areas. *International Journal of Remote Sensing, 23*, 4235-4246

Dong, J., Kaufmann, R.K., Myneni, R.B., Tucker, C.J., Kauppi, P.E., Liski, J., Buerman, W., Alexeyev, V., & Hughes, M.K. (2003). Remote sensing estimates of boreal and temperate forest woody biomass: carbon pools, sources, and sinks. *Remote Sensing of Environment, 84*, 393-410

Doraiswamy, P.C., & Cook, P.W. (1995). Spring wheat yield assessment using NOAA AVHRR data. *Canadian Journal of Remote Sensing, 21*, 43-51

Dorman, J.L., & Sellers, P.J. (1989). A Global Climatology of Albedo, Roughness Length and Stomatal Resistance for Atmospheric General Circulation Models as Represented by the Simple Biosphere Model (SiB). *American Meteorological Society, 28*, 833-855

Dye, D.G., & Tucker, C.J. (2003). Seasonality and trends of snow-cover, vegetation index, and temperature in northern Eurasia. *Geophysical Research Letters, 30*, 58-51, 58-54

Epstein, H.E., Calef, M.P., Walker, M.D., Chapin, F.S., & Starfield, A.M. (2004). Detecting changes in arctic tundra plant communities in response to warming over decadal time scales. *Global Change Biology, 10*, 1325-1334

FAO (1978). *Report on the Agroecological Zone Project*. Rome: Food and Agriculture Organization of the UN

Feng, S., & Hu, Q. (2004). Changes in agro-meteorological indicators in the contiguous United States: 1951-2000. *Theoretical Applications in Climatology, 78*, 247-264

Field, C.B., Randerson, J.T., & Malmstrom, C.M. (1995). Global Net Primary Production: Combining Ecology and Remote Sensing. *Remote Sensing of Environment, 51*, 74-88

Flannigan, M.D., Stocks, B.J., & Wotton, B.M. (2000). Climate change and forest fires. *The Science of the Total Environment, 262*, 221-229

Foley, J.A., & Ramankutty, N. (2004). A primer on the terrestrial carbon cycle: What we don't know but should. In C.B. Field & M.R. Raupauch (Eds.), *The global carbon cycle: Integrating humans, climate and the natural world* (pp. 279-294). Washington D.C.: Island Press

Frich, P., Alexander, L.V., Della-Marta, P., Gleason, B., Haylock, M., Tank, A.M.G.K., & Peterson, T. (2002). Observed coherent changes in climatic extremes during the second half of the twentieth century. *Climate Research, 19*, 2559-2566

Friedlingstein, P., Cox, R., Betts, R., Bopp, L., Bloh, W.v., Brovokin, V., Doney, S., Eby, M., Fung, I., Govindasamy, B., John, J., Jones, C., Joos, F., Kato, T., Kawamiya, M., Knorr, W., Lindsay, K., Mathews, H.D., Weaver, T., Yoshikawa, C., & Zeng, N. (2006). Climate-carbon cycle feedback analysis, results from the C^4 MIP model intercomparison. *Journal of Climate, 19*, 891-899

Friedlingstein, P., Fung, I., Holland, E., John, J., Brasseur, G., Erickson, D., & Schimel, S. (1995). On the contribution of CO_2 fertilization to the missing biosphere sink. *Global Biogeochemical Cycles, 9*, 541-556

Friedlingstein, P., Joel, G., Feild, B., & Fung, I.Y. (1999). Toward an allocation scheme for global terrestrial carbon models. *Global Change Biology, 5*, 755-770

Fung, I., Field, C.B., Berry, J.A., Thompson, M.V., Randserson, J.T., Malmstrom, C.M., Vitousek, P.M., Collatz, G.J., Sellers, P.J., Randall, D.A., Denning, A.S., Badeck, F., & John, J. (1997). Carbon 13 exchanges between the atmosphere and biosphere. *Global Biogeochemical Cycles, 11*, 507-533

Fung, I.Y., Doney, S.C., Lindsay, K., & John, J. (2005). Evolution of carbon sinks in changing climate. *Proceedings of the National Academy of Sciences of the United States of America, 102*, 11201-11206

Goetz, S.J., Bunn, A.G., Fiske, G.J., & Houghton, R.A. (2005). Satellite-observed photosynthetic trends across boreal North America associated with climate and fire disturbance. *Proceedings of the National Academy of Sciences of the United States of America, 102*, 13521-13525

Goetz, S.J., Fiske, G.J., & Bunn, A.G. (2006). Using satellite time-series data sets to analyze fire disturbance and forest recovery across Canada. *Remote Sensing of Environment, 101*, 352-365

Gong, D.Y., & Shi, P.J. (2003). Northern hemispheric NDVI variations associated with large-scale climate indices in spring. *International Journal of Remote Sensing, 24*, 2559-2566

Goodale, C.L., Apps, M.J., Birdsey, R.A., Field, C.B., Heath, L.S., Houghton, R.A., Jekkins, J.C., Kohlmaier, G.H., Kurz, W., Liu, S., Nabuurs, G., Nilsson, S., & Shvidenko, A.Z. (2002). Forest Carbon Sinks in the Northern Hemisphere. *Ecological Applications, 12*

Goudrian, J., Groot, J.J.R., & Uithol, P.W.J. (2001). Productivity of Agro-Ecosystems. In J. Roy & B. Saugier (Eds.), *Terrestrial Global Productivity* (p. 573). San Diego: Academic Press

Gregory, P.J., Ingram, J.S.I., Campbell, B., Goudrian, L.A., Hunt, J.J., Linder, S., Stafford, S., Smith, M., Sutherst, R.W., & Valentin, C. (1999). Managed production systems. In B. Walker, W. Steffen, J. Canadell & J. Ingram (Eds.), *The Terrestrial Biosphere and Global Change: Implications for natural and managed ecosystems*

Guild, L.S., Cohen, W.B., & Kauffman, J.B. (2004). Detection of deforestation and land conversion in Rondonia, Brazil using change detection techniques. *International Journal of Remote Sensing, 25*, 731-750

Gurney, K.R., Law, R.M., Denning, A.S., Rayner, P.J., Baker, D., Bousquet, P., Bruhwiler, L., Chen, Y.H., Cias, P., Fan, S., Fung, I.Y., Gloor, M., Heimann, M., Higuchi, K., John, J., Maki, T., Maksyutov, S., Massaric, K., Peylin, P., Prather, M., Pak, B.C., Randerson, J., Sarmiento, J., Taguchi, S., Takahsi, T., & Yue, C.W. (2002). Towards robust regional estimates of CO2 sources abd sinks using atmospheric transport models. *Nature, 415*, 626-630

Gurney, K.R., Law, R.M., Denning, A.S., Rayner, P.J., Pak, B.C., Baker, D., Bousquet, P., Bruhwiler, L., Chen, Y.H., Cias, P., Fung, I.Y., Heimann, M., John, J., Maki, T., Maksyutov, S., Peylin, P., Prather, M., & Taguchi, S. (2004). Transcom 3 inversion intercomparison: Model mean results for the estimation of seasonal carbon sources and sinks. *Global Biogeochemical Cycles, 18*, GB1010, 1011-1018

Hall, F., Masek, J., & Collatz, G. (2006). Evaluation of ISLSCP Initiative II FASIR and GIMMS NDVI products and implications for carbon cycle science. *Journal of Geophysical Research, 111*, D22808 22801-22815

Hansen, J., Nazarenko, L., Ruedt, R., Sato, M., Willis, J., Genio, A.D., Koch, D., Lacis, A., Lo, K., Menon, S., Novakov, T., Perlwitz, J., Russell, G., Schmidt, G.A., & Tausnev, N. (2005). Earth's energy imbalance: confirmation and implications. *Science, 308*, 1431-1435

Hansen, J., Ruedy, R., Glascoe, J., & Sato, M. (1999). GISS Analysis of Surface Temperature Change. *Journal of Geophysical Research, 104*, 30997-31022

Hansen, J.E. (2007). Scientific reticence and sea level rise. *Environmental Resarch Letters, 2*, 1-6

Hay, R.K.M. (1995). Harvest index: a review of its use in plat breeding and crop physiology. *Annals of Applied Biology, 126*, 196-216

Hicke, J., Asner, G., Kasischke, E., French, N., Randerson, J., Collatz, G.J., Stocks, B.J., Tucker, C.J., Los, S.O., & Field, C.B. (2003). Postfire Response of North American Boreal Forest Net Primary Productivity Analyzed with Satellite Observations. *Global Change Biology, 9*, 1145-1157

Hicke, J.A., Asner, G.P., Randerson, J.T., Tucker, C.J., Los, S., Birdsey, R., Jenkins, J.C., Field, C., & Holland, E. (2002). Satellite-derived increases in net primary productivity across North America 1982-1998. *Geophysical Research Letters, 29*, 1427

Hicke, J.A., Lobell, D.B., & Asner, G.P. (2004). Cropland Area and Net Primary Production Computed from 30 years of USDA Agricultural Harvest Data. *Earth Interactions, 8*, 1-20

Higgins, D.G., & Ramsey, G.S. (1992). Canadian Forest Fire Statistics. Canadian Forest Service Information Report PI-X-16. In (p. 32). Chalk River, Canada: Petawawa National Forest Institute

Hobbie, S.E., Nadelhofer, K.J., & Hogberg, P. (2002). A synthesis: The role of nutrients as constraints on carbon balances in boreal and arctic regions. *Plant and Soil, 242*, 163-170

Houghton, D.D., Gallimore, R.G., & Keller, L.M. (1991). Stability and Variability in a Coupled Ocean-Atmosphere Climate Model: Results of 100-year Simulations. *Journal of Climate, 4*, 557-577

Houghton, R. (2007). Balancing the Global Carbon Budget. *Annual Review of Earth Planet Science, 35*, 313-347

Houghton, R.A. (1999). The annual net flux of carbon to the atmosphere from changes in land use 1850-1990. *Tellus Series B-Chemical and Physical Meteorology, 51B*, 298-313

Houghton, R.A. (2003). Revised estimates of the annual net flux of carbon to the atmosphere from changes in land use and land management 1850-2000 *Tellus, 55B*, 378-390

Houghton, R.A., Davidson, E.A., & Woodwell, G.M. (1998). Missing sinks, feedbacks and understanding the role of terrestrial ecosystems in the global carbon balance. *Global Biogeochemical Cycles, 12*, 25-34

Houghton, R.A., Hackler, J.L., & Lawrence, K.T. (1999). The U.S. carbon budget: contributions from land-use change. *Science, 285*, 574-578

Howard, E.A., Gower, S.T., Foley, J.A., & Kucharik, C.J. (2004). Effects of logging on carbon dynamics of jack pine forest in Saskatchewan, Canada. *Global Change Biology, 10*, 1267-1284

Huang, C., Wylie, B., Yang, L., Homer, C., & Zylstra, G. (2002). Derivation of a tasselled cap transformation based on Landsat 7 at-satellite reflectance. *International Journal of Remote Sensing, 23*, 1741-1748

Ichii, K., Kawabata, A., & Yamaguchi, Y. (2002). Global correlation analysis for NDVI and climatic variables and NDVI trends:1982-1990. *International Journal of Remote Sensing, 23*, 3873-3878

Imhoff, M.L., Tucker, C.J., Lawrence, W.T., & Stutzer, D.C. (2000). The use of multisource satellite and geospatial data to study the effect of urbanization on primary productivity in the United States. *IEEE Transactions on Geoscience and Remote Sensing, 38*, 2549-2556

IPCC (2001). North America. In S. Cohen & K. Miller (Eds.), *Climate Change 2001 Impacts, Adaptation, and Vulnerability* (pp. 735-800). Cambridge: Cambridge University Press

IPCC (2007). *Climate Change 2007 The Physical Science Basis*. Cambridge: Cambridge University Press

Jarvis, P.G., Saugier, B., & Schulze, E.D. (2001). *Productivity of Boreal Forests*. San Diego: Academic Press

Jensen, J.R. (2006). *Remote Sensing of the Environment: An Earth Resource Perspective*. Upper Saddle River: Prentice Hall

Jia, G.J., Epstein, H.E., & Walker, D.A. (2003). Greening of Arctic Alaska, 1981-2001. *Geophysical Research Letters, 30*, hls3-1,3-4

Jin, S., & Sader, S.A. (2005). Comparison of time series tasseled cap wetness and the normalized difference moisture index in detecting forest disturbances. *Remote Sensing of Environment, 94*, 364-372

Joos, F., & Prentice, I.C. (2004). A paleo perspective on the future of atmospheric CO_2 and climate. In C.B. Field & M.R. Raupach (Eds.), *The Global Carbon Cycle: Integrating Humans, Climate, and the Natural World* (pp. 165-186). Washington D.C.: Island Press

Kasischke, E.S., French, N.H.F. (1997). Constraints on using AVHRR composite index imagery to study patterns of vegetation cover in boreal forests. *International Journal of Remote Sensing, 18*, 2403-2426

Kauth, R.J., Lambeck, P.F., Richardson, W., Thomas, G.S., & Pentland, A.P. (1978). Feature extraction applied to agricultural crops as seen by Landsat. *The LACIE Symposium Proceedings of the Technical Session*, 705-722

Kauth, R.J., Lambeck, P.F., Richardson, W., Thomas, G.S., & Pentland, A.P. (1979). Feature extraction applied to agricultural crops as seen by Landsat. *The LACIE Symposium Proceedings of the Technical Session*, 705-722

Keeling, C.D., & Whorf, T.P. (2005). Atmospheric CO_2 records from sites in the SIO air sampling network. In: Trends: A Compendium of Data on Global Change. In O.R.N.L. Carbon Dioxide Information Analysis Center (Ed.). Oak Ridge, TN, USA: U.S. Department of Energy

Kettela, E. (1983). A Cartographic History of Spruce Budworm Defoliation from 1967 to 1981 in Eastern North America. In M.F.R. Center (Ed.) (p. 14): Fredericton

Knoor, W., & Heimann, M. (1995). Impact of drought stress and other factors on seasonal land biosphere CO2 exchange studied through an atmospheric tracer transport model. *Tellus, 47B*, 471-489

Kroodsma, D.A., & Feild, C.B. (2006). Carbon Sequestration In California Agriculture, 1980-2000 *Ecological Applicaitons, 16*, 1975-1985

Labus, M.P., Nielsen, G.A., Lawrence, R.L., & Engel, R. (2002). Wheat yield estimates using multi-temporal NDVI satellite imagery. *International Journal of Remote Sensing, 23*, 4169-4180

LaMotte, M., & Bourliere, F. (1983). Energy flow and nutrient cycling in tropical savannas. In F. Bourliere (Ed.), *Ecosystems of the World. Tropical Savannas* (pp. 583-603). New York: Elsevier

Lanjeri, S., Segarra, D., & Mella, J. (2004). Interannual vineyard crop variability in the Castilla-La Mancha region during the period 1991-1996 with Landsat Thematic Mapper images. *International Journal of Remote Sensing, 25*, 2441-2457

Larson, D.L. (1995). Effects of climate on numbers of northern prairie wetlands. *Climatic Change, 30*, 169-180

Leemans, R., & Cramer, W. (1991). The IIASA database for mean monthly values of temperature, precipitation and cloudness of a global terrestrial grid. *International Institute for Applied Systems Analysis (IIASA)*, RR-91-18

Lemly, A.D., Kingsford, R.T., & Thompson, J.R. (2000). Irrigated Agriculture and Wildlife Conservation: Conflict on a Global Scale. *Environmental Management, 25*, 485-512

Lobell, D.B., Hicke, J.A., Asner, G.P., Field, C.B., Tucker, C.J., & Los, S.O. (2002). Satellite estimates of productivity and light use efficiency in United States agriculture, 1982-98. *Global Change Biology, 8*, 722-735

Los, S.O., Collatz, G.J., Sellers, P.J., Malmstrom, C.M., Pollack, N.H., DeFries, R.S., Bounoua, L., Parris, M.T., Tucker, C.J., & Dazlich, D.A. (2000). A Global 9-year Biophysical Land Surface Dataset from NOAA AVHRR data. *Journal of Hydrometerology, 1*, 183-199

Lotsch, A., Friedl, M.A., & Anderson, B.T. (2003). Coupled vegetation-precipitation variability observed from satellite and climate records. *Geophysical Research Letters, 30*, 8-1-8-4

Lotsch, A., Friedl, M.A., Anderson, B.T., & Tucker, C.J. (2005). Response of terrestrial ecosystems to recent Northern Hemispheric drought. *Geophysical Research Letters, 32*, L06705

Lucht, W., Prentice, I.C., Myneni, R.B., Sitch, S., Friedlingstein, P., Cramer, W., Bousquet, P., Buermann, W., & Smith, B. (2002). Climatic Control of the High-Latitude Vegetation Greening Trend and Pinatubo Effect. *Science, 296*, 1687-1689

Lunetta, R.S., Ediriwickrema, J., Johnson, D.M., Lyon, H.J.G., & McKerrow, A. (2002). Impacts of vegetation dynamics on the identification of land-cover change in a biologically complex community in North Carolina, USA. *Remote Sensing of Environment, 82*, 258-270

Malhi, S.S., Gill, K.S., & Heier, K. (2001). Effectiveness of banding versus broadcasting of establishment-time and annual phosphorus applications on yield, protein, and phosphorus uptake of bromegrass. *Journal of Plant Nutrition, 24*, 1435-1444

Malmstrom, C.M., Thompson, M.V., Juday, G.P., Los, S.O., Randerson, J.T., & Field, C.B. (1997). Interannual variation in global scale net primary production: Testing model estimates. *Global Biogeochemical Cycles, 11*, 367-392

Masek, J.G., & Collatz, G.J. (2006). Estimating forest carbon fluxes in a disturbed southerstern landscape: Integration of remote sensing, forest inventory, and biogeochemical modeling. *Journal of Geophysical Research, 111*, G01006

Masek, J.G., Lindsay, F.E., & Goward, S.N. (2000). Dynamics of urban growth in the Washington DC metropolitan area, 1973-1996, from Landsat observations. *International Journal of Remote Sensing, 21*, 3473-3486

McGuire, A.D., Melillo, J.M., Randerson, J., Parton, W.J., Heimann, M., Meier, R.A., Clein, J.S., Kicklighter, D.W., & Sauf, W. (2000). Modeling the effects of snowpack on heterotrophic respiration across northern temperate and high latitude regions: Comparison with measurements of atmospheric carbon dioxide in high latitudes. *Biogeochemistry, 48*, 91-114

McNaughton, S.J., Oesterheld, M., Frank, D.A., & Williams, K.J. (1989). Ecosystem-level paterns of primary production and herbivory in terrestrial habitats. *Nature, 341*, 142-144

Menzel, A., & Fabian, P. (1999). Growing season extended in Europe. *Nature, 397*, 659

Monson, R.K., Lipson, D.L., Burns, S.P., Turnipseed, A.A., Delany, A.C., Williams, M.W., & Schmidt, S.K. (2006). Winter forest soil respiration controlled by climate and microbial community composition. *Nature, 439*, 711-714

Monteith, J. (1977). Climate and Efficiency of Crop Production in Britain. *Philosophical Transactions of the Royal Society of London Series B-Biological Sciences, 281*, 277-294

Monteith, J.L. (1981). Climatic variation and the growth of crops. *Quarterly Journal of The Royal Meteorological Society, 107*, 749-774

MSC (2007). Meteorological Service of Canada. Available Online at: http://www.msc-smc.ec.gc.ca (accessed 2-12-2007)

Murayama, S., & Taguchi, S. (2004). Imterannual variation in the atmospheric CO_2 growth rate: Role of atmospheric transport in the Northern Hemisphere. *Journal of Geophysical Research, 109*, D02305, 02301-02314

Myneni, R.B., Dong, J., Tucker, C.J., Kaufmann, R.K., Kauppi, P.E., Liski, J., Zhou, L., Alexeyev, V., & Hughes, M.K. (2001). A large carbon sink in the woody biomass of Northern forests. *Proceedings of the National Academy of Sciences of the United States of America, 98*, 14784-14789

Myneni, R.B., Hall, F.G., Sellers, P.J., & Marshak, A.L. (1995). The Interpretation of Spectral Vegetation Indexes. *IEEE Transactions Geoscience and Remote Sensing, 33*, 481-486

Myneni, R.B., Keeling, C.D., Tucker, C.J., Asrar, G., & Nemani, R.R. (1997). Increased Plant Growth in the Northern High Latitudes from 1981 to 1991. *Nature, 386*, 698-702

Nackerts, K., Vaesen, K., Muys, B., & Coppin, P. (2005). Comparative performance of a modified change vector analysis in a forest change detection. *International Journal of Remote Sensing, 26*, 839-852

Nazarenko, L., Tausnev, N., & Hansen, J. (2007). The North Atlantic Thermohaline Ciruclation Simulated by the GISS Climate Model during 1970-99. *Canadian Meteorlogical and Oceanographic Society, 45*, 81-92

Neigh, C.S.R., Tucker, C.J., & Townshend, J.R.G. (2007). Synchronous NDVI and surface temperature trends in Newfoundland: 1982-2003. *International Journal of Remote Sensing, 28*, 2581-2598

Neigh, C.S.R., Tucker, C.J., & Townshend, J.R.G. (2008). North American Vegetation Dynamics observed with multi-resolution satellite data. *Remote Sensing of Environment, 112*, 1749-1772

Nemani, R.R., Keeling, C.D., Hashimoto, H., Jolly, W.M., Piper, S.C., Tucker, C.J., Myneni, R.B., & Running, S.W. (2003). Climate-Driven Increases in Global Terrestrial Net Primary Production from 1982 to 1999. *Science, 300*, 1560-1563

NFS (2007). National Forestry Database Program Available Online at: http://pndf.ccmf.org (accessed 1-31-07)

Nowak, R.S., Ellsworth, D.S., & Smith, S.D. (2004). Functional responses of plants to elevated atmospheric CO_2 - do photosynthetic and productivity data from FACE experiments support early predictions? *New Phytologist, 162*, 253-280

NRC (2007). Forestry Statistics. Available Online at: http://www.nrcan.gc.ca/cfs (accessed 7-29-07)

Odum, E.P. (1969). The Strategy of Ecosystem Development. *Science, 164*, 262-270

Ogle, S.M., Breidt, F.J., Eve, M.D., & Paustian, K. (2003). Uncertainty in estimating land use and management impacts on soil organic carbon storage for US agricultural lands between 1982 and 1997. *Global Change Biology, 9*, 1521-1542

Olson, J.S. (1975). *Productivity of Forests Ecosystems, Productivity of World Ecosystems*. Washington, DC: National Academy of Sciences

Opie, J. (2000). *Ogallala: water for a dry land*. Lincoln: University of Nebraska Press

Pacala, S.W., Hurtt, G.C., Baker, D., Peylin, P., Houghton, R.A., Birdsey, R.A., Heath, L., Sundquist, E.T., Stallard, R.F., Ciais, P., Moorcroft, P., Caspersen, J.P., Shevliakova, E., Moore, B., Kohlmaier, G., Holland, E., Gloor, M., Harmon, M.E., Fan, S.-M., Sarmiento, J.L., Goodale, C.L., Schimel, D., & Field, C.B. (2001). Consistent Land- and Atmosphere-Based U.S. Carbon Sink Estimates. *Science, 292*, 2316-2320

Parmesan, C., Ryrholm, N., Stefanescu, C., Hill, J.K., Thomas, C.D., Descimon, H., Huntely, B., Kaila, L., Kullberg, J., Tammaru, T., Tennent, W.J., Tomas, J.A., & Warren, M. (1999). Poleward shifts in geographical ranges of butterfly species associated with regional warming. *Nature, 399*, 579-583

Parton, W., Hartman, M., Ojima, D., & Shimel, D. (1998). DAYCENT and its land surface submodel: description and testing. *Global and Planetary Change, 19*, 35-48

Parton, W.J., Schimel, D.S., Cole, C.V., & Ojima, D.S. (1987). Analysis of Factors Controlling Soil Organic-Matter Levels in Great-Plains Grasslands. *Soil Science Society of America, 51*, 1173-1179

Patra, P.K., Maksyutov, S., & Nakazawa, T. (2005). Analysis of atmospheric CO2 growth rates at Mauna Loa using CO2 fluxes derived from an inverse model. *Tellus, 57B*, 357-365

Paustian, K., Six, J., Elliott, E.T., & Hunt, H.W. (2000). Management options for reducing CO_2 emissions from agricultural soils. *Biogeochemistry, 48*, 147-163

Pavelsky, T.M., & Smith, L.C. (2004). Spatial and temporal patterns in Arctic river ice breakup observed with MODIS and AVHRR time series. *Remote Sensing of Environment, 93*, 328-338

Pham, A.T., Grandpre, L.D., Gauthier, S., & Bergeron, Y. (2004). Gap dynamics and replacement patterns in gaps of the northeastern boreal forest of Quebec. *Canadian Journal of Forest Research, 34*, 353-364

Pickett, S.T.A., & White, P.S. (1985). *The Ecology of Natural Disturbance and Patch Dynamics*. Orlando: Academic Press, INC.

Pisaric, M.F.J., Carey, S.K., Kokelj, S.V., & Youngblut, D. (2007). Anomalous 20th century tree growth, Mackenzie Delta, Northwest Territories, Canada. *Geophysical Research Letters, 34*, L05714

Potter, C., Klooster, S., Hiatt, S., Fladeland, M., Genovese, V., & Gross, P. (2007a). Satellite-derived estimates of potential carbon sequestration through afforestation of agriculture lands in the United States. *Climatic Change, 80*, 323-336

Potter, C., Klooster, S., Huete, A., & Genovese, V. (2007b). Terrestrial Carbon Sinks for the United States Predicted from MODIS Satellite Data and Ecosystem Modeling. *Earth Interactions, 11*, 1-21

Potter, C., Klooster, S., Myneni, R., Genovese, V., Tan, P.-N., & Kumar, V. (2003a). Continental-scale comparisons of terrestrial carbon sinks estimated from satellite data and ecosystem modeling 1982-1998. *Global Planetary Change, 39*, 201-213

Potter, C., Klooster, S., Tan, P., Steinbach, M., Kumar, V., & Genovese, V. (2003b). Variability in Terrestrial Carbon Sinks over Two Decades. Part I : North America. *Earth Interactions, 7*, 1-14

Potter, C., Randerson, J., Field, C., Matson, P.A., Vitousek, P., Mooney, H., & Klooster, S. (1993). Terrestrial ecosystem production: A process model based on global satellite and surface data. *Global Biogeochemical Cycles, 11*, 99-109

Potter, C., Tan, P.-N., Steinbach, M., Klooster, S., Kumar, V., Myneni, R., & Genovese, V. (2003c). Major disturbance events in terrestrial ecosystems detected using global satellite data sets. *Global Change Biology, 9*, 1005-1021

Potter, C.S. (1999). Terrestrial biomass and the effects of deforestation on the global carbon cycle. *Bioscience, 49*, 769-778

Powell, R.L., Matzke, N., deSouza, C., Clark, M., Numata, I., Hess, L.L., & Roberts, D.A. (2004). Sources of error in accuracy assessment of thematic land-cover maps in the Brazilian Amazon. *Remote Sensing of Environment, 90*, 221-234

Prince, S.D. (1991). A Model of Regional Primary Production for use with Course Resolution Satellite Data. *International Journal of Remote Sensing, 12*, 1313-1330

Prince, S.D., Haskett, J., Steininger, M., Strand, H., & Wright, R. (2001). Net primary production of US Midwest croplands from agricultural harvest yield data. *Ecological Applications, 11*, 1194-1205

Rahmstorf, S. (2007). A Semi-Empirical Approach to Projecting Future Sea-Level Rise. *Science, 315*, 368-370

Randerson, J.T., Chapin, F.S., Harden, J.W., Neff, J.C., & Harmon, M.E. (2002). Net Ecosystem Production: A Comprehensive Measure of Net Carbon Accumulation By Ecosystems. *Ecological Applications, 12*, 937-947

Randerson, J.T., Thompson, M.V., Conway, T.J., Fung, I.Y., & Field, C.B. (1997). The Contribution of Terrestrial Sources and Sinks to Trends in the Seasonal Cycle of Atmospheric Carbon Dioxide. *Global Biogeochemical Cycles, 11*, 535-560

Randerson, J.T., Thompson, M.V., Malmstrom, C.M., Field, C.B., & Fung, I.Y. (1996). Substrate limitations for heterotrophs: Implications for models that estimate the seasonal cycle of atmospheric CO_2. *Global Biogeochemical Cycles, 10*, 585-602

Rasmussen, M.S. (1992). Assessment of millet yields and production in northern Burkina Faso using integrated NDVI from the AVHRR. *International Journal of Remote Sensing, 13*, 3431-3442

Richards, J.A. (1984). Thematic mapping from multitemporal image data using principal components transformation. *Remote Sensing of Environment, 16*, 35-46

Richards, J.A. (1993). *Remote sensing digital image analysis. An introduction*. Berlin: Springer-Verlag

Rigina, O. (2003). Detection of boreal forest decline with high-resolution panchromatic satellite imagery. *International Journal of Remote Sensing, 24*, 1895-1912

Robertson, G.P., & Grace, P.R. (2004). Greenhouse gas fluxes in tropical and temperate agriculture: the need for a full-cost accounting of global warming potentials. *Environment, Devlopment and Sustainability, 6*, 51-63

Roe, G., & Baker, M. (2007). Why is Climate Sensitivity So Unpredictable. *Science, 318*, 629-632

Ruimy, A., Dedieu, G., & Saugier, B. (1996). TURC: a diognostic model of continental gross primary productivity and net primary productivity. *Global Biogeochemical Cycles, 10*, 269-286

Ruimy, A., Kergoat, L., & Bondeau, A. (1999). Comparing global models of terrestrial net primary productivity (NPP): analysis of differences in light absorption and light-use efficiency. *Global Change Biology, 5*, 56-64

Sabine, C.L., Heiman, M., Artaxo, P., Bakker, D.C.E., Chen, C.T.A., Field, C.B., Gruber, N., LeQuere, C., Prinn, R.G., Richey, J.E., Romero-Lanko, P., Sathaye, J.A., & Valentini, R. (2004). Current status and past trends of the carbon cycle. . In C.B. Field & M.R. Raupach (Eds.), *The Global Caron Cycle: Integrating Humans, Climate, and the Natural World*. Washington D.C.: Island Press

Sabol, D.E., Gillespie, A.R., Adams, J.B., Smith, M.O., & Tucker, C.J. (2002). Structural stage in Pacific Northwest forests estimated using simple mixing models of multispectral images. *Remote Sensing of Environment, 80*, 1-16

Sainju, U.M., Singh, B.P., & Whitehead, W.F. (2002). Long-term effects of tillage, cover crops, and nitrogen fertilization on organic carbon and nitrogen concentrations in sandy loam soils in Georgia, USA. *Soil and Tillage Research, 63*, 167-169

Saxton, K.E., Rawls, W.J., Romberger, J.S., & Papendick, R.J. (1986). Estimating generalized soil-water charcteristics from texture. *Soil Science Society of America, 50*, 1031-1036

Scanlon, B.R., Reedy, R.C., Stonestrom, D.A., Pridic, D.E., & Dennehy, K.F. (2005). Impact of land use and land cover change on groundwater recharge and quality in the southwestern US. *Global Change Biology, 11*, 1577-1593

Schaefer, K., Denning, A.S., Suits, N., Kaduk, J., Baker, I., Los, S., & Prihodko, L. (2002). Effect of climate on interannual variability of terrestrial CO_2 fluxes. *Global Biogeochemical Cycles, 16*, doi:10.1029/2002GB001928

Schimel, D.S., House, J.I., Hibbard, K.A., Bousquet, P., Cias, P., Peylin, P., Braswell, B.H., Apps, M.J., Baker, D., Bondeau, A., Canadell, J., Churkina, G., Cramer, W., Denning, A.S., Field, C.B., Friedlingstein, P., Goodale, C., Heimann, M., Houghton, R.A., Melillo, J.M., More, B., Murdiyarso, D., Noble, I., Pacala, S.W., Prentice, I.C., Raupach, M.R., Rayner, P.J., Scholes, R.J., Steffen, W.L., & Wirth, C. (2001). Recent patterns and mechanisms of carbon exchange by terrestrial ecosystems. *Nature, 414*, 169-172

Schlesinger, W.H. (1997). *Biogeochemistry: an analysis of global change*. San Diego, USA: Academic Press

Schulze, E.D., & Heimann, M. (1998). *Carbon and water exchange of terrestrial ecosystems*. Cambridge: Cambridge University Press

Schulze, E.D., Wirth, C., & Heinmann, M. (2000). Managing forests after Kyoto. *Science, 289*, 2058-2059

Sellers, P.J. (1985). Canopy reflectance, photosynthesis, and transpiration. *International Journal of Remote Sensing, 6*, 1335-1372

Sellers, P.J. (1987). Canopy Reflectance, Photosynthesis and Transpiration. II. The Role of Biophysiscs in the Linearity of Their Interdependence. *Remote Sensing of Environment, 21*, 143-183

Sellers, P.J., Hall, F.G., Kelly, R.D., Black, A., Baldocchi, D., Berry, J., Ryan, M., Ranson, K.J., Crill, P.M., Lettenmaier, D.P., Margolis, H., Chilar, J., Newcomer, J., Fitzjarrald, D., Jarvis, P.G., Gower, S., Halliwell, D., Williams, D., Goodison, B., Wickland, D.E., & Guertin, F.E. (1997). BOREAS in 1997: Experiment

overview, scientific results, and future directions. *Journal of Geophysical Research (JGR), BOREAS Special Issue II, 102*, 28,731-728,769

Sellers, P.J., Randall, D.A., Collatz, G.J., Berry, J.A., Field, C.B., Dazlich, D.A., Zhang, C., Collelo, G.D., & Bounoua, L. (1996). A Revised Land Surface Parameterization (SiB2) for Atmospheric GCMs. Part I: Model Formulation. *Journal of Climate, 9*, 676-705

Sitch, S., McGuire, A.D., Kimball, J., Gedney, N., Gamon, J., Engstrom, R., Wolfe, A., Zhuang, Q., Clein, J., & Mcdonald, K.C. (2007). Assessing The Carbon Balance Of Circumpolar Arctic Tundra Using Remote Sensing and Process Modeling. *Ecological Applications, 17*, 213-234

Sitch, S., Smith, B., Prentice, I.C., Arneth, A., Bondeau, A., Cramer, W., Kaplan, J., Levis, S., Lucht, W., Sykes, M., Thonicke, K., & Venevsky, S. (2003). Evaluation o fecosystem dynamics, plant geogaphy and terrestrial carbon cycling in the LPJ Dynamic Vegetation Model. *Global Chnage Biology, 9*, 161-185

Six, J., Ogle, S.M., Briedt, F.J., Conant, R.T., Mosier, A.R., & Paustian, K. (2004). The potential to mitigate global warming wih no-tillage management is only realized when practices in the long term. *Global Change Biology, 10*, 155-160

Slayback, D., Pinzon, J., Los, S., & Tucker, C.J. (2003). Northern hemisphere photosynthetic trends 1982-99. *Global Change Biology, 9*, 1-15

Soja, A.J., Tchebakova, N.M., French, N.H.F., Flannigan, M.D., Shugart, H.H., Stocks, B.J., Sukinin, A.I., Parfenova, E.I., Chapin, F.S., & Stackhouse, P.W. (2007). Climate-induced boreal forest change: Predictions versus current observations. *Global and Planetary Change, 56*, 274-296

Steingrobe, B., Schmid, H., Guster, R., & Claassen, N. (2001). Root production and root mortality of winter wheat grown on sandy and loamy soils in different farming systems. *Biology and Fertility of Soils, 33*, 331-339

Stocks, B.J., Mason, J.A., Todd, J.B., Bosch, E.M., Wotton, B.M., Amiro, B.D., Flannigan, M.D., Hirsch, K.G., Logan, K.A., Martell, D.L., & Skinner, W.R. (2003). Large forest fires in Canada, 1959-1997. *Journal of Geophysical Research, 108*, 5-1, 5-12

Stokstad, E. (2004). Deforesting the Carbon Freezer of the North. *Science, 304*, 1619-1620

Stow, D., Daeschner, S., Hope, A., Douglas, D., Petersen, A., Myneni, R., Zhou, L., & Oechel, W. (2003). Variability of the Seasonality Integrated Normalized Difference Vegetation Index Across the North Slope of Alaska in the 1990s. *International Journal of Remote Sensing, 24*, 1111-1117

Sturm, M., Douglas, T., & Racine, R. (2005). Changing snow and shrub conditions affect albedo with global implications. *Journal of Geophysical Research, 110*, 1-13

Sturm, M., McFadden, J., & Liston, G. (2001). Snow-shrub interactions in Arctic tundra: a hypothesis with climatic implications. *Journal of Climate, 14*, 336-344

Tape, K., Sturm, M., & Racine, C. (2006). The evidence for shrub expansion in Northern Alaska and the Pan-Arctic. *Global Change Biology, 12*, 686-702

Thompson, M.V., & Randerson, J.T. (1999). Impulse response functions of terrestrial carbon cycle models: method and application. *Global Change Biology, 5*, 371-394

Tilman, D. (1999). Global environmental impacts of agriculture expansion: The need for sustainable and efficient practices. *Proceedings of the National Academy of Sciences of the United States of America, 96*, 5995-6000

Tompson, M., Randerson, J., Malmstrom, C., & Field, C. (1996). Change in net primary production and heterotrophic respiration: How much is necessary to sustain the terrestrial carbon sink? *Global Biogeochemical Cycles, 10*, 711-726

Tou, J.T., & Gonzales, R.C. (1974). *Pattern Recognition Principles*: Addison-Wesley

Townshend, J.R.G., Justice, C.O., Gurney, C., & McManus, J. (1992). The Impact of Misregistration on Change Detection. *IEEE Transactions Geoscience and Remote Sensing, 30*, 1054-1060

Trenberth, K.E., Branstator, G.W., & Arkin, P. (1988). Origins of the 1988 North American Drought. *Science, 242*, 1640-1645

Tucker, C.J. (1979). Red and Photographic Infrared Linear Combinations for Monitoring Vegetation. *Remote Sensing of Environment, 8*, 127-150

Tucker, C.J., Grant, D.M., & Dykstra, J.D. (2004). NASA's Global Orthorectified Landsat Data Set. *Photogrammetric Engineering and Remote Sensing, 70*, 313-322

Tucker, C.J., Pinzon, J.E., Brown, M.E., Slayback, D.A., Pak, E.W., Mahoney, R., Vermote, E.F., & Saleous, N.E. (2005). An Extended AVHRR 8-km NDVI Data Set Compatible with MODIS and SPOT Vegetation NDVI Data. *International Journal of Remote Sensing, 26*, 4485-4498

Tucker, C.J., Slayback, D.A., Pinzon, J.E., Los, S.O., Myneni, R.B., & Taylor, M.G. (2001). Higher northern latitude normalized difference vegetation index and growing season trends from 1982 to 1999. *International Journal of Biometeorology, 45*, 184-190

USDA (2005). Forest Insect and Disease Conditions in the United States 2004. In F.H.P.O. Forest Service (Ed.) (p. 154). Missoula, MT

USDA (2007). National Agriculture Statistics. Available Online at: http://www.nass.usda.gov (accessed 07-29-07)

vanCleve, K., Oliver, L., Schlenter, R., Viereck, L.A., & Dyrness, C.T. (1983). Productivity and nutrient cycling in taiga forest ecosystems. *Canadian Journal of Forest Research - Revue Canadienne De Recherche Forestiere, 13*, 747-766

vanderWerf, G.R., Randerson, J.T., Collatz, G.J., Giglio, L., Kasibhatla, P.S., Arellano, A.F., Olsen, S.C., & Kasischke, E.S. (2004). Continental-scale partitioning of fire emissions during the 1997 to 2001 El Nino/La Nina period. *Science, 303*, 73-76

vanderWerf, G.R., Randerson, J.T., Giglio, L., Collatz, G.J., Kasibhatla, P.S., & Arellano, A.F. (2006). Interannual variability in global biomass burning emissions from 1997 to 2004. *Atmospheric Chemistry and Physics, 6*, 3423-3441

Vowinckel, T., Oechel, W.C., & Boll, W.G. (1975). The effect of climate on the photosynthesis of *Picea mariana* at the subarctic tree line. *Canadian Journal of Botany*, 604-620

Walker, D.A., Epstein, H.E., Jia, G.J., Balser, A., Copass, C., Edwards, E.J., Gould, W.A., Hollingsworth, J., Knudson, J., Maier, H.A., Moody, A., & Raynolds, M.K. (2003). Phytomass, LAI, and NDVI in northern Alaska: Relationships to summer warmth, soil pH, plant functional types, and extrapolation to the circumpolar Arctic. *Journal of Geophysical Research-Atmospheres, 108*

Wang, J., Price, K.P., & Rich, P.M. (2001). Spatial patterns of NDVI in response to precipitation and temperature in the central Great Plains. *International Journal of Remote Sensing, 22*, 3827-3844

Warner, T. (2005). Hyperspherical direction cosine change vector analysis. *International Journal of Remote Sensing, 26*, 1201-1215

Wein, R.W., & MacLean, D.A. (1983). *The Role of Fire in Northern Circumpolar Ecosystems*. New York: J. Wiley and Sons

Winter, T.C., & Rosenberry, D.O. (1998). Hydrology of Prairie Pothole Wetlands During Drought and Deluge: A 17-year study of the cottonwood lake wetland complex in North Dakota in the perspective of longer term measured and proxy hydrological records. *Climatic Change, 40*, 189-209

Wofsy, S.C., & Harris, R.C. (2002). The North American Carbon Program (NACP). In (pp. 1-56): U.S. Carbon Cycle Science Steering Group

Wright, H.E., & Heinselman, M.L. (1973). The ecological role of fire in natural conifer forests of western and northern North America. *Quaternary Research, 3*, 317-513

Zhou, L., Kaufmann, R.K., Tian, Y., Myneni, R.B., and Tucker, C.J. (2003). Relation Between Interannual Variations in Satellite Measures of Vegetation Greenness

and Climate Between 1982 and 1999. *Journal of Geophysical Research, 108*, ACL 3-1, ACL 3-11

Zhou, L., Tucker, C.J., Kaufmann, R.K., Slayback, D., Shabanov, N.V., & Myneni, R.B. (2001). Variations in northern vegetation activity inferred from satellite data of vegetation index during 1981 to 1999. *Journal of Geophysical Research, 106*, 20,069-020,083